Federal University of Rio Grande do Sul

Institute of Chemistry

Preparing Jet Engine and Diesel Engine Range Fuels from Biomass Pyrolysis Oil Through Hydrogenation Using NiMo as a Catalyst

Doctorate candidate: **ZEBAN SHAH**

September 2017

Porto Alegre, RS, Brazil

Federal University of Rio Grande do Sul

Institute of Chemistry

Preparing Jet Engine and Diesel Engine Range Fuels from Biomass Pyrolysis Oil Through Hydrogenation Using NiMo as a Catalyst

This thesis is submitted in fulfilment of the requirements
of the degree of Doctor in Chemistry.

Doctorate candidate: **ZEBAN SHAH**

Supervisor:

Renato CataluñaVeses

(Professor at UFRGS)

September 2017

Porto Alegre, RS, Brazil

CONTENTS

Abstract ……..... 14

Graphical Abstract ……..……...……15

Resumo ……..……16

Objectives ……..…….…..……..18

1. Introduction …….....19

2. Literature review ……..……...……23

2.1. Pyrolysis ……..……..……23

2.2. Catalytic pyrolysis ……..……...…….29

2.3. Factors effecting pyrolysis ……..…..…….……34

2.4. Upgrading of bio-oil ……..….36

2.4.1. Esterification ……...……...……...…….……..41

2.4.2. Hydrogenation ……...……..…….……...43

2.4.3. Supercritical fluids (SCFs) ……..…….……48

2.4.4. Steam reforming …….…...…49

2.5. Physico-chemical properties of bio-oil ……51

2.6. Formulations ……52

3. Experimental ……..…….....54

3.1: Materials and methods …….54

3.2. Production of LFP and HFP ……..……..……57

3.3. Production of LFH and HFH …… ……..57

3.4. Characterization of LFP, HFP, LFH and HFH……..…….58

4. RESULTS AND DISCUSSIONS ……..……...…..……65

4.1. Characterization of all fractions of bio-oil after and before hydrogenation ……..….. 65

4.2. GC-MS characterization of all fractions of bio-oil ...……...……...….....…65

4.3. NMR of all fractions ...……..……...……65

4.4. FTIR characterization of all fractions of bio-oil ...…...……..…….67

4.5. TGA analysis of all fractions……..……..…69

4.6. Enthalpy of combustion ...…… ……....…..72

4.7. Freezing point ……..…73

4.8. Density and Viscosity of AF, DF, LFH and HFH …….……..……..….75

4.9 Distillation curves ……..…….…….…….79

4.10. Flash point of AF, DF, LFH and HFH ……..…….....……..……81

4.11. Enrichment of hydrocarbons in bio-oil after hydrogenation …….……82

4.12. Nitrogen and Oxygen contents ……...…84

5. Analysis of LFH and HFH after formulations With DF And AF ……....85

5.1. Density of aviation and diesel fuels with 20% and 10% bio-oil ……..……..…..85

5.2. Viscosity of aviation and diesel fuels with 20% and 10% bio-oil …….....…..86

5.3. Distillation curves of pure AF, HFH, 10% and 20% formulations of HFH with AF..….88

5.4. Distillation curves of pure DF, LFH, 10% and 20% formulations of LFH with DF…...89

6. Conclusions 90

7. References 93

8. ANNEXES ……...……..…….....101

FIGURE INDEX

Figure 1. Schematic diagram of biomass pyrolysis system ……..…..……58

Figure 2. Calorimeter used for the determination of enthalpy of combustion …….....60

Figure 3. Schematic diagram of freezing point determination system ……..…61

Figure 4. Diagram of open cup method for flash point determination ……..…….62

Figure.5. Diagram of a atmospheric distillation system ……..……....63

Figure 6. Oswald viscometer ……...…….…..…..…64

Figure 7. ^{1}H-NMR spectrums of LFP, HFP, LFH and HFH ……..67

Figure 8. FTIR spectras of LFP, HFP, LFH and HFH ……..……..... 69

Figure 9. TGA thermograms of LFP, HFP, LFH and HFH ……...…72

Figure 10. Graphical representation of density of LFH, HFH, AF and DF …….……....76

Figure 11. Graphical representation of viscosity of LFH, HFH, AF and DF ……...78

Figure 12. Distillation curves of HFH and AF ……..……..……...…...…80

Figure 13. Distillation curves of LFH and DF ……..……...……...….....….81

Figure 14. Percentage area of chemical classes for bio-oil after and before hydrogenation...84

Figure 15. Relationship between temperature and density of all formulations …….....86

Figure 16. Relationship between temperature and viscosity of all formulations…….....….87

Figure 17. Distillation curves of HFH formulations with AF ……..……...…...88

Figure 18. Distillation curves of LFH formulations with DF ……..……...…..89

TABLE INDEX

Table I. Changes in pyrolysis yields at different temperatures ……..……...….....……..….56

Table II. Different properties of LFP, HFP, LFH, HFH, DF, and AF .…… …….…..….75

ACKNOWLEDGEMENTS

"In the Name of ALLAH the Most Merciful and Mighty"

Firstly, I would like to pay infallible gratitude and deepest thanks to my venerate and sincere supervisor Prof. Dr. Renato Cataluña Veses who gave me an opportunity to complete my Ph.D. in his research laboratory. He always encouraged my research work and allowing me to grown up as a research scientist. His guidance on both my research skills as well as on my career has been priceless.

I am also very thankful to Prof. Veneza De Oliveira for her sympathetic treatments, constant encouragement and inspiring guidance which enabled me to complete my research work successfully. My sincere thanks to Prof. Dr. Rosangela da Silva, Prof. Dr. Silvio L.P. Dias, Dr. Julio C.P. Waghetti, all the professors of Institute of Chemistry UFRGS and all PPGQ team especially Giuliana Rissi. I extremely appreciate all of my friends, especially my heartiest friend Mr. Sardar Ali **(**Bhutto**),** Dr. Muhammad Nisar, Mr. Muhammad Shafiq, Mr. Muhammad Yaseen and my dearest cousin Abdul Qayyum Khan for their sympathetic behavior, nice company, and ethical support.

My heartily thanks are for my father Gul Muhammad (Late) and for my loving and caring mother Halima Jan (Late). They have always prayed for my well-being and for success. It is due to their encouragement, valuable guidance, prayers and moral support which have helped me to achieve my goal. My gratitudes are to my brothers Said Kamal Shah, Saleman Shah, Muhammad Raza and my loving and caring sisters, whose sympathies, financial assistance and love paved the way for me to achieve this mere dream.

Dr. Zeban Shah

List of Publications

1: **Zeban Shah***, Renato Cataluña Veses, and Rosangela da Silva

Using GC-MS to Analyze Bio-Oil Produced from Pyrolysis of Agricultural Wastes - Discarded Soybean Frying Oil, Coffee and Eucalyptus Sawdust in the Presence of 5% Hydrogen and Argon.

Journal of Analytical & Bioanalytical Techniques

Volume 7, Issue 2, 7:300, 2- 24- 2016

2: Zeban Shah*, Renato Cataluña Vases, Inam Ullah, Muhammad Yaseen, Rafaela A. Aguilhera, Salma Jamal, Vanessa de A. Amorim, Rosangela da Silva

Analysis of Bio-Oil Obtained from pyrolysis of Scenedesmus and Spirogyra mixture (Algal Biomass).

Journal of ongoing chemical research

Volume 2. Issue. 2. 1-13, 05-09- 2016.

3: Zeban Shah*, Renato Cataluña Veses, Rafaela Aguilhera, Rosangela da Silva

Bio-Oil Production from Pyrolysis of Coffee and Eucalyptus Sawdust in the Presence of 5% Hydrogen.

International Journal of Engineering Research & Science (IJOER)

Volume-2, Issue-5, 103-111, 5-30-2016

4: **Zeban Shah***, Renato Cataluña Veses, Inam Ullah, Rosangela da Silva

GC-MS and FTIR analysis of bio-oil obtained from freshwater algae (spirogyra) Collected from Freshwater.

International Journal of Environmental & Agriculture Research (IJOEAR)

Vol-2, Issue-2, 134-141, 2-10- 2016

5: **Zeban Shah**,***** , Renato Cataluña Veses, Rosangela da Silva

A Comparative Study and Analysis of Two types of Bio-Oil Samples Obtained from Freshwater Algae and Microbial treated Algae through Pyrolysis.

Journal of Modern chemistry and applications

Volume 4, Issue 3, 4:185, 07-02-2016

6: Renato Cataluña*, **Zeban Shah**, Pedro Motifumi Kuamoto, Elina B. Caramão, Maria Elisabete Machado and Rosângela da Silva

Bio-Oil Production by Thermal Cracking in the Presence of Hydrogen.

International Journal of Engineering Research & Science (IJOER)

Volume 2, Issue 1, 88-107, 01-2016

7: Renato Cataluña*, **Zeban Shah**, Leidimara Pelisson, Nattan R. Caetano, Rosângela da Silva and Carla M. N. Azevedo

Biodiesel Glycerides from the Soybean Ethylic Route Incomplete Conversion on the Diesel Engines Combustion Process.

Journal of Brazilian chemical society

Volume 00, No. 00, 1-8, 2017

8: Zeban Shah,***,** Renato Cataluña Veses, Marco A. Ceschi, Rosangela da Silva

Separation of Phenol from Bio-oil Produced from Pyrolysis of Agricultural wastes.

Modern chemistry and Applications journal

Volume.5. issue1, 5:199, 01-02-2017

9*:* Muhammad Yaseen**,** **Zeban Shah,** Renato Cataluña, Silvio L.P Dias, Khalid Mehmood, Éder C. Lima, Julio C.P. Vaghetti.

Photocatalytic Studies of TiO_2/SiO_2 Nanocomposite Xerogels.

Journal of Analytical and Bioanalytical techniques

Volume 8, issue 1, 8:348, 02-25-2017

10: Zeban Shah*, Renato C. Veses, Rosangela da Silva

Preparing Jet Engine Range Fuels from Biomass Pyrolysis Oil through Hydrogenation Using NiMo as a Catalyst

Under review

11. Zeban Shah*, Renato Cataluña Veses**,** Silvio L.P. Dias**,** Eder C. Lima, Anderson J.B. Leite, Julio C.P Vaghetti

Bio-Oil Production from Pyrolysis of Brazilian Ironwood Seeds (Caesalpinia Ferrea).

Under review

ABBREVIATIONS:

HFH: Heavy fraction of bio-oil after hydrogenation (160-240 ^{o}C)

LFH: Light fraction of bio-oil after hydrogenation (80-160 ^{o}C)

HFP: Heavy fraction of bio-oil after pyrolysis (160-240 ^{o}C)

LFP: Light fraction of bio-oil after pyrolysis (80-160 ^{o}C)

AF: Aviation fuels

DF: Diesel fuels

GC-MS: Gas chromatography–mass spectrometry

NMR: Nuclear magnetic resonance spectroscopy

TGA: Thermal Gravimetric Analysis

FTIR: Fourier Transform Infrared Spectroscopy

NiMo: Nickel Molybdenum

CaO: Calcium oxide

HDS: Hydrodesulfurization

HDO: Hydrodeoxygenation

HDN: Hydrodenitrogenation

ABSTRACT

In this work, the use of bio-oil was proposed as an alternative to fossil fuels (petroleum). The bio-oil was produced by pyrolysis of Eucalyptus sawdust and discarded soybean frying oil, while calcium oxide (CaO) was used as pyrolysis catalyst to improve the bio-oil yield. The temperature of the pyrolysis system was initiated at 25 °C and increased to 850 °C. The atmospheric distillation of crude bio-oil was carried out after pyrolysis and two fractions were separated at a temperature 80−160 °C (LFP, light fraction of pyrolysis oil) and 160−240 °C (HFP, heavy fraction of pyrolysis oil) and were analyzed by TGA (Thermal gravimetric analysis), GC-MS (gas chromatography and mass spectrometry), FTIR (Fourier transform infrared spectroscopy) and NMR (nuclear magnetic resonance spectroscopy). There was an abundance of oxygen and nitrogen containing compounds, as well as other reactive species in the bio-oil after pyrolysis. In order to reduce the amount of these species, because they not only lead to high corrosiveness and acidity, but also set up many obstacles to applications, both fractions LFP and HFP were subjected to the thermal cracking process in the presence of hydrogen (hydrogenation) and again subjected to catalytic hydrogenation in the presence of the NiMo (catalyst). After the catalytic hydrogenation, the second atmospheric distillation was carried out, obtaining more two fractions at temperature 80−160 ºC (LFH, light fraction after hydrogenation) and 160−240 ºC (HFH, heavy fraction after hydrogenation), which were also characterized by the same techniques and we observed that more than 60% of oxygenated, nitrogenated and other reactive species were converted into hydrocarbons. Both LFH and HFH were also compared with S-10 diesel fuels (DF) and jet A aviation fuels (AF) respectively. The differences amongst LFP, HFP, LFH, HFH, DF and AF were presented and critically discussed in this work, where it was verified after the physico-chemical analyzes such as chemical composition, enthalpy of combustion, freezing

point, flash point, density and viscosity, that the fractions obtained by the hydrogenation process (LFH and HFH) can be used as petroleum fuels because both fractions have very close similarities in the important physico-chemical properties with diesel fuels (DF) and aviation fuels (AF). From these fractions, formulations were prepared with 10% and 20% m/m fractions: LFH with diesel oil (DF) and HFH with aviation fuels (AF). The physico-chemical analyzes of these formulations were compared to the pure AF and DF which showed the potential to use these fractions as additives and consequent contribution to the mitigation of the global energy crisis.

GRAPHICAL ABSTRACT

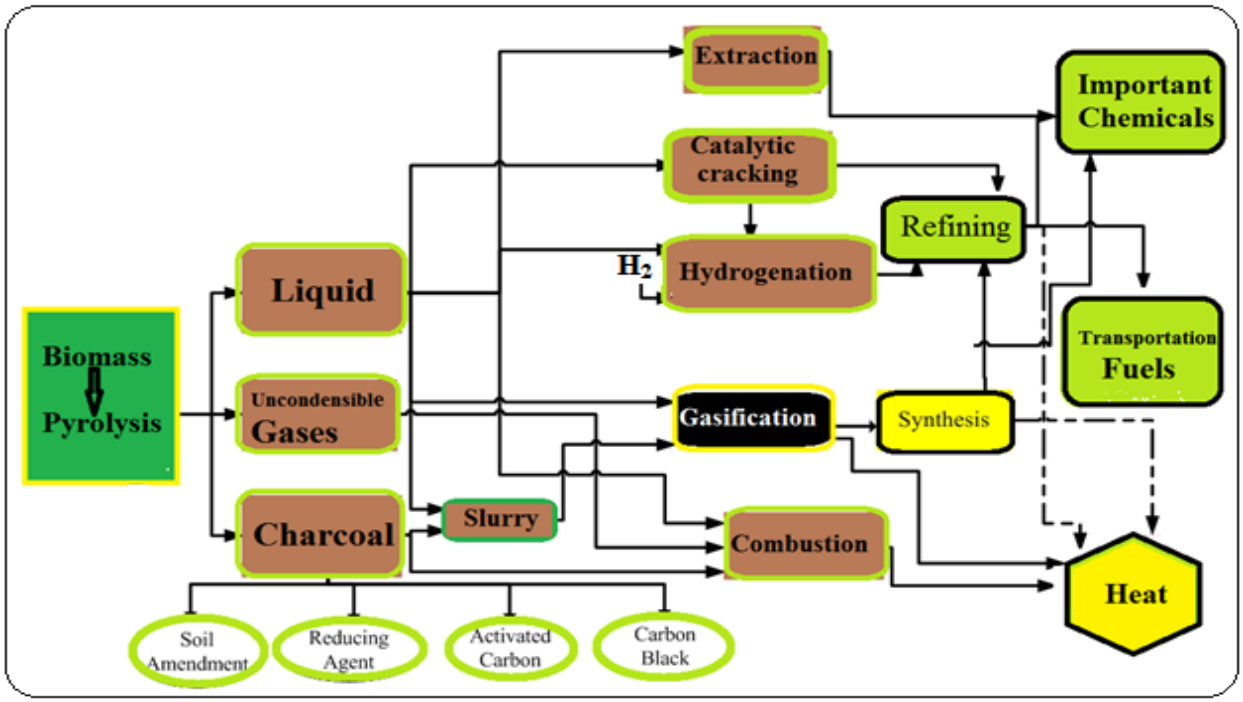

RESUMO

Neste trabalho, o uso de bio-óleo foi proposto como alternativa aos combustíveis fósseis (petróleo). O bio-óleo foi produzido por pirólise de serragem de eucalipto e óleo de fritura de soja descartado, enquanto que o óxido de cálcio (CaO) foi usado como catalisador de pirólise para melhorar o rendimento de bio-óleo. A temperatura do sistema de pirólise foi iniciada a 25 °C e aumentada para 850 °C. A destilação atmosférica de bio-óleo bruto foi realizada após a pirólise e duas frações foram separadas à temperatura de 80−160 ºC (LFP, Fação Leve da Pirólise do bio- óleo) e 160−240 ºC (HFP, Fração Pesada da Pirólise do bio-óleo) e as quais foram analisadas por TGA (análise térmica gravimétrica), GC-MS (cromatografia gasosa acoplada a espectrometria de massa), FTIR (espectroscopia de infravermelho de transformação de Fourier) e RMN (espectroscopia de ressonância magnética nuclear) verificando-se que havia uma abundância de espécies contendo nitrogênio e oxigênio, bem como outras espécies reativas. Com o objetivo de reduzir a quantidade destas espécies após a pirólise, as frações LFP e HFP foram submetidas ao processo de craqueamento térmico na presença de hidrogênio (hidrogenação) e, novamente submetido a hidrogenação catalítica na presença do catalisador de NiMo. Após a hidrogenação catalítca, foi realizada a segunda destilação atmosférica obtendo-se duas frações à temperatura de 80−160 ºC (LFH, Fração Leve da Hidrogenação) e 160−240 ºC (HFH, Fração Pesada da Hidrogenação) as quais foram igualmente caracterizadas pelas técnicas acima enumeradas, observando-se que mais de 60% de espécies nitrogenadas, oxigenadas e outras espécies reativas foram convertidas em hidrocarbonetos. As diferenças entre LFP, HFP e LFH, HFH foram apresentadas e discutidas criticamente neste trabalho, onde verificou-se após as análises fisico-químicas como composição química, entalpia de combustão, ponto de congelamento, densidade, viscosidade e volatilidadeque as frações obtidas pelo processo de

craqueamento e hidrogenação catalítica (LFH e HFH) podem ser usadas como combustíveis, porque apresentaram semelhanças muito próximas nas propriedades fisico-quimicas importantes do óleo de aviação (AF) e óleo diesel (DF). A partir destas informações foram preparadas formulações com 10 e 20% (m/m) das frações: HFH com óleo de aviação (AF) e LFH com oleo diesel (DF). As análises fisico quimicas destas formulações comparadas com o AF e DF mostraram o potencial uso destas frações como aditivos e consequente contribuição para a amenização da crise energética mundial.

OBJECTIVES OF THIS WORK

The main six objectives of this work are as follows:

1. To examine the influence of pre-treatment of agricultural wastes (biomass) on the pyrolysis process and fuel quality.
2. To study the influence of NiMo as a catalyst on pyrolysis oil of agricultural wastes.
3. To study and compare the important analysis as density, viscosity, freezing point, flash point, distillation curve and enthalpy of combustion of bio-oil with aviation fuels and diesel fuels after hydrogenation.
4. To analyze 10% and 20% formulations of bio-oil with aviation fuels and diesel fuels.
5. To understand and define the concept of upgrading and bio-oil quality.
6. To determine a proper pyrolysis temperature for waste biomass to obtain the maximum pyrolysis yield.

1. INTRODUCTION

The thermochemical conversion of biomass is a promising route for the production of chemicals and energy from renewable resources like woody biomass, residues etc[1]. Among all the possible thermochemical processes, pyrolysis is one of the most beneficial and easy technologies used for biomass conversion. This process converts the biomass into bio-oil, a burnable liquid that is easy to store[2-4]. The recent environmental restrictions on the use of fossil fuels have intensified research into new alternative energy sources and many alternative fuel production technologies have been developed, among which the use of biomass offers a promising potential[5,6].

Biomass is a renewable source which has received attention due to various characteristics, particularly its low cost, wide availability and regrowth or regeneration. Biomass can be converted into biofuels by means of different processes, e.g., reductive combustion, liquefaction, pyrolysis, and gasification[7,8]. The use of biomass is particularly interesting when it involves waste products such as waste vegetable oil, fruit seeds, sugarcane bagasse, sugarcane straw, rice husks, coconut fibers, and coffee grounds, which are also potential sources of energy[9,10].

Bio-oil from biomass pyrolysis, also known as pyrolysis oil, is a dark brown almost black liquid with a characteristic smoke odor, whose elemental composition is analogous to that of the biomass from which it derives. It is a complex mixture of oxygenated and nitrogenated compounds with a significant amount of water originating from the moisture of the biomass and from crackingreactions[11-13]. Bio-oil may also contain small coal particles and dissolved alkali metals coming from the ash. Its composition depends on the raw material and on the operating

conditions used in its production. Bio-oil is an aqueous microemulsion resulting from the products of fragmentation of cellulose, hemicelluloses and lignin[14,15].

The biomass pyrolysis process is an economically feasible option for producing chemicals andfuels[16]. The bio-oil resulting from the pyrolysis process consists of a mixture of more than 300organiccompounds, but it's processing, separation, and characterization poses technological challenges. In the thermal cracking process, the volatile compounds generated during pyrolysis also present a promising potential for energy generation[17-19]. Moreover, the upgrading process, which involves the reduction of oxygenates is necessary to improve the quality of bio-oil, normally requires processes such as catalytic cracking, hydrogenation and steam reforming[20,22].

Hydrogenation is an important technique for improving the quality of bio-oil produced from biomass pyrolysis. Hydrogen is a reducing gas and cracking biomass in the presence of hydrogen can reduce the oxygen and nitrogen content in bio-oil[23]. Pyrolysis oil exhibits some inferior properties, such as high water content, high oxygen content, high viscosity low flash point, and strong corrosiveness and these drawbacks make it difficult to be directly used as a vehicle fuel. Therefore, several upgrading technologies have been developed to improve the quality of bio-oil, including catalytic hydrodeoxygenation, hydrodesulfurization and hydrodenitrogenation, catalytic cracking, steam reforming, catalytic esterification, supercritical upgrading and so on[24-26].

Many zeolites also have been applied as solid acid catalysts for oxygen removal from bio-oil and as a resolution multi-stage hydrodeoxygenation has been proposed in which first the pyrolysis oil is stabilized in a low-temperature reactor and then a deeper hydrodeoxygenation is

accomplished in the second-stage reactor at a higher temperature[27-30]. It is reported that Al-MCM-41 (a mesoporous catalysts used for converting the pyrolysis vapours of wood in order to obtain better bio-oil properties) is a promising catalyst for production of high-quality bio-oil. However, it is found that high amount of coke always deposited on this catalyst due to its specific properties such as high acidity and large pore volume[31-33]. The bio-oil can be upgrade by using various kinds of catalysts, such as NiMo, CoMo, FCC, ZnO, H-ZSM-5 etc[34-36]. The use of bio-oil has been proposed as an alternative to the fossil fuels in this work. Bio-oil was produced from pyrolysis of Eucalyptus sawdust and soybean frying oil. After pyrolysis the bio-oil was subjected into thermal cracking in the presence of hydrogen and after hydrogenation bio-oil was again subjected to catalytic hydrogenation in the presence of NiMo as a catalyst. The bio-oil was obtained from pyrolysis where the temperature of the system was initiated at 25 ºC and increased up to 850 ºC. Atmospheric distillation of crude bio-oil was performed and two fractions were separated at temperature 80-160 ºC and 160-240 ºC and these fractions were analyzed by thermal gravimetric analysis, Gas chromatography–mass spectrometry, Fourier transform infrared spectroscopy, and Nuclear magnetic resonance spectroscopy to identify different hydrocarbons and other groups present in pyrolysis oil. After conducting the above-mentioned analysis, it was noticed that there was an abundance of nitrogen and oxygen containing species as well as other reactive species in the bio-oil. To reduce the amount of these species, the bio-oil was subjected to hydrogenation in the presence of NiMo as a catalyst. After second atmospheric distillation of hydrogenated bio-oil two more fractions were obtained at temperature 80-160 ºC and 160-240 ºC and again these hydrogenated fractions were analyzed by the same techniques like TGA, GC-MS, FTIR and NMR. We have noticed that after hydrogenation more than 60% of oxygenated, nitrogenated and other reactive species were converted into hydrocarbons. The differences

amongst all fractions of bio-oil, after and before hydrogenation were presented and critically discussed in this work, where we have seen that hydrogenated fractions of bio-oil can be used as fuels because it showed almost the same important properties and characteristics of petroleum fuels. For example, a light fraction (80-160 ºC) of bio-oil and a heavy fraction (160-240 ºC) showed close similarities in density, viscosity, freezing point, flash point, the presence of lower molecular weight hydrocarbons and enthalpy of combustion as that of diesel fuels and aviation fuels respectively.

1. LITERATURE REVIEW

This literature review explains the origin, progress, and upgrading of pyrolysis oil as well as various catalysts for bio-oil pyrolysis and upgrading. This includes a basic introduction, types, and methods of bio-oil upgrading and types of some catalysts used by previous researchers and scientists.

2.1. PYROLYSIS

Pyrolysis is a thermal process for converting various biomasses, residues and wastes to produce high-energy-density fuels. while avoiding the high cost of transportation and technical difficulties that occur when bio-oil is used directly as fuel[37]. The fixed-bed pyrolysis experiments on a sample of hazelnut shells to determine the possibility of being a potential source of renewable fuels and chemical feedstocks. The effects of pyrolysis temperature and well-sweep gas atmosphere (N_2) on the pyrolysis yields and chemical compositions have been also investigated[38]. Pyrolysis of tires is the thermochemical recycling of rubber from old tires by pyrolysis and Hydropyrolysis. Pyrolysis is a thermal decomposition (500 – 700 ^oC) that occurs in the absence of oxygen and is classified as slow or fast depending on the heating rate, residence time and rate of product condensation. During pyrolysis, the biomass components are thermally depolymerized producing condensable vapors, incondensable gas, aerosol, and char. Depending on the operating conditions, the pyrolysis process can be divided into three subclasses: conventional pyrolysis,pyrolysis, and flash pyrolysis[39].

The pyrolysis of fats has been investigated for more than 100 years, especially in those areas of the world that lack deposits of petroleum[40]. The first pyrolysis of vegetable oil was conducted as an attempt to synthesize petroleum from vegetable oil. A thermogravimetric is used

to obtain the effect of heating rate on the pyrolysis rate in experimental runs. It is interesting to determine how the heating rate affects the pyrolysis rate[41].

Thepyrolysis oil is a suitable source for chemicals, however, the composition of bio-oil from woody biomass pyrolysis varies considerably and it is a function of several parameters such as the source of biomass, its pretreatment, reactor technology, heating, quenching rates, and residence time of the products inside the reactor. The determination ofpyrolysis oil composition is a great analytical challenge. The best methodology among the most commonly available analytical techniques is a merging between gas and liquid chromatography. They allow complementary qualitative and quantitative analysis of a wide variety of compounds, giving complementary information. Gas chromatographic (GC) analyses provide reliable insight on volatile compounds with boiling points below 350^{o}C. Among several biomass energy conversion methods, microwave assisted pyrolysis offers low temperature and energy efficient route to convert solid waste biomass resources to energy products[43,44]. The microwave assisted pyrolysis oil was found rich in valuable chemicals, such as phenol high content syngas and high quality bio-char. The pyrolysis performance of uniform distribution method was reported to improve microwave penetration depth, biomass heating profile and bio-oil yield[44,45]. Previous studies on microwave assisted pyrolysis of waste biomass indicated that the process factors influencing bio-oil yield are MWA loading and microwave power. In addition, factors that are assumed to have minimal effects on bio-oil yield can be eliminated, as well as the factors that are categorical[55]. Investigation of the effects of uniformly distributed coconut activated carbon (CAC) at various levels of CAC loading, microwave power and N_2 flow rate on heating profile, bio-oil yield and its composition. The response surface methodology was used to establish model to predict bio-oil yield. Moreover, bio-oil obtained under various microwave operating conditions was analyzed

using GC–MS for phenol and other chemicals. However, the use of thermocouple in microwave cavity environment can measure accurate temperature provided that it is thin with grounded metal sheath and held exactly at 90ºC to the electric field component of microwave[64].

The combination of pyrolysis-GC/MS and TLC–FID techniques for whole sample analysis of bio-oil samples obtained from different lignocellulosic biomasses, (i.e., birch wood, pine wood, barley straw and forest residue and thermal-cracking fractions) were used. Both techniques showed the ability to analyze the whole sample without cleanup or fractionation and to distinguish among the bio-oils based on their feedstock sources. They reported that forest residue bio-oil and its thermal cracking fractions could be effectively characterized by TLC–FID (and Py-GC/MS) whereby the light fraction was composed of a wide range of lower polarity compounds while the heavy fraction had higher polarity compounds[47]. Catalytic pyrolysis of green algae for hydrocarbon production using H-ZSM-5as a catalyst was performed and it was found that when a fresh water green alga, Chlorella vulgaris, was taken for pyrolysis study, the average activation energy for pyrolysis zone was found to be 109.1 kJ/mol. Fixed-bed pyrolysis of algae gave a bio-oil yield of 53 wt.% which accounts for 60.7 wt.% carbon yield. In addition, analytical pyrolysis of Chlorella vulgaris was carried out in a Py/GC–MS to identify major compounds present in bio-oil with and without catalyst (H-ZSM-5). In catalytic pyrolysis, as the catalyst loading increased from zero to nine times of the biomass, the carbon yield of aromatic hydrocarbons increased from 0.9 to 25.8 wt.%. Bio-oil and bio-char produced from Spirulina Sp. by slow pyrolysis were analyzed by thermo gravimetric analyzer (TGA) to investigate the pyrolytic characteristics and essential components of algae. It was found that the temperature for the maximum degradation, 322 ºC, is lower than that of other biomass. With their fixed-bed reactor, 125 g of dried Spirulina Sp. algae was fed under a nitrogen atmosphere until the

temperature reached a set temperature between 450 and 600 ^{o}C. It was found that the suitable temperature to obtain bio-char and bio-oil were at approximately 500 and 550 ^{o}C respectively. The bio-oil components were identified by a gas chromatography-mass spectrometry (GC-MS). The saturated functional carbon of the bio-oil was in a range of heavy naphtha, kerosene and diesel oil. The energy consumption ratio (ECR) of bio-oil and bio-char was calculated, and the net energy output was positive. The ECR had an average value of 0.49[48].

In 2011 a report about extraction of cardanol and phenol from bio-oils obtained through vacuum pyrolysis of biomass using supercritical fluid extraction was published and feasibility of extraction of phenol rich oil from the bio-oils obtained through pyrolysis of cashew nut shells and sugarcane bagasse also studied. The extraction rate of phenol rich oil using CO_2 as a supercritical fluid is discussed. Operating parameters are optimized for the maximum concentration of phenol and cardanol. Higher yield of oil (50% by weight) along with higher concentration of phenols and cardanol by present method is found encouraging. The experiments were conducted in the pressure range of 120 - 300 bar, the temperature range of 303 - 333 K and the mass flow rate range of 0.7- 1.2 kgh^{-1}. Also process parameters were optimized to maximize the yield of extracts and its contents of phenols and substituted phenols from sugarcane bagasse pyrolysis oil. The oil samples at various operating parameters, analyzed by Gas Chromatograph-Mass Spectroscopy (GC-MS) and Fourier Transform Infra-Red Spectroscopy (FTIR) were obtained.

The biomass pyrolysis is a promising path toward renewable liquid fuels. However, the calorific value of the pyrolysis oil also known as bio-oil, is low due to the high content of organic oxygenates and water. The oxygen content of bio-oil can be reduced by hydrodeoxygenation, in which hydrogen is used to remove oxygen[49,50]. An economic

disadvantage of hydrodeoxygenation pathway is its dependence on hydrogen as an expensive feedstock. An alternative technology is to upgrade bio-oil in hot, high pressure water, known as hydrothermal processing. They studies upgrading pyrolysis oil derived from Norwegian spruce by hydrodeoxygenation in a liquid hydrocarbon solvent using nanodispersed sulphide catalysts and hydrothermal treatment in near-supercritical water. Experimental results and simulation studies suggested that if water soluble products are reformed for hydrogen production, the hydrodeoxygenation pathway would be a net consumer of hydrogen, while the hydrothermal pathway could produce a significant hydrogen excess. By comparison, the fuel yield from hydrodeoxygenation was significantly higher than hydrothermally treated fuel[51].

For pyrolysis more than 100 types of biomass have been tested, ranging from agricultural wastes such as straw, olive pits, corncobs, tea waste and nut shells to energy crops such as miscanthus and sorghum. Forestry wastes such as bark, thinning and other solid wastes, including sewage sludge and leather wastes have also been studied by other researcher. But most of the research work has been done on wood.

Bio-oil from wood pyrolysis is dark brown, free-flowing organic liquid that is comprised of highly oxygenated compounds. It is very viscous, relatively unstable and susceptible to aging. Chemically, bio-oil is a complex mixture of water, guaiacols, catechols, syringols, vanillins, furancarboxaldehydes, isoeugenol, pyrones, acetic acid, formic acid, and other carboxylic acids. It also contains other major groups of compounds, including hydroxyaldehydes, hydroxyketones, sugars, carboxylic acids, and phenolics[52].

To develop a separation process for phenolic fraction recovery from various pyrolysis-oils, produced by pyrolysis process of wood and forest residues in the framework of the EU Project BIOCOUP[25], two slightly different schemes, namely the first one starting with an

aqueous extraction of pyrolysis oil and the second one with the simultaneous use of a hydrophobic-polar solvent and antisolvent for the extraction of bio-oil were introduced. In both cases the distribution coefficients of phenolic components between the phases as well as extraction factors for major separation stages are presented. Different aqueous solutions were applied and alkali solution was found to be more efficient in comparison to water or aqueous $NaHSO_3$ solution. From various hydrophobic-polar solvents tested, methyl isobutyl ketone (MIBK) was shown to be the most efficient solvent for extraction of phenolics from bio-oil in combination with 0.1 M or 0.5 M aqueous NaOH solution, followed by butyl acetate[53].

In 2013 a microwave pyrolysis of lignin were performed, an aromatic polymer byproduct from paper-pulping industry, produces char, gases, and lignin pyrolysis oil. A method using switchable hydrophilicity solvents (SHS) to extract phenols as a mixture from lignin microwave pyrolysis oil at the scale of 10 g of bio-oil was described. Even at a small scale, losses are small, 96% of the bio-oil was recovered in its three fractions, 72% of guaiacol and 70% of 4-methylguaiacol, the most abundant phenols in the bio-oil were extracted and 91% of the solvent SHS was recovered after extraction. The starting material (lignin microwave-pyrolysis oil) and the three fractions resulted from SHS extraction were characterized by GC–MS and quantitative $^{13}C\{^1H\}$ and $^{31}P\{^1H\}$ NMR spectroscopy[54].

Recently, in 2017 the pyrolysis of several Canadian straw biomasses, using a thermogravimetric analyzer and a bench-scale horizontal fixed-bed reactor, in order to better understand the devolatilization process and to obtain information about the product yields of these biomasses. They converted the straw biomasses through pyrolysis performed in a fixed-bed reactor at temperatures of 500 °C to study the influence of the feedstock on product yields. They also discussed the effects of various catalysts on product yields. When using zeolite catalysts, the

bio-oil and bio-char yields of the straw pyrolysis were increased to 46% and 38%, respectively, while the bio-gas yield was decreased to 13%. The use of catalyst zeolite ZSM-5 (Zeolite Socony Mobil–5, a zeolites catalyst, used for pyrolysis to obtain high quality of bio-oil) had the most significant effect on overall bio-oil yield, increasing the bio-oil yield by about 20%. This catalyst had the most significant effect on the pyrolysis of flax straw, where the bio-oil yield was increased to 40%. In the pyrolysis of oat straw, the use of the catalyst consistently decreased the bio-gas yield. However, the bio-oil yield increased the most significantly to 53% with the use of catalyst zeolite ZSM-5[54,55].

2.2. CATALYTIC PYROLYSIS

Recently, catalytic pyrolysis has aroused a great interest for the advantages of operating at atmospheric pressure and the lack of need for hydrogen, which has been demonstrated in literature. Catalysts, namely, H-ZSM-5, (zeolite catalyst, used to decreases the yield of uncondensable gases and increases the yields of liquid and char) silicalite and silica-alumina for the upgrading of pyrolysis bio-oil were used. They examined for their relative performance in the production of organic distillate fraction, hydrocarbon formation and minimization of char, coke and tar formation.

A catalyst effectiveness criterion based on yield and selectivity for each product was defined and correlated with the performance of each catalyst. Amongst the five catalysts studied, H-ZSM-5 was the most effective catalyst for the production of organic distillate fraction, overall hydrocarbons and aromatic hydrocarbons. Also, it provided the least coke formation[56].

Silica-alumina catalyst was most effective for minimizing the char formation and H-Y catalyst was superior in minimizing tar formation as well as maximizing the production of aliphatic hydrocarbon. The experiments on catalytic pyrolysis of biomass were generally carried out in a fixed bed reactor or fluidized bed under nitrogen flow with some catalysts, such as H-ZSM-5[57], Al-SBA-15[58], alumina[59] and Cu [60] etc.

Many aspects of catalytic pyrolysis have been studied, including a screening of feasible catalysts with high deoxygenating activities or preferred selectivities influence of temperature and catalyst-to-material ratio on product yields**.** Characteristics analysis of bio-oil using elemental GC–MS and FTIR technologies, both in a fixed bed reactor and in a fluidized bed, the investigation indicated that catalytic pyrolysis lowered the oxygen content of the bio-oil and aggrandized the calorific values compared to the direct pyrolysis without catalysts. This conclusion can be drawn in many experiments with different biomass, including green microalgae, corncob, herb residue and waste woody biomass. Besides, catalytic pyrolysis can lead to the higher content of aromatic hydrocarbons in bio-oil with H-ZSM-5, alumina or H-ZSM- 5/γ-Al_2O_3 as a catalyst while direct pyrolysis promoted the increase of carbon chain compounds[61]. However, the addition of an H-ZSM-5 zeolite catalyst in the experiments caused a significant increase of heavy oil fraction and a decrease of the coke, water, and non-condensable gas yields. This was because the H-ZSM-5 zeolite catalyst could promote the conversion of oxygen in biomass into hydrocarbons. Choosing proper catalysts is crucial to catalytic pyrolysis so, catalyst should be chosen according to the nature of biomass[62].

The catalytic cracking of pyrolysis oil of different starting compositions over H-ZSM-5 was studied to inform the extent of upgrading in the liquid phase. After establishing a catalyst

bed temperature of 500 °C as the optimum operating condition with regard to deoxygenation and yield of mono-aromatics in the products obtained, the performances of conventional pyrolysis and tail gas reactive pyrolysis (TGRP) bio-oils as starting liquids for the cracking were compared. The results indicated that the formation of naphthalenes was favored, while the formation of benzene, toluene, ethylbenzene, and xylenes (BTEX) compounds were slightly depressed in the case of the TGRP oil. The results obtained from this study will help to determine the issues that need to be addressed when developing a catalytic cracker with H-ZSM-5 for regular pyrolysis oil and TGRP oil[63]. Rope-like bundles of single-walled carbon nanotubes (SWNTs) similar to those obtained by laser vaporization and electric-arc techniques were synthesized on a relatively large scale and at low cost by the catalytic decomposition of hydrocarbons at a temperature of about 1200 °C using an improved floating catalyst method. The SWNTs thus obtained have larger diameters and are self-organized into ropes. The addition of thiophene was found to be effective in promoting the growth of SWNTs and in increasing the yield of either SWNTs or multiwalled carbon nanotubes under different growth conditions[102].

Pyrolysis bio-oil currently produced in demonstration and semi-commercial plants have potential as a fuel for stationary power production using boilers or turbines but they require significant modification to become an acceptable transportation fuel. Catalytic upgrading of pyrolysis vapors using zeolites is a potentially promising method for removing oxygen from organic compounds and converting them to hydrocarbons. A set of commercial and laboratory-synthesized catalysts for their hydrocarbon production performance evaluated via the pyrolysis/catalytic cracking route. Three types of biomass feedstocks; cellulose, lignin, and wood were pyrolyzed (batch experiments) in quartz boats in physical contact with the catalysts at temperature ranging from 400 °C to 600 °C and catalyst-to-biomass ratios of 5–10 by weight.

Molecular-beam mass spectrometry (MBMS) was used to analyze the product vapor and gas composition. The highest yield of hydrocarbons (approximately 16 wt.%, including 3.5 wt.% of toluene) was achieved using nickel, cobalt, iron, and gallium-substituted ZSM-5. Tests performed using a semi-continuous flow reactor allowed us to observe the change in the composition of the volatiles produced by the pyrolysis/catalytic vapor cracking reactions as a function of the catalyst time-on-stream. The deoxygenation activity decreased with time because of coke deposits formed on the catalyst[103].

2.3. KEY FACTORS EFFECTING PYROLYSIS

2.3.1. TEMPERATURE

Currently, many effective methods for pyrolysis and upgrading are known. Effect of temperature on pyrolysis yields for catalytic pyrolysis follows the same trend as for the non-catalytic experiments. The organic yields reach a maximum at approximately 600^{o}C and further temperature increase results in a reduction of liquid yields. In contrast, reaction water yields rise with an increase in temperature. In the case of gas yields, an increase is observed with rising temperature. The opposite trend is observed with char yields. Temperature has an effect on the chemical distribution for catalytic pyrolysis. Specifically, for both studies with temperature increase, the amount of monocyclic and bicyclic aromatic hydrocarbons was greater when ZSM-5 was applied. This is an interesting finding since hydrocarbons are a desirable product in terms of bio-oil quality[64].

2.3.2. PYROLYSIS TIME OR RESIDENCE TIME

The pyrolysis time in the reactor plays an important role to the catalytic pyrolysis products yields. The increase of pyrolysis time in the reactor results in an increase of the thermal

cracking of pyrolysis gas. While the effect of pyrolysis time using a ZSM-5 catalyst was also studied. Concerning the products yields, an increase of residence time, decreased the pyrolysis liquid yields, coke and char yields. The gas yields showed an opposite trend. In terms of chemical distribution, the monocyclic and bicyclic aromatic hydrocarbons were greater. The residence time also depends upon the amount and quality of biomass present in pyrolysis furnace or reactor[65].

2.3.3. CATALYSTS

A substance able to increase the rate of a chemical reaction without itself being consumed or changed by the reacting chemicals is called a catalyst. The action of a catalyst is called catalysis. Catalysts are used by chemists to speed up chemical reactions that otherwise would be inconveniently slow. There are many catalysts used for pyrolysis to increase the pyrolysis yields. There are also many catalyst used for upgrading of bio-oil to increase the number of hydrocarbons in bio-oil. A few pyrolysis catalysts are given below:

Research was undertaken in terms of the effect of ZSM-5 on pyrolysis products yields and chemical distribution, the influence of the regeneration of the former zeolite; the influence of deactivation of ZSM-5 on pyrolysis vapors; catalyst dilution; operating conditions[66].

Nickel molybdenum (NiMo) is also used in the hydrotreating process. Since research showed that Cobal molybdenum has a potential in pyrolysis process, NiMo could also prove to be an interesting catalyst for bio-oil upgrading[67]. As well as catalysts of cobalt molybdenum (CoMo) is known as a catalyst that enhances deoxygenation reactions in the hydrotreating process. CoMo was also used in the pyrolysis process. This catalyst improved cracking reactions, increased light hydrocarbons and deoxygenates the bio-oil[68].

Fluid catalytic cracking **(**FCC) is a commercial proprietary catalyst and previous research showed that it is a promising catalyst for phenol and hydrocarbon production[69].

Zinc oxide (ZnO) is a metal oxide catalyst that seemed promising to improve viscosity and stability of bio-oil[70]. Metal oxides conventionally as a selective oxidation catalyst are used to synthesize intermediate chemicals. Currently, they are being used as catalysts in various applications, including the petroleum, chemical and environmental industries[71].

The zirconium oxide catalysts (ZrO), iron oxide ($Fe_3O_{2)}$ and titanium oxide (TiO) seemed to be a potential catalyst for improvement of viscosity and stability of bio-oil, it is worth it to investigate more metal oxides. The selection of ZrO was due to its market availability, as well as its potential for cracking the lignin derivative compounds in bio-oil. This was indicated from the oxidation of tar and ammonia in gasification gas cleaning process by ZrO. A red mud based catalyst was used to upgrade bio-oil and it was showed that the upgraded bio-oil contained less carbonyl-containing and polar oxygenated compounds and more saturated hydrocarbons. This result caused interesting to test red mud based catalyst, such as Fe_3O_2 and TiO. Additionally, the low cost and high availability of the red mud based catalysts made the catalysts attractive was noticed[72].

Copper-chromium (CuCr) as a catalyst has the potential for improving bio-oil stability and deoxygenates the bio-oil. Additionally, it was used for hydrogenation of carbonyl groups, under a hydrogen atmosphere and high pressure. It was also noticed that through low temperatures biomass pyrolysis within the presence of zinc chloride ($ZnCl_2$) proposed a new technique to produce furfural (FF). The result showed that in the presence of $ZnCl_2$ reduce the temperature for biomass, It cause devolatilization of lignin and pyrolysis ring scission of holocellulose to form the FF and three anhydrosugars i.e.(levoglucosenone) (LGO),1-hydroxy-

3,6dioxabicyclo[3.2.1]octane-2-1(LAC) and 1,4:3,6-dianhydro-α-d glucopyranose (DGP)) as the major primary pyrolytic products. It promoted depolymerization and dehydration of holocellulose. By increasing $ZnCl_2$ content, the three anhydrosugars are increased firstly and then decreased, while steadily FF was increased. Secondary catalysis by $ZnCl_2$, could convert the anhydrosugars to FF, leaving FF as the main product. The acetic acid is produced as the only significant liquid by-product[73]. Biomass experimental study by catalytic pyrolysis at low temperature through nickel / aluminum (Ni/Al) Co-precipitated catalyst fed into the reaction bed were study where the thermochemical breakdown of biomass occurred at temperature 600 °C–750 °C. Pyrolysis process (WFPP) technology, the hydrogen stream rate of catalyst and the influence of the calcinations temperature (750–850 °C) were analyzed. The properties and performance of catalyst were significantly influenced by the temperature of calcination. The temperature of the two reactions, 650 and 700 °C, with the presence of a catalyst at 850 °C, higher CO, and H_2 products be obtained with the reduced catalyst (flow rate 3080 cm^3 (STP) min^{-1}; WHSV=0.826 h^{-1}) than without reduction. By considering the experimental results and characterization, it was concluded that the catalyst calcined at 750 °C[74].

2.4. UPGRADING OF BIO-OIL

Pyrolysis can produce a considerable amount of bio-oil, for example, a yield up to 56% was reported in domestic research, their direct applications as fuels are limited by the problems of high viscosity, high oxygen content, and corrosion, as well as their thermal instability. Therefore, bio-oil should be upgraded using proper methods before they can be used in diesel or gasoline engines.

2.4.1. CATALYTIC CRACKING

Catalyticcracking for upgrading pyrolysis bio-oil can be divided into two patterns, the traditional catalytic cracking and the combination of catalytic pyrolysis and catalytic cracking. Traditionally, the catalytic cracking referred to a thermal conversion process of bio-oil under certain conditions, including hydrogen flow, proper catalysts like H-ZSM-5 and a specific temperature higher than 350 ^{o}C as well as rather high pressure[75]. Hydrogenation with simultaneous cracking occurred during the catalytic cracking process. The products of the catalytic cracking process consist of solid, liquid and gasses. The solid is called coke, and the liquid can be divided into two phases, aqueous phase and an organic phase and an uncondensable burnable gas. The traditional catalytic cracking had been carried out in a tubular fixed bed reactor and micro-fixed bed reactor[76]. The advantage of this technique was the probability of obtaining a good deal of light product, but catalyst coke deposition was a bottleneck for sustainable application of catalysts e.g., H-ZSM-5 made the combination of catalytic pyrolysis and catalytic cracking to upgrade pyrolysis bio-oil. It adopted a sequential biomass pyrolysis reactor which consisted of a traditional pyrolysis reactor followed by the subsequent apparatus that supported decomposition of gaseous intermediate.

The largest reactor for this kind of investigation was made of the 316 stainlesstube, with a length of 1000 mm and an inner diameter of 20 mm. For example, researchers applied this method and found that biomass could be fully converted into gaseous products, such as H_2, CH_4 and CO etc. Catalyst (Fe/γ-Al_2O_3) activities were affected by several factors, including calcination temperature, the temperature of catalytic pyrolysis and Fe/Al mass ratio[77].

Pyrolysis bio-oil is a promising source of liquid fuels, but requires upgrading to remove excess oxygen and produce a satisfactory fuel oil. Nickel phosphide (Ni_2P) has been shown to be

an active composition for hydrodeoxygenation (HDO) of bio-oil model compounds. Nickel phosphide catalysts were used for direct upgrading of an actual pyrolysis bio-oil derived from cedar chips. The activity of Ni_2P deposited on an amorphous SiO_2 support for HDO was first verified using the model compound, 2-methyltetrahydrofuran (2-MTHF), at the temperature of the pyrolysis oil treatment of 350 ^oC. TheNi_2P/SiO_2 catalyst showed high activity for 2-MTHF hydrodeoxygenation under atmospheric pressure hydrogen with low cracking activity. Pyrolysis and catalytic upgrading were conducted sequentially using a laboratory-scale, two-stage system consisting of a fluidized bed pyrolyzer and a fluidized bed catalytic reactor both operating at0.1 MPa, with a hydrogen partial pressure of 0.06 MPa. The Ni_2P/SiO_2 catalyst is moderately effective in upgrading the biomass pyrolysis vapors and producing a refined bio-oil with decreased oxygen content.

The moderate deoxygenation of the bio-oil is confirmed by elemental analysis and Fourier transform ion cyclotron resonance mass spectrometry (FT-ICR MS) analysis. Gas chromatography–mass spectrometry (GC–MS) analysis showed that the treated bio-oil mainly consisted of phenolic compounds and the MS spectra before and after upgrading suggested that reactions including hydrodeoxygenation, hydrogenation, decarbonylation, and hydrolysis occurred during the upgrading.

Furthermore, Ni_2P supported on ZSM-5 zeolite eliminated oxygen in the bio-oil with smaller reduction in the oil yield than Ni_2P supported on SiO_2. The deoxygenation activity of the nickel phosphide catalysts is higher than that of conventional catalysts such as Ni/SiO_2, Pd/C and an FCC catalyst[108].

Micro algae are promising attractive energy carriers. Their biomass productivity is 5-30 times higher than that of first and second generation biomass. Additionally, they utilize CO_2 for

their photosynthetic process thereby protects possibly the environment and contributes towards CO_2 remediation at higher rates. Their cultivation can be combined with wastewater and industrial effluents which consequently leads to the bioremediation of inorganic elements more effectively. Among the conversion technologies for the biofuels production from the micro algal biomass, thermochemical conversion is an enduring sustainable alternative path in the view of engineering as this process utilizes all kinds of the biochemical moieties from the micro algal biomass cellular constitution.

This article reviews the bio moieties of micro algal biomass, and subsequent use of them in thermochemical liquefaction (TCL) technologies like pyrolysis and hydrothermal liquefaction (HTL) for the extraction of liquid fuels and upgrading of bio-oil processes via decarbonylation, decarboxylation (DCO) and hydrogenation for palmitic/oleic using suitable catalysts viz activated carbon with noble metals & cost-effective tungsten based catalysts. These two technically feasible processes in an appropriate technical downstream path are dependent on the oil upgrading process. Moreover, a comparative study of pyrolysis and HTL processes has been evaluated towards the challenges and opportunities of a commercial-scale microalgae-to-fuels process in the consideration for mitigating technical, environmental, and logistical concern[103].

Upgrading of bio-oil from biomass pyrolysis over Cu-modified β-zeolite catalyst in a down-draft fixed-bed reactor, in which the pyrolysis and upgrading processes are integrated, is investigated in details. It is found that high silica β-zeolite has high selectivity to the hydrocarbon during the upgrading process. When it is modified by a small amount of Cu, the selectivity can be obviously promoted. Especially, when 0.50 wt% of Cu is loaded on it, almost only hydrocarbons can be detected in the light oil of upgraded bio-oil and its activity can be remained for several reuses even without regeneration treatment. However, if more Cu is loaded, the selectivity

decreases to some extent. Interestingly, low Cu loading on β-zeolite results in the increase of surface area as well as the formation of more micropores. The surface area reaches the maximum in the case of 0.50 wt% of Cu doping. Based on XRD analysis, when the loading amount is over 1.00 wt%, Cu species aggregate on the surface of zeolite, resulting the blockage of zeolite pores and the decrease of surface area. Doping of Cu decreases the coke deposit on spent catalyst but overloading of Cu results in the increase of coking and the decrease of activity and selectivity. These results indicate that the synergetic effect between the doped metal sites and the protonic sites on the zeolite structure should be benefit for the promising catalytic performance and thus, a proper loading amount is very important for this kind of catalyst[104.]

Due to the negative effects of acids and aldehydes, crude bio-oil has to be upgraded before its application as a high-graded fuel. A novel method for bio-oil upgrading by simultaneous catalytic esterification and alkylation with azeotropic water removal using n-butanol and 2-methylfuran is investigated. Under the optimum upgrading conditions, water content is evidently decreased from27.82% to 3.21%, and acid number is reduced from 41.12 mg NaOH/g to 6.17 mg NaOH/g. High heating value of upgraded bio-oil is more than 2 times higher than crude bio-oil and the other properties are also improved significantly. GC-MS analysis indicated that labile acids, aldehydes, ketones and lower alcohols are transformed to stable target products.

The introduction of 2-methylfuran effectively suppressed acetalization reactions and the yields of more stable alkylation products are higher than acetals. In addition, oxygenated liquid fuel and sugars and their derivatives could be effectively separated from upgraded bio-oil by H_2O/CH_2Cl_2 extraction. The main product in crude sugars part is butyl-β-D-glucopyranoside, which is formed by means of hydrolysis of levoglucosan and the following glycosidation[105,109].

2.4.2. ESTERIFICATION

There are also many drawbacks of bio-oil such as low heating value, high viscosity, high corrosiveness and poor stability, due to the drawbacks of pyrolysis bio-oil, upgrading of bio-oil before the practical application is necessary to acquire high-grade fuel. Organic acids in bio-oil can be converted into their corresponding esters by catalytic esterification and this greatly improves the quality of bio-oil[78].

Upgrading the bio-oil through catalytic esterification has been carried out widely in all over the world. During the etherification process, the experiment was generally conducted in a 250 ml or 300 ml autoclave and the catalysts included ion exchange resins, MoNi/γ-Al_2O_3[79]. The results showed that the upgraded bio-oil had lower acid numbers, watercontents, and viscosities. Meanwhile, stability and corrosion properties of bio-oil were also promoted.

Recently, researchers reported their observations on ozone oxidation of bio-oil and production of upgraded bio-oil using subsequent esterification where they found good results of upgrading bio-oil. In 2009 developed a simple reactive condensation technique to decrease the concentration of reactive species in the oily phase of two-phase pyrolysis oil as a means to increase the storage stability, heating value, and overall quality of the bio-oil.

Bio-oil vapours were esterified from the reaction of in situ organic acids with ethanol during condensation resulting in the production of water and esters[80].

The bio-oil from pyrolysis of biomass cannot be used directly as engine fuel because of its high corrosiveness and instability mainly due to substantial amounts of organic acids and reactive aldehydes. A treatment of acids and aldehydes in the bio-oil is focused on.

A novel upgrading method named one-step hydrogenation−esterification (OHE) is established to convert acids and aldehydes to stable and combustible components. Acetaldehyde (butyl aldehyde) and acetic acid are chosen as model compounds for the OHE reaction over platinum catalysts that acidic supports such as H-ZSM-5 or amorphous aluminum silicate are adopted. The catalysts are bifunctional, which means they have properties of hydrogenation and esterification. Experiments showed this, and it is a feasible route to convert these main unstable components of bio-oil to esters through this simple and effective OHE reaction. The catalysts with high surface area, large pore size distribution, small metal particles and strong acid sites may be beneficial for the OHE reaction[106,108].

The crude bio-oil is upgraded in supercritical ethanol under hydrogen atmosphere by using $Pd/SO_4^{2-}/ZrO_2$/SBA-15 catalyst. This is a novel way to upgrade bio-oil with the combination of hydrotreatment, esterification, and cracking under supercritical conditions. The results indicated that the upgrading process performed effectively and the properties of the upgraded bio-oil were improved significantly. After the upgrading process, a trace amount of tar or coke was produced and most of the organic components were kept in the upgraded bio-oil. No phase separation was observed. The amount of aldehydes and ketones decreased evidently. In particular, aldehydes were almost completely removed. Most acids were converted into corresponding esters, and at the same time many new types of esters were produced. The results of TGA and DTA indicated that macromolecular compounds were decomposed and much more volatile compounds were produced after the upgrading process. The pH value and heating value of the upgraded bio-oil increased; meanwhile, the kinematical viscosity and density decreased compared to those of the crude bio-oil[107].

2.4.3. HYDROGENATION

The ultimate aim of hydrogenation is to improve stability and fuel quality by decreasing the contents of organic acids and aldehydes as well as other reactive compounds, because they not only lead to high corrosiveness and acidity but also set up many obstacles to applications.

Recently many researchers have achieved considerable progress in upgrading pyrolysis bio-oils using hydrogenation technology. Traditionally, researchers generally upgraded bio-oil by single hydrogenation technology[81]. Traditional hydrogenation is the treatment of pyrolysis bio-oil under specific conditions, such as high pressure (10–20 MPa), certain temperature and hydrogen flow rate as well as a proper catalyst.

The bio-oil can be obtained by various kinds of pyrolysis using several catalysts, such as Al_2O_3- based catalysts and Ru/SBA-15 catalysts etc. In the upgrading experiments, the following results generally could be observed, the pH value, the water content as well as the H_2 contents all increased in varying degrees while the dynamic viscosity decreased to some extent. These experiments also simultaneously indicated that the properties of the pyrolysis oil were improved by hydrotreating and esterifying carboxyl groups over these catalysts.

Recently, an over upgrading method named one-step hydrogenation esterification (OHE) was established to convert acids and aldehydes to stable and combustible components. The catalysts for OHE reaction were bifunctional, such as Al-SBA-15 supported palladium bifunctional catalysts and bifunctional Pd catalysts which meanthey have properties of hydrogenation and esterification[82]. This is the advantage over the traditional hydrogenation process for OHE screened out 5% $Pd/Al_2(SiO_3)_3$ with the best catalytic performance among tested bifunctional catalysts, and demonstrated that it is viable to convert these unstable constituents of bio-oil to esters and alcohols through this simple and effective OHE reaction.

Besides, for the OHE reaction, tests. While in 2001 researcher demonstrated the effectiveness of the bifunctional catalyst system for combined hydrogenation/esterification and a synergistic effect between metal sites and acid sites over respective catalyst[83]. Moreover, in2011, some measures were taken to improve the catalytic performance of the bifunctional catalyst and they showed the new hydrogenation method is much better than the traditional method[84].

In 2010 the application of the Shvo catalyst (The Shvo catalyst, named after Youval Shvo, is an organoruthenium compound that is used for transfer hydrogenation) in homogeneous hydrogenation of bio-oil obtained from pyrolysis of white poplar (New mild upgrading conditions) were studied. They focused on the use of the ruthenium based Shvo homogeneous catalyst for the hydrogenation of model mixtures (vanillin, cinnamaldehyde, methylacetophenone, glycolaldehyde, acetol, acetic acid) and of a real bio-oil. They investigated the hydrogenation of model compounds both in mono- and biphasic mixtures under a $P(H_2)$ = 10 atm in the temperature range of 90–145 °C varying the substrate to catalyst molar ratio from 2000:1 to 200:1.

Employing the most active reaction conditions (substrate/catalyst 200:1, T = 145 °C, $P(H_2)$ = 10 atm) the Shvo catalyst maintains its performances under acidic "bio-oil conditions" leading to the almost quantitative conversion of the polar double bonds within 1 h. They also investigated the activity of the Shvo catalyst for the hydrogenation of a bio-oil. They noticed that hydrogenation deeply changed the chemical nature of the pyrolysis oil. Aldehydes, ketones and non-aromatic double bonds were almost totally hydrogenated. The catalytic system also promoted the hydrolysis of sugar oligomers into monomers[85].

In 2008, a catalytic hydroprocessing of chemical models for bio-oil presented. They reported that bio-oil (product liquids from pyrolysis of biomass) is a complex mixture of oxygenates

derived from the thermal breakdown of the biopolymers in biomass. In the case of lignocellulosic biomass, the structures of three major components, cellulose, hemicellulose and lignin, are well-represented by the bio-oil components.

To study the chemical mechanisms of catalytic hydroprocessing of bio-oil, three model compounds were chosen to represent those components. Guaiacol represents the large number of mono- and dimethoxy phenols found in bio-oil derived from soft- or hardwood, respectively. Furfural represents a major pyrolysis product group from cellulosics. Acetic acid is a major product from biomass pyrolysis, derived from the hemicellulose, which has important impacts on the further processing of the bio-oil because of its acidic character[86].

The liquid phase upgrading of a model bio-oil over a series of supported Pt catalysts were studied. Pt/Al_2O_3 showed the highest activity for deoxygenation, the oxygen content of the model oil decreasing from an initial value of 41 wt% to 28 wt% after upgrading.

GC–MS analysis of the oil showed it to be highly aromatic, the major components corresponding to alkyl-substituted benzenes and cyclohexanes. CO_2 was formed as the major gaseous product, together with lower yields of H_2 and C_1–C_6 hydrocarbons. Based on the product distribution, they proposed a reaction scheme in which light oxygenates predominantly undergo reforming to CO_2 and H_2, with C–O bond breaking/hydrogenation (to afford alkanes) as a minor pathway. In a parallel process, aromatics undergo C–O cleavage/hydrogenation, affording benzenes and cyclohexanes. The highly alkylated nature of the products appears to be a consequence of the acidic nature of the reaction medium, favoring the occurrence of aromatic electrophilic substitution reactions[87].

2.4.4. HYDRODEOXYGENATION

Hydrodeoxygenation (HDO) is a bio-oil upgrading process which removes the oxygen under high pressure of hydrogen with a catalyst. It can reduce the oxygen content of many kinds of oxygenated chemical groups, such as acids, aldehydes, esters, ketones, and phenols, etc. Hydrodeoxygenation has been considered to be one of the most promising methods for bio-oil upgrading. Recently, a 500 ml autoclave reactor with a diameter of 10 mm and length of 420 mm is the largest experimental facility for hydrodeoxygenation. Additionally, the largest dosage of the catalyst for this kind of research is 1.5 g.

Most of the previous researches on hydrodeoxygenation of bio-oil focused on industrial NiMo or CoMo sulfide/supported hydrotreating catalysts[87]. For instance, it is demonstrated that Pt supported on mesoporous ZSM-5 showed better performance than Pt/ZSM-5 and Pt/Al_2O_3 in dibenzofuran hydrodeoxygenation. However, it was reported that these catalysts have several inherent shortcomings in hydrodeoxygenation, such as production contamination and catalyst deactivation. The noble metal catalyst exhibits high catalytic activity in the HDO reactions but with a high cost. So, novel and economical catalysts that can be used for hydrodeoxygenation of bio-oil with high oxygen content should be developed[88].

An idealized reaction is,

cyclohexa-1,3,5-triene-1,2-diol + H_2 → Hexane + water

$C_6H_5O_2 + H_2 \rightarrow C_6H_6 + H_2O$

2.4.5. HYDRODESULFURIZATION (HDS)

Hydrodesulfurization (HDS) is a catalytic chemical process widely used to remove sulfur (S) from natural gas and from refined petroleum products such as gasoline or petrol, diesel fuels,

kerosene, jet fuels and Bio-oil. The purpose of removing the sulfur and creating products such as ultra-low sulfur diesel is to reduce the sulfur dioxide (SO_2) emissions that result from using those fuels in automotive vehicles, aircraft, railroad locomotives, ships, gas or oil burning power plants, residential and industrial furnaces and other forms of fuels combustions, e.g.

Ethanethiol + Hydrogen → Ethane + Hydrogen sulfide

$C_2H_5SH + H_2 \rightarrow C_2H_6 + H_2S$

2.4.6. HYDRODENITROGENATION (HDN)

The hydrogenolysis reaction is also used to reduce the nitrogen content of a fuel stream in a process referred to as hydrodenitrogenation (HDN). The process flow is the same as that for an HDS unit. Using pyridine (C_5H_5N), a nitrogen compound present in bio-oil, as an example, the hydrodenitrogenation reaction has been postulated in 1996, as occurring in three steps below:

Pyridine + Hydrogen→ Piperdine + Hydrogen→ Amylamine + Hydrogen→ Pentane +Ammonia

$$C_5H_5N + 5H_2 \rightarrow C_5H_{11}N + 2H_2 \rightarrow C_5H_{11}NH_2 + H_2 \rightarrow C_5H_{12} + NH_3$$

And the overall reaction may be simply expressed as:

$$C_5H_5N + 5H_2 \rightarrow C_5H_{12} + NH_3$$

Many HDS units for desulfurizing naphthas within petroleum refineries are actually simultaneously denitrogenating to some extent as well.

2.4.7. SATURATION OF OLEFINS

The hydrogenolysis reaction may also be used to saturate or convert olefins into paraffin. The process used is the same as for an HDS unit. As an example, the saturation of the olefin pentene can be simply expressed as:

$C_5H_{10} + H_2 \rightarrow C_5H_{12}$

or

$C_4H_6 + H_2 \rightarrow C_4H_8 + H_2 \rightarrow C_4H_{10}$

2.4.8. SUPERCRITICAL FLUIDS (SCFs)

Recently, a new method for upgrading bio-oil from pyrolysis using supercritical fluids (SCFs) has drawn a great attention in all over the world. This method takes full advantage of the unique and superior properties of supercritical reaction media, such as liquid-like density, faster rates of mass and heat transfer, dissolving power and gas-like diffusivity and viscosity.

They also reported that SCFs can be not only used as a reaction condition to produce bio-oils, but also can be used as a superior medium to upgrade bio-oil, and have shown great potential for producing bio-oils with much lower viscosity and higher caloric values. In order to enhance the oil yields and qualities, some organic solvents, such as ethanol, methanol, water and CO_2 etc. were adopted in many relative researches.

Usually, the upgrading method using SCFs performed effectively in improving the quality and yield with the help of some catalysts, such as aluminum silicate and H-ZSM-5[89]. The upgrading experiments were mainly performed in the autoclave reactor, with a volume of 100 ml or 150 ml. After upgrading, the components of the bio-oil were optimized significantly and the properties of the bio-oil were improved greatly. The catalysts in supercritical media can facilitate the conversion of most acids into various kinds of esters in the upgrading process. As a result, kinematic viscosity and the density of upgraded bio-oil decreased compared to that of crude bio-oil, while the heating value and pH value of upgraded bio-oil increased to a certain degree[90].

2.4.9. STEAM REFORMING

The steam reforming is also an effective method to upgrade pyrolysis oil or bio-oil. It could simultaneously produce renewable and clear gaseous hydrogen along with bio-oil upgrading, which was a big advantage for steam reforming among various upgrading technologies. Steam reforming generally used a fluidized bed reactor system or a fixed bed reactor system. In the steam reforming process, high temperature (800 – 900 ^{o}C) and proper catalysts were generally necessary. However, coke formation caused catalyst deactivation, which was a big problem in steam reforming of the bio-oil for sustainable hydrogen production[91]. Carbon deposition behavior in the steam reforming process of bio-oil for hydrogen production and demonstrated that for the competition of carbon deposition and carbon elimination, a peak value of coking formation rate was obtained in a broad range of temperature (575 – 900 ^{o}C), while high ratio of steam to carbon contributed to the carbon elimination. Also, regenerated catalyst showed slight drops in activity due to Fe contamination and Ni redispersion. Above all, upgrading bio-oil methods were feasible but more appropriate catalysts and dependable and fully developed reactor systems still, need to be developed in the future for maximum product yields and a maximum number of hydrocarbons in bio-oil[92].

The use of noble metal-based catalysts for the steam reforming of a few model compounds and that of an actual bio-oil were studied and he steam reforming of the model compounds was investigated in the temperature range 650 – 950 °C over Pt, Pd and Rh supported on alumina and a ceria–zirconia sample. The model compounds used were acetic acid, phenol, acetone and ethanol.

The nature of the support appeared to play a significant role in the activity of these catalysts. The use of ceria–zirconia, a redox mixed oxide, lead to higher H_2 yields as compared to

the case of the alumina-supported catalysts. They noticed that the supported Rh and Pt catalysts were the most active for the steam reforming of these compounds, while Pd-based catalysts poorly performed. The activity of the promising Pt and Rh catalysts was also investigated for the steam reforming of bio-oil obtained from beech wood pyrolysis[93].

Catalytic steam reforming of condensable vapours of bio-oil derived from pyrolysis of biomass is a technically viable process for hydrogen production. In their study, the aqueous fraction of bio-oil, generated from pyrolysis, was catalytically steam reformed at 825 ºC and 875 °C and low residence time (26 ms). They used a fixed-bed micro-reactor interfaced with a molecular beam mass spectrometer (MBMS), a variety of research and commercial nickel-based catalysts were tested. They used Magnesium and Lanthanum as support modifiers to enhance steam adsorption while Cobalt and Chromium additives were applied to reduce coke formation reactions.

The cobalt-promoted nickel and chromium-promoted nickel supported on $MgO\text{-}La_2O_3\text{-}\alpha\text{-}Al_2O_3$ catalysts showed the best results in the laboratory tests. At the reaction conditions, progressive catalyst deactivation was observed leading to a decrease in the yields of hydrogen and carbon dioxide and an increase in carbon monoxide. The loss of activity also resulted in the formation of higher amounts of methane, benzene and other aromatic compounds[94].

Commercial catalysts that were developed for steam reforming of natural gas and crude oil fractions proved to be more efficient for hydrogen production from bio-oil than most of the research catalysts mainly due to the higher water–gas shift activity[95]. Hydrogen and synthesis gas can be produced in an environmentally friendly and sustainable way through steam reforming of bio-oil and the state-of-the-art of steam reforming of bio-oil and model compounds presented and

reported that several catalytic systems with Ni, Ru, or Rh can achieve good performance with respect to initial conversion and yield of hydrogen[96].

2.5. PHYSICO-CHEMICAL PROPERTIES OF BIO-OIL

2.5.1. HOMOGENEITY OF BIO-OIL

Bio-oil is not considered to be homogeneous single-phase liquids. There are a number of reasons why two or more phases might be gone through during product recovery, handling or storage. If ignored, this phenomenon may cause serious problems in combustion applications. Especially due to water and other immiscible species, bio-oil shows many layers after pyrolysis but these immiscible species can be removed from bio-oil applying various methods, like water can be removedthrough the simple separatory flask. While for other immiscible species have other techniques[97].

2.5.2. SOLUBILITY OF BIO-OIL

Bio-oil is a polar mixture of different compounds and the solubility of bio-oil in organic solvents is affected by the degree of polarity. Proper and good solvents for polar bio-oil are methanol, ethanol and acetone etc. These solvents dissolve practically all the bio-oil and some extractives. However polar bio-oil does not dissolve in hydrocarbons such as hexane, diesel fuels or polyolefins but after hydrogenation, the high molecular weight polar compounds, nitrogenated and oxygenated species get convert into low molecular weight hydrocarbons.

2.5.3. ACIDITY OF BIO-OIL

There are no strong acids, like hydrochloric acid (HCl) or sulfuric acid (H_2SO_4) in wood pyrolysis oil but still, this bio-oil contains some acids like acetic and formic acid. However,

phenolic compounds also increase the acidity of this bio-oil and this acidity can be determined as pH.

2.5.4. STABILITY OF BIO-OIL

Stability is the main factor in fuels. However, bio-oil is thermally and chemically unstable or less stable than conventional petroleum fuels because of its high content of reactive nitrogen and oxygen-containing species that's why few hours after distillation it changes its color, which means that bio-oil is also highly reactive to oxygen present in the air. But by using a little amount of hydroquinone we can stop or reduce this phenomenon or we should store bio-oil at a very low temperature like 0 to -5 ^{o}C to reduce its reactivity[98].

2.6. FORMULATIONOF BIO-OIL

Bio-oil is very viscous, highly acidic and does not ignite easily as it contains a substantial amount of structural water. To circumvent these problems pyrolytic bio-oil was formulated with petroleum fuel.

The fuel properties such as heating values, cetane number, viscosity and corrosivity were characterized and the heating value of centrifuged bio-oil was about one third of that of diesel, reducing the heating values of formulation accordingly. Formulation viscosities, particularly in the 10 – 20% bio-oil concentration range, are substantially lower than the viscosity of bio-oil itself, making these products very easy to handle[99]. In order to promote the application of bio-oil as a combustion fuel, formulation was performed as a feasible method to upgrade the bio-oil. They demonstrated that formulation was a cheaper and convenient method for utilization of bio-oil.

Without any surfactants, pyrolysis oils can be formulated with diesel fuels. The bio-oil formulations fuels using bio-oil and 0# diesel by power ultrasound. The effects of treating time and ultrasound power on the stability of the emulsion fuels were studied. The results indicated that the formulations fuels with a stable time as long as 35 h could be obtained under ultrasound power of 80 W with a treating time of 3 minutes [22].

The combustion characteristics of a blended fuel of bio-oil and diesel with different proportion of the two fuels using a numerical simulation method were investigated. The factors, such as combustion components distribution, ignition delay, and temperature distribution in the combustor were studied.

The lubricity of the bio-oil/diesel fuel using a High-Frequency Reciprocating Test Rig (HFRR) also studied. It is found that the lubrication ability of the bio-oil/diesel fuel was better compared with the conventional diesel fuel (number zero). The bio-oil formulations with different percentages of diesel oil were conducted and evaluated the lubrication properties of oil samples using a four-ball tester. It is found that several properties, such as friction-reduction, anti-wear, and extreme pressure were better. The difference was likely to be caused by the use of the different device in their experiments. Meanwhile, increasing content of the bio-oil in the formulations could promote the lubrication ability of the formulation. Moreover, the solid char particles in the pyrolysis bio-oil could enhance its lubrication performance.

An attempt was made in 2011, to use modified bio oil blended with diesel fuel in a single cylinder, four stroke, air cooled, DI diesel engine. The performance and exhaust emissions such as unburned hydrocarbons [UBHC], carbon monoxide [CO], carbon-di-oxide [CO_2] and nitric oxide [NO] were measured from the diesel engine at different power outputs. The performance and exhaust emissions were studied from the engine with three different pyrolysis oil based fuels

such as pyrolysis oil diesel emulsion, and two pyrolysis oil diesel emulsions with addition of 2% and 4% diethylether. The results were compared with the diesel fuel data analyse. It is observed from the results that there was an increase in the brake thermal efficiency. The NO and HC emissions were lower with only pyrolysis oil diesel emulsion. For the other formulations the HC and NO emissions were higher than diesel fuel operation[100].

The effect of biomass pyrolysis oil on the formulation of diesel fuels was studied. It was analyzed that parameters like, ignition delay time, emission of particulate matter and unburned hydrocarbons, and specific fuel consumption. The fraction of pyrolysis oil used as fuel was obtained by vacuum distillation at 80 − 240 °C. The use of this fraction resulted in a decrease in the ignition delay time in the combustion process, with the resulting increase in the cetane number due to the presence of phenolic groups in the pyrolysis oil, which modify the formation mechanism of peroxyl radicals by altering the temperature of the flame front. Additionally, it was reported that particulate matter emissions are reduced significantly by up to 30% when compared with the base fuel. Their results indicated the promising potential of bio-oil for use in the formulation of diesel fuel, decreasing ignition delay and increasing the cetane number, as well as significantly reducing particulate matter emissions[110].

3. EXPERIMENTAL

3.1: MATERIALS AND METHODS

The bio-oil was obtained by pyrolysis of a mixture of discarded soybean frying oil, CaO (calcium oxide), sand and Eucalyptus sawdust. Sand was used for thermal resistance, soybean oil was used to make a malleable mixture of biomass as well as a high bio-oil yield while CaO was used as a catalyst to increase the bio-oil yield from 48% to 55% (CaO increases the bio-oil yield up to 7%) and also to improve biochar quality. The discarded soybean frying oil was mixed with the Eucalyptus sawdust after their particle size was reduced to 0.21 mm. Sand was added to this mixture to produce a malleable mass that could be moulded into cylindrical samples (50 mm × 180 mm). The samples were allowed to dry at room temperature and many pyrolysis experiments were performed and many attempts were made to obtain a maximum pyrolysis yield by changing the amount of discarded soybean frying oil, sand and CaO in the mixture. Sawdust, CaO and sand were mixed to discarded soybean frying oil with different ratios and mixed well before pyrolysis. After preparation, the mixture was subjected to pyrolysis where the temperature of the pyrolysis system was changed in every experiment to discover a proper temperature for a maximum pyrolysis yield. The flow of hydrogen gas was kept 100 mL min^{-1}.

In all experiments, CaO was mixed to discarded soybean frying oil with different ratios (by mass) before pyrolysis and then Eucalyptus sawdust was added to the same mixture and sand was also added to those mixtures by different ratios and mixed well. The pyrolysis temperature was initiated at 25^{0}C in all experiments and then increased up to 600 ^{0}C, 700 ^{o}C, 850 ^{o}C and 900 ^{o}C at different heating rates of 10 ^{0}C min^{-1}, 15 ^{0}C min^{-1} and 20 ^{0}C min^{-1}. The pyrolysis yields in all experiments are given below in **Table I**.

Table I. Changes in the pyrolysis yields at different temperatures

N^{O}	Weight of the sample (grams)	Temperature (^{0}C)	Bio-oil (%)	Uncondensable Gas (%)	Residues (%)	Water fraction (%)
1	300	600	30	27	25	11
2	300	700	36	35	24	10
3	300	850	55	17	20	10
4	300	900	42	37	23	9

In the first pyrolysis experiment, CaO was mixed to discarded soybean frying oil 10% and 30% (by mass) respectively before pyrolysis and 50% Eucalyptus sawdust (by mass) was added to the same mixture and 10% sand was also added to this mixture and mixed well. The pyrolysis temperature was initiated at 25 ^{0}C and increased up to 600 ^{0}C at a heating rate of 10 ^{0}C min^{-1} where the pyrolysis yield was only 30%, which was not a good yield, and we also observed a blockage of the system at such a low temperature and slow heating rate, therefore the temperature, heating rate, catalyst, and biomass ratios were changed in next pyrolysis experiment.

In the second case CaO was mixed to discarded soybean frying oil 15% and 25% (by mass) respectively before pyrolysis and 50% Eucalyptus sawdust was added to the same mixture and 10% sand was also added to this mixture and mixed well. In this case, the pyrolysis temperature was initiated at 25 ^{0}C and increased up to 700 ^{0}C at a heating rate of 15 ^{0}C min^{-1}. In this pyrolysis experiment, the pyrolysis yield was only 36%, and there was also an abundance of

incondensible gases and residues, which was also not a good yield, therefore, the temperature, heating rate, biomass, and catalyst amount, were changed in the third experiment.

In the third pyrolysis experiment, CaO was mixed to discarded soybean frying oil 25% and 25% (by mass) respectively before pyrolysis and 50% Eucalyptus sawdust was added to the same mixture and 5% sand was also added to this mixture and mixed well. In this case, the pyrolysis temperature was initiated at 25 ^{0}C and increased up to 850 ^{0}C at a heating rate of 20 ^{0}C min^{-1} where the pyrolysis yield was 55% and there was a little appearance of incondensable gases and residues. Although 55% bio-oil yield is enough in the case of wood pyrolysis, anyhow, another pyrolysis experiment was done comparatively at a high temperature and different biomass and catalyst ratios only for the sake curiosity.

In the fourth pyrolysis experiment CaO was mixed to discarded soybean frying oil 20% and 20% (by mass) respectively before pyrolysis and 50% Eucalyptus sawdust was added to the same mixture by and 10% sand was also added to this mixture and mixed well. In this case, the pyrolysis temperature was kept at 25 ^{0}C and increased up to 900 ^{0}C at a heating rate of 25 ^{0}C min^{-1} where the pyrolysis yield was only 42% and there was a high appearance of incondensable gases and blockage of the system were observed due to high temperature and high heating rate. Therefore, we concluded that at a very low or very high temperature the blockage of the system occurs and the third pyrolysis experiment was considered as best one, where the bio-oil yield was 55%.

3.2. PRODUCTION OF LFP AND HFP

The biomass sample was kept inside a stainless steel reactor of pyrolysis system which was connected to two condensers as shown in **Figure 1**. The temperature of the reactor which had biomass was increased from 25 ºC to 850 ºC with the help of electric heater and temperature controller cabinet. In this system, biomass was converted to biogas and the biogas was condensed to bio-oil. The condensed bio-oil fractions were collected from both condensers, the water contents were removed by simple separatory flask and subjected to atmospheric distillation, where two fractions were obtained at the temperature range of 80−160 ºC (LFP) and 160−240 ºC (HFP). These two fractions were subjected to hydrogenation after TGA, GC-MS, NMR and FTIR analysis.

3.3. PRODUCTION OF LFH AND HFH

Hydrogenation was performed for the LFP and HFP in the presence of NiMo as a catalyst. NiMo was used as a catalyst because it is easily available and more suitable and productive for hydrogenation of bio-oil as compared to other catalysts like cobalt-molybdenum and nickel phosphide ect.[25] During hydrogenation, relatively lower temperature and pumping pressure were used as compare to pyrolysis. After hydrogenation, more two fractions were separated at the same range of temperature 80−160 ºC (LFH) and 160−240 ºC (HFH) through atmospheric distillation. Both fractions were subjected to TGA, GC/MS, NMR and FTIR analysis. Other important analyses like density, viscosity, flash point, freezing point and enthalpy of combustion were also performed and compared with aviation and diesel fuels.

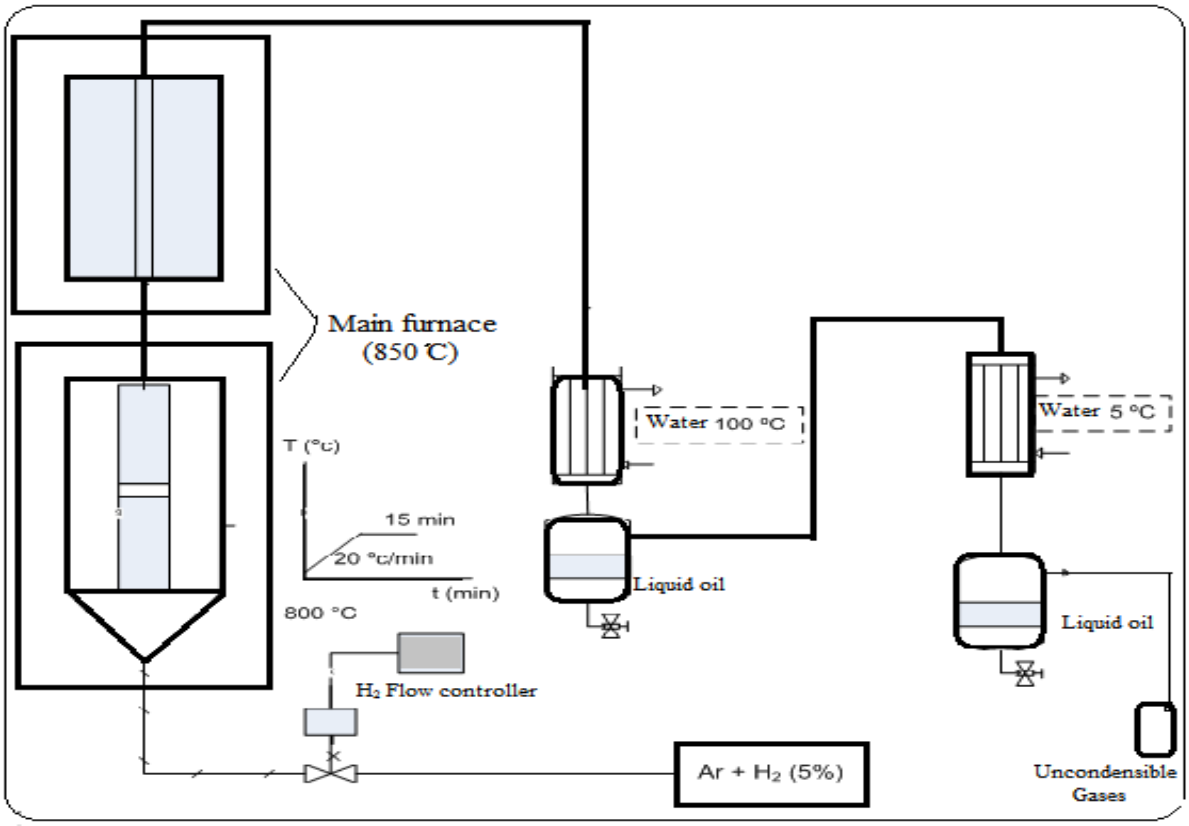

Figure 1. Schematic diagram of biomass pyrolysis system

3.4. CHARACTERIZATION OF LFP, HFP, LFH, AND HFH

The bio-oil was produced in a fixed bed reactor from a mixture of discarded soybean frying oil, calcium oxide, and Eucalyptus sawdust, applying a heating rate of 20 °C min^{-1} from room temperature to 850 °C. The bio-oil thus produced was separated from the water and fractionated by atmospheric distillation between 80 and 240 °C in two fractions, the LFP and a HFP. Both fractions were subjected to hydrogenation after pyrolysis and fractionated by atmospheric distillation between 80 and 240 °C in two fractions, the LFH and a HFH.

All fractions HFH, LFH, HFP and LFP were characterized by Fourier transform infrared spectroscopy (FTIR), proton nuclear magnetic resonance spectroscopy (^{1}H-NMR), Gas chromatography–mass spectrometry (GC-MS), and Thermal Gravimetric Analysis (TGA). The

infrared spectrums of the both bio-oil fractions were obtained in the form of a film on a potassium bromide (KBr) wafer, using an FTIR spectrophotometer (AIM-8800) in the frequency range of 4000 − 400 cm^{-1}. A nuclear magnetic resonance (NMR) analysis was performed in deuterated chloroform, using a Varian VRMN-300 MHz spectrometer. TGA analysis was performed with gas used ultra-pure Nitrogen 100 mL min^{-1}, a device used was SDT Q600 from TA Instruments, and type of crucible was Alumina.

The bio-oil composition was also determined by gas chromatography with mass spectrometric detection (GC-MS), using a GC Agilent series 6890 with an Agilent mass selective detector of series 5973, a capillary polar wax column, polyethylene glycol (PEG)-coated (length of 30 m, internal diameter of 0.25 mm, and film thickness of 0.25 μm). Chromatographic conditions were: Injection volume of 0.2 μL, oven at 40 °C min^{-1} 6 °C min^{-1} up to 300 °C (10 °C min^{-1}) split mode with a ratio of 100:1 and injection temperature of 290°C. Time taken was 54 minutes, He (helium) as a carrier gas with a flow rate of 2.9 mL min^{-1}. Library Wiley and NIST were used for identification of compounds based on probability score and each compound was detected very clearly and with a high probability value and a mixture of standards of linear hydrocarbons was used to calculate the compound Retention Index.

The bomb calorimeter (VEB Vereinigte Babelsberger App-Nr. 081036) was used to determine the enthalpy of combustion by measuring the temperature variation resulting from the heat transfer caused by the combustion reaction. For this purpose, the bio-oil to be analysed was burned in the presence of excess oxygen in an adiabatic calorimeter. The calorimeter is equipment used to determine the enthalpy of combustion by measuring the temperature variation resulting from the heat transfer caused by the combustion reaction. For this, the samples of bio-oil fractions to be analyzed were burned in the presence of oxygen in an adiabatic calorimeter.

For burning, the samples were placed in a hermetically sealed calorimetric pump and in contact with a conductive wire through which electric current passes which promoted the burning of the sample after the activation of the ignition source. To ensure the material burns, after purging with O_2, the system is subjected to 30 bars of the same gas. The calorimetric pump is submerged in water so that the energy generated during the combustion was transferred to it. In order to minimize thermal losses, the system is enveloped by an air layer that provides insulation, making the system adiabatic. **Figure 2** illustrates this phenomenon.

After assembling the system, in order to optimize the transfer of energy, the agitation is activated. However, it was necessary to check the temperature change due to the transfer of mechanical energy to the system, accompanying the stabilization of the temperature for 5 minutes. After this procedure, ignition is given, which promoted the flow of electric current by the resistance and consequently it's burning. The temperature change is monitored during the next 15 minutes to verify the variation of this as a result of the combustion reaction.

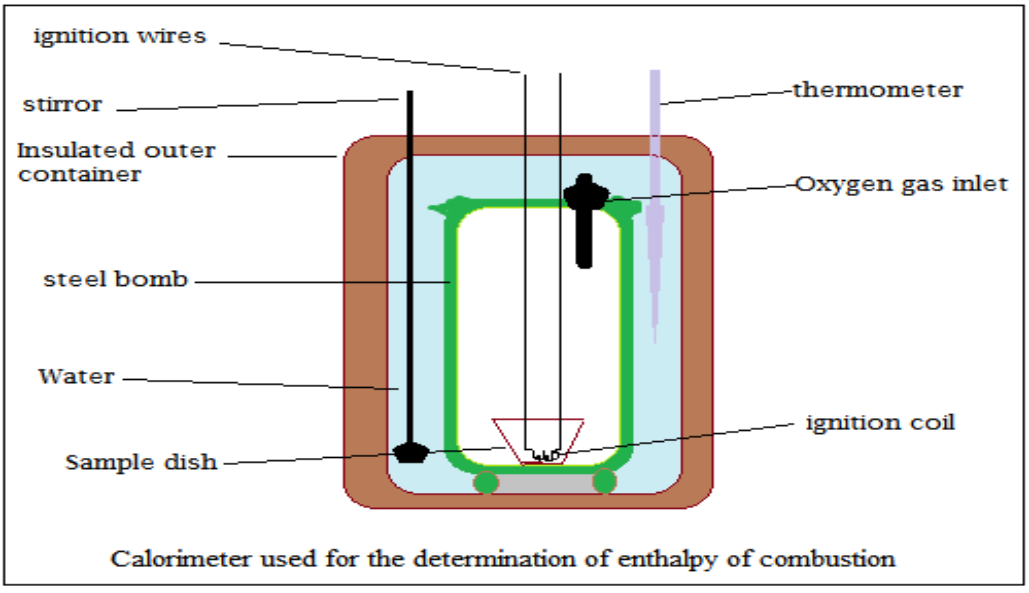

Figure 2. Calorimeter used for the determination of enthalpy of combustion

A simple freezing point determination method and system were used to determine freezing point of bio-oil. Liquid nitrogen is used to determine the freezing point of all samples. A Hofmann bottle, liquid nitrogen, thermocouple, air cylinder and a computer system were connected to determine the freezing point as shown in **Figure 3**. The air was passed from liquid nitrogen to carry and pass liquid nitrogen in the Hofmann bottle which had bio-oil. After passing the liquid N_2 from bio-oil, the air gets eliminate from Hofmann bottle and more cold air (liquid nitrogen) was entering to Hofmann bottle. This cycle was continuous until the temperature reaches to a point where the bio-oil starts freezing because the liquid nitrogen possesses a very low temperature.

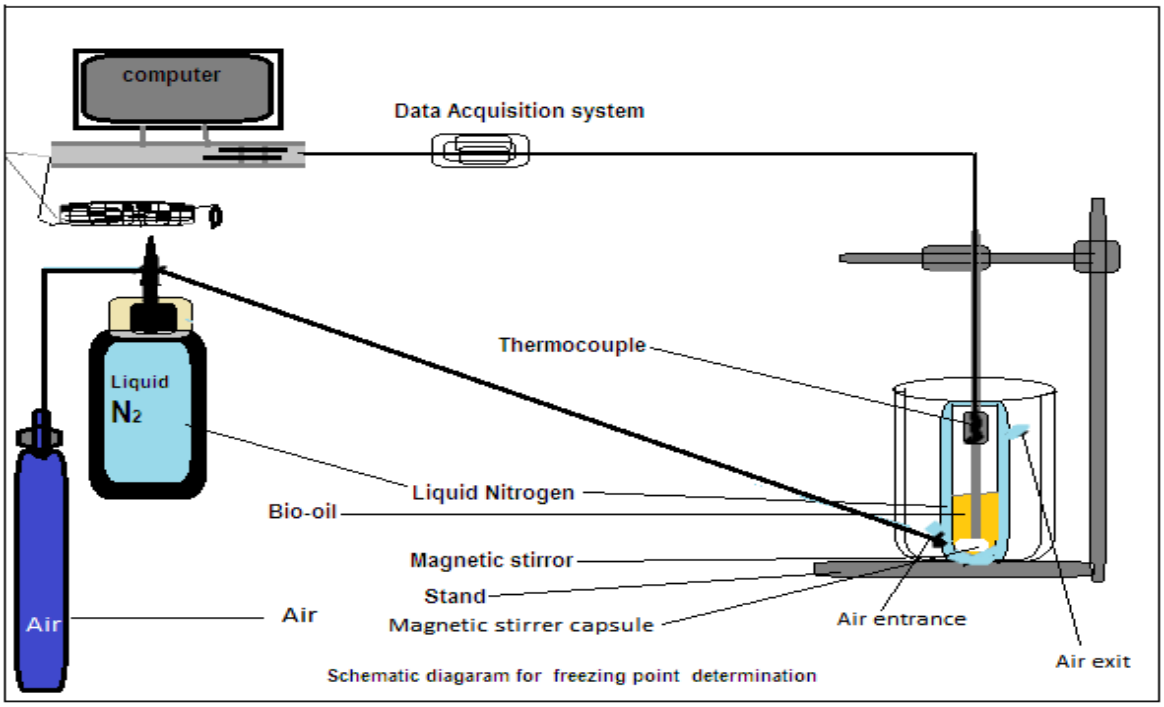

Figure 3. Schematic diagram of freezing point determination system

The flash point of LFP, HFP, LFH, HFH, DF and AF was determined by simple open cup method with the help of a heater, water bath, thermometer, gas ignition flame and a sample in a little bottle, as shown in **Figure 4**. The sample was kept in the bath and the temperature was increased from 25 ^{o}C. At every degree Celsius the flash point was checked by gas ignition flame and here also the same method was repeated three times for each sample. The flash points all fractions were discovered according to standard ASTM D56.

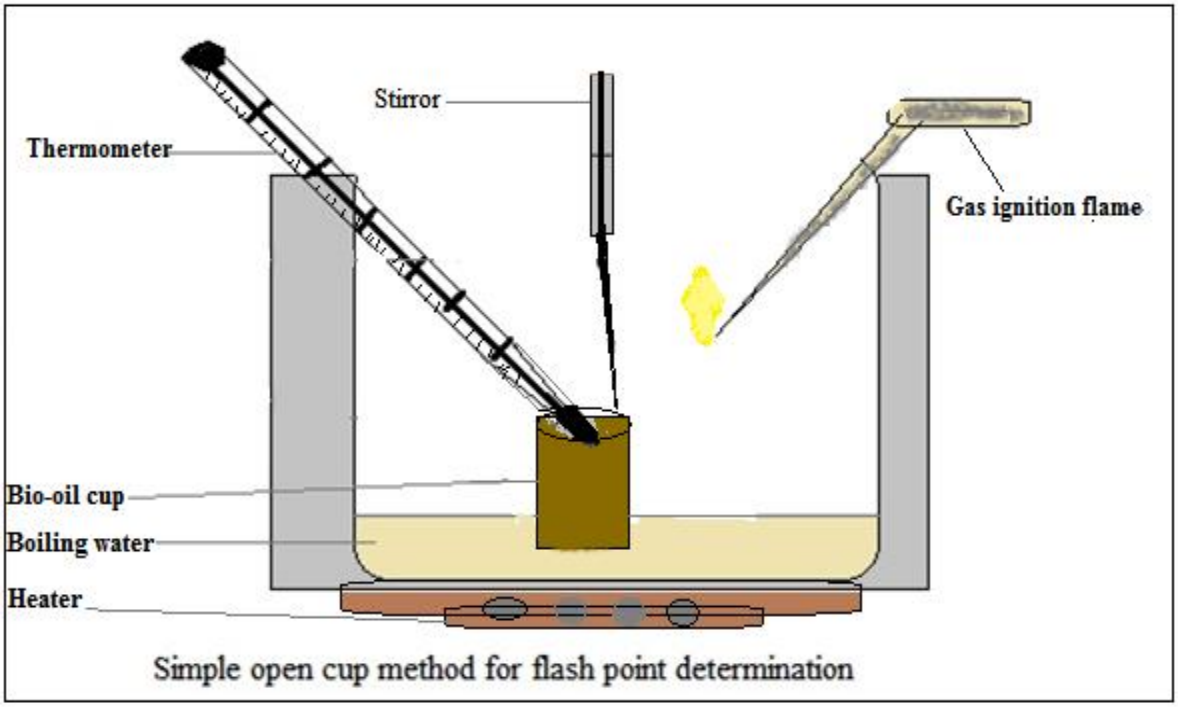

Figure 4. Open cup method diagram for determination of flash point

A simple atmospheric distillation as shown in **Figure 5** was performed with the help of a heater, a distillation flask, a condenser, a cooler, a thermometer and a graduated cylinder to separate the crude bio-oil into two fractions, a light fraction 80−160 ^{o}C and a heavy fraction 160−240 ^{o}C (LFP & HFP) and also to separate hydrogenated bio-oil into two fractions a light

fraction 80−160 °C and a heavy fraction 160−240 °C (LFH & HFH). The 10% and 20% formulations of HFH and LFH with AF and DF were also distillated to obtain their distillation curves. As bio-oil was a mixture of many hundred organic compounds including water, so it was not an easy task to distillate it. Although the water fraction was separated by a simple separatory funnel but there were still some water molecules inside the crude bio-oil as well as in the hydrogenated fractions. Those water molecules were creating problems during distillation. After a long struggle the bio-oil was distillated according to ASTM D86 method and distillation curves were built for all fractions (LFH, HFH and their formulations) and compared with AF and DF.

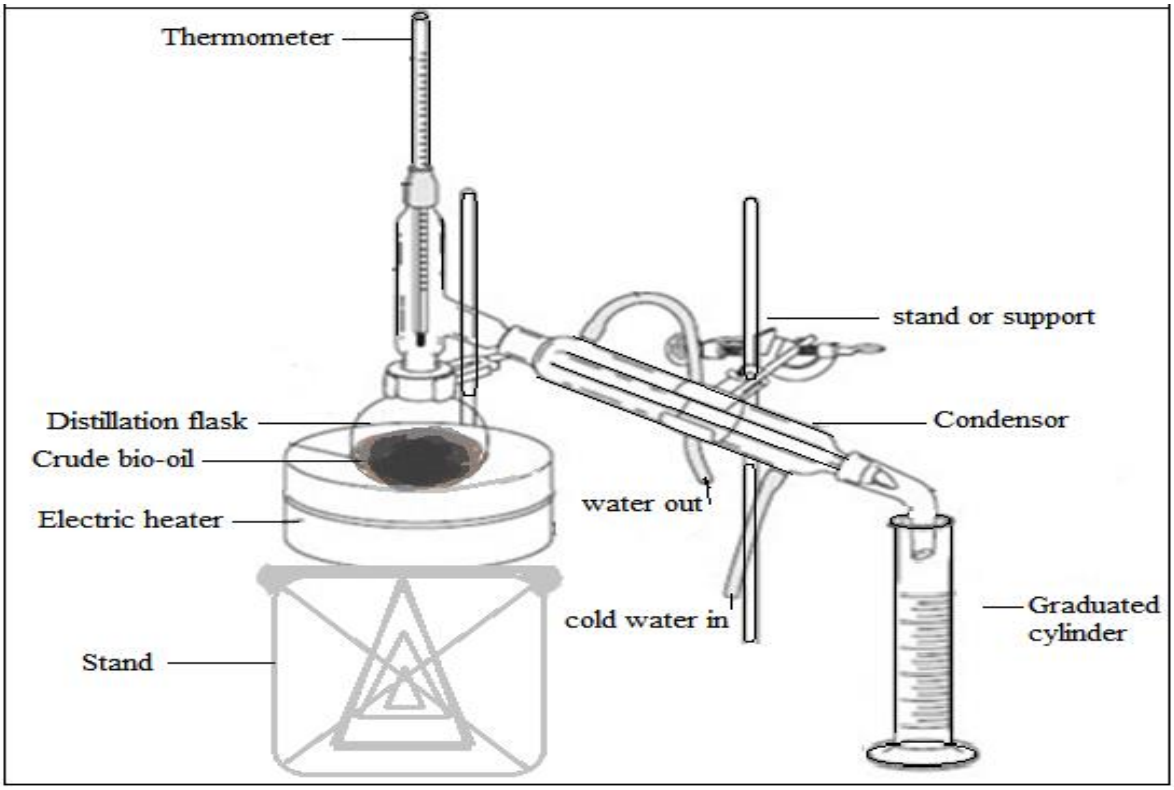

Figure 5. A simple fractional distillation system

Ostwald Viscometer, also known as U-tube viscometer or capillary viscometer as shown in **Figure 6** was used to determine the viscosity of the AF, AD and both bio-oil fractions HFH, LFH and their formulation with AF and DF at different temperatures. A bath having temperatures of -10 to 100 °C was used to determine the viscosity all fraction at different temperatures like -10 ^{o}C to 50 ^{o}C and then it was extrapolated to -20 ^{o}C.

The same bath having temperatures of -10 to 100 °C was used to determine the density all fraction at different temperatures like -10 ^{o}C to 50 ^{o}C and then it was extrapolated to -20 ^{o}C. A simple g/mL method was used to determine the density of bio-oil. A mass (10 gm) of sample was taken in test tube and its volume was checked at various temperatures and then the density was determined by simple formula m/v. The same method was repeated three times for each sample.

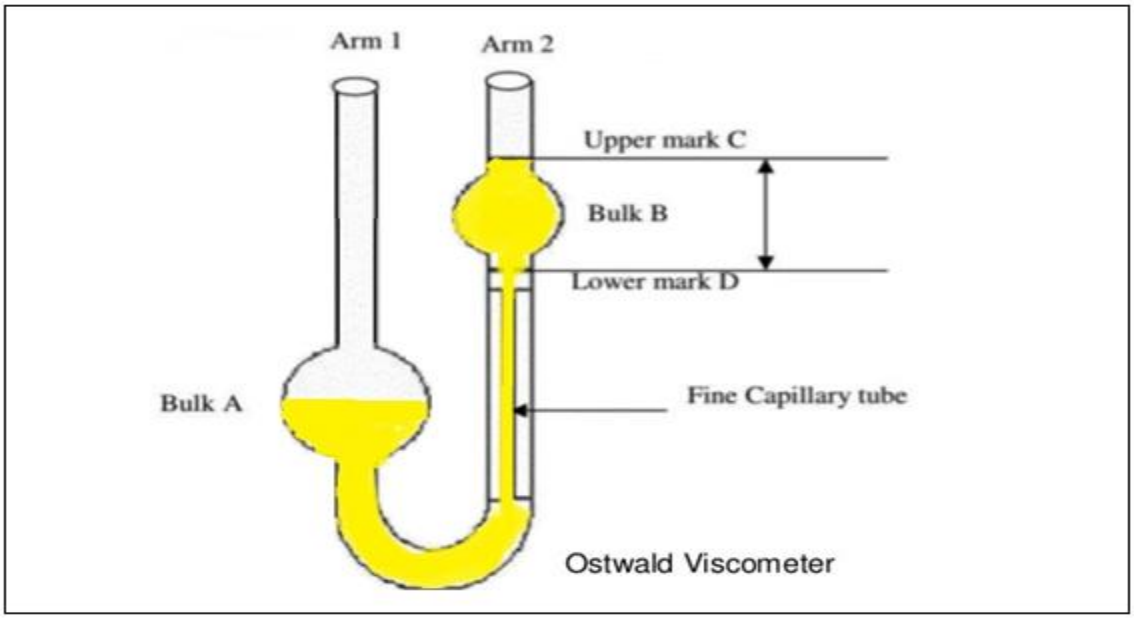

Figure 6. Ostwald Viscometer

4. RESULTS AND DISCUSSIONS

4.1 GC-MS CHARACTERIZATION OF LFP, HFP, LFH AND HFH

All four fractions of bio-oil were analysed by GC-MS (two fractions before hydrogenation LFP and HFP and two fractions after hydrogenation LFH and HFH) and the resulting compounds are given in **ANNEXES 1** and **2**, while the main hydrocarbons of the respective fractions are presented in **ANNEX 3**. A total of 72 peaks (only large peaks were considered) were identified in each fraction considering a minimum signal-to-noise ratio (S/N). The bio-oil composition showed chemical class like alcohols, ketones, ethers, phenols, aromatics and aliphatic hydrocarbons and nitrogen compounds. The sample obtained by pyrolysis before hydrogenation was composed mainly of ketones and nitrogen compounds, with minor amounts of alcohols, ethers, phenols and hydrocarbons. The predominant classes in the samples before hydrogenation were oxygen and nitrogen containing compounds: 30% nitrogen and 45% ketone compounds. The nitrogen compounds in the bio-oil were due discarded soybean frying oil which had proteins after used in restaurants to fry meet or chickens (meet and chickens are sources of proteins and protein contains nitrogen in each amino acid)

4.2. 1H-NMR SPECTRAS OF LFP, HFP, LFH, AND HFH

Figure 7 (a, b, c, d) are representing the ^{1}H-NMR spectrums of HFP, LFP, HFH and LFH respectively. In all cases, the same equipment and conditions were used. As the biomass was a mixture of two products (wood and soybean) so the NMR data of **Figure 7 (a)** and **(b)** showed the presence of (uncertainty $\pm$ 0.2%, according to manufacturer of the equipment) aromatic and vinylic hydrogens, indicated by the signals in the region of 5 to 7.5 ppm, as well as of hydrogens

bound to oxygenated carbons (CH−O) between 5 and 6 ppm and of hydrogens neighboring carbonyl in the region of 1.9 to 2.9 ppm. The intense peaks between 0.7 and 1.5 are typical of aliphatic hydrogens. In the NMR data confirm the presence of many groups by the signals in region 0 to 8 before hydrogenation.

Figure 7 (c) and **(d)** are the ^{1}H-NMR spectrums of the HFH and LFH respectively. According to **Figure 7 (c)** and **(d)** as there were many hydrocarbons in both fractions after hydrogenation that's why both spectrums are showing very few groups where the hydrocarbons are dominant. As the aromatic hydrogens normally have similar chemical shifts and may appear as either a broad singlet or complex multiplet in the region of 7 to 8 ppm in **Figure 7 (c)** and **(d)** after hydrogenation.

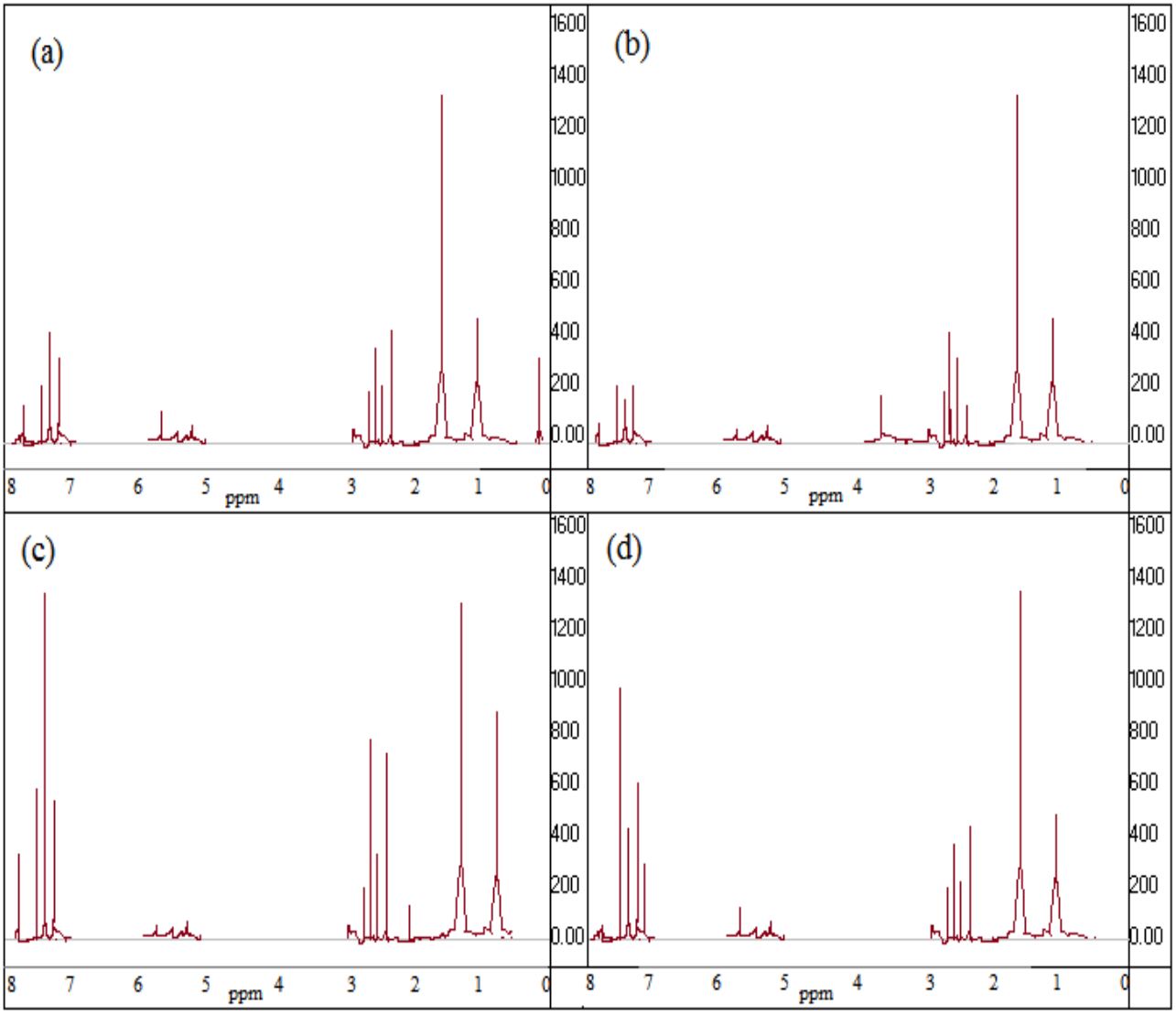

Figure 7. ^{1}H-NMR spectrums of (a) HFP, (b) LFP, (c) HFH and (d) LFH

4.3. FTIR SPECTRAS OF LFP, HFP, LFH, AND HFH

The FTIR spectrums in **Figure 8** (a) and 8 (b) were used to investigate the chemical structure of both HFP and LFP (uncertainty $\pm$ 0.1% according to manufacturer of the equipment). Since the pyrolysis oil obtained from the mixture of soybean oil and Eucalyptus sawdust, the absorption bands at 1592, 1453, 1414, 1376, 1266, 1165, 991, 745 and 695 cm^{-1} are characteristic of lignocellulosic materials and are consistent with the spectrum of wood before hydrogenation.

The absorption bands at around 3000 cm^{-1} are attributed to the symmetric and asymmetric vibration of saturated C-H bonds. The signal at 1704 cm^{-1} is related to the stretching vibration of the C=O bond of compounds derived from the fragmentation of soybean oil triglycerides. The absorption band at 1453 cm^{-1} is associated with the asymmetric deformation of the CH methyl and methoxyl groups, while the broadened band at 3367 cm^{-1} is characteristic of the stretching vibration of the OH bond.

The FTIR spectrums in **Figure 8 (c)** and **Figure 8 (d)** were used to investigate the chemical structure of both HFH and LFH. In **Figure 8 (c)** the absorption bands around 3000 cm^{-1} are attributed to the symmetrical and asymmetrical stretching of the C-H bonds. The peak at 1713 cm^{-1} occurs due to the vibrational stretch of the C=O bond. The absorption bands at 1457 cm^{-1} refer to the asymmetric deformation of CH of the methyl and methoxyl groups. The absorption bands at 1377 and 729 cm^{-1} are characteristic of lignocellulosic materials. In **Figure 8 (d)** also the absorption bands around 3000 cm^{-1} are attributed to the symmetrical and asymmetrical stretching of the C-H bonds. The peak at 1709 cm^{-1} occurs due to the vibrational stretch of the C = O bond. The absorption bands at 1457 cm^{-1} refer to the asymmetric deformation of CH of the methyl and methoxyl groups. The absorption bands at 1377, 909, 782, 728 and 696 cm^{-1} are characteristic of lignocellulosic materials. In **Figure 8 (d)** a double bond of an alkene gives C=C stretching at 1640 cm^{-1} and we can see that a sharp vibration band near 1500 cm^{-1} indicates the presence of a benzene ring.

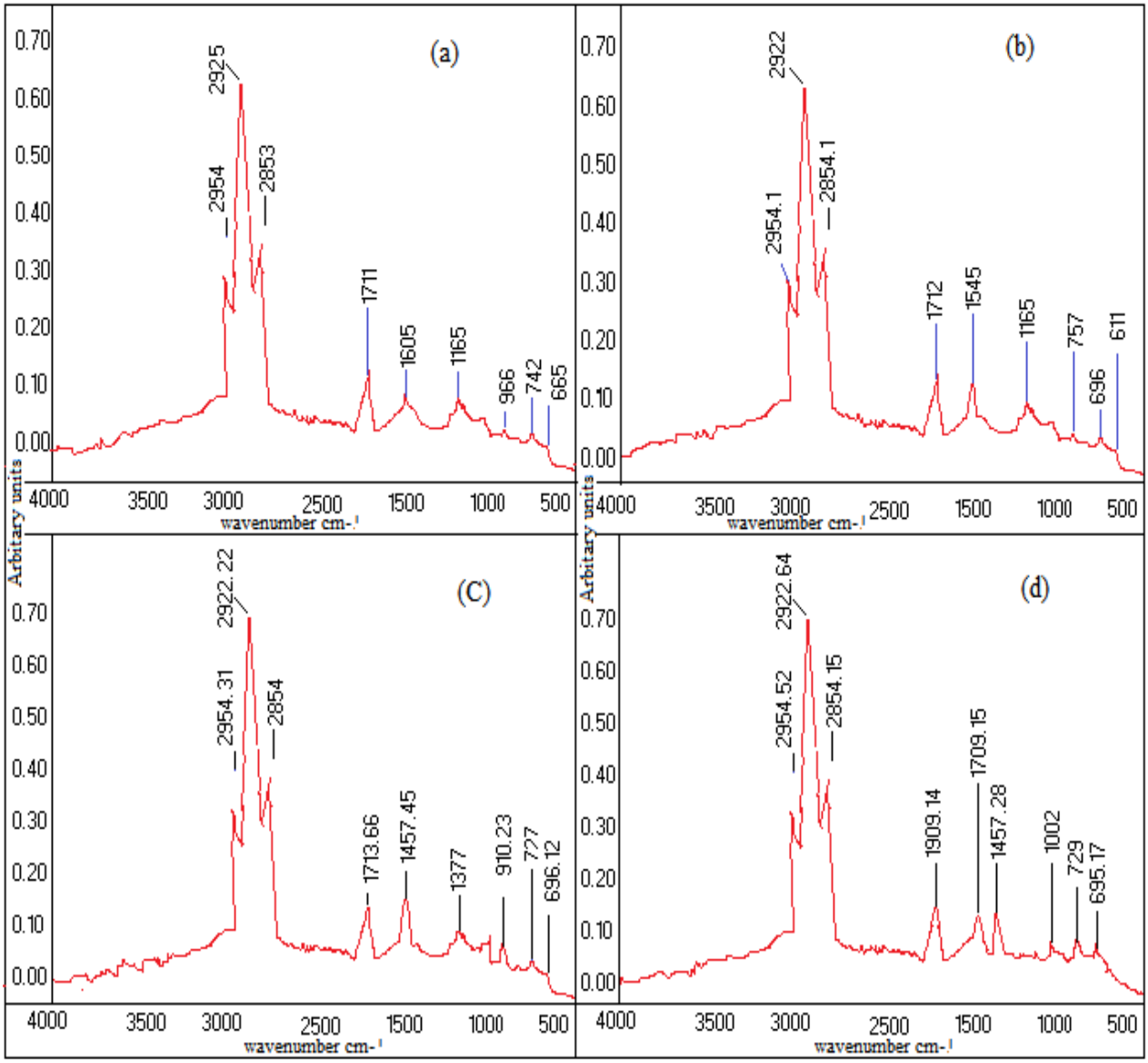

Figure 8. FTIR spectra of (a) HFP, (b) LFP, (c) HFH and (d) LFH

4.4. TGA THERMOGRAMS OF ALL FRACTIONS OF BIO-OIL

Figure 9 (a, b, c, d) are the thermograms of LFP, HFP, LFH and HFH. **Figure 9 (a)** represents the thermogram of the LFP where 96% of the mass is decomposed at temperatures below 150 °C (uncertainty $\pm$ 0.5%, according to manufacturer of the equipment). In this

thermogram also presents a material that does not undergo decomposition at temperatures between 150 and 300 °C and can be attributed to organic substances of high molecular weight (4%). It would not be used as fuel compatible with blends or formulation in petroleum fuels checking compatibility issues, miscibility and the main problem is that its thermal stability is very low and generates waste of 4%. Because after pyrolysis there are many oxygenated and other reactive organic species which boil or ignite very fast but never ignite 100%. That's why they left 4% of residues after ignition. On other hand,

Figure 9 (b) is the thermogram of the HFP. **Figure 9 (b)** shows that most of the mass (95%) is decomposed at temperatures below 150 °C like the LFP. In this thermogram also presents a material that does not undergo decomposition at temperatures between 150 and 300 °C and can be attributed to organic substances of high molecular weight (5%). It would not be used as fuel compatible with blends or formulation in petroleum fuels checking compatibility issues, miscibility and the main problem is that it generates waste or residues of 5%. Because after pyrolysis there are many oxygenated and other reactive organic species which boil or ignite very fast but never ignite 100%. That's why they left 5% of residues after ignition.

Figure 9 (c) is the thermogram of LFH. There was a 100% augmentation or increase in the thermal stability (250−300 ºC) of the sample conferred by the hydrogenation reaction. This increase is evidenced by the total boiling temperature which goes from 250 to 300 °C. Another interesting factor that this graph offers is the low waste or residue content (0.50%). The residues of LFH decreased from 4% to 0.50%, which favors the use of this fuel fraction in mixtures with diesel fuel. After hydrogenation, the analysis of LFH shows that the process residue or waste has a lower value due to the decrease of highly reactive organic compounds and other heavy species that do not ignite 100% as showed in the both fraction before hydrogenation.

In **Figure 9 (d)** is the thermogram of the HFH and there is also almost the same increase in the thermal stability of the sample conferred by the hydrogenation reaction. There was also a 100% augmentation in the thermal stability (250−300 ºC) of the sample conferred by the hydrogenation reaction. This increase is evidenced by the total boiling temperature which increases from 250 to 300 °C. Another interesting factor that this graph offers is the lowest amount of waste or residue contents decreased from 5% to 0.53%, which favors the use of this fuel fraction in mixtures with aviation fuels. The thermograms after hydrogenation show that the process residue has a lower value due to the non-existence of highly reactive organic compounds. Because after hydrogenation, almost all oxygenated, nitrogenated and other reactive species have converted into hydrocarbons or lower molecular weight stable compounds.

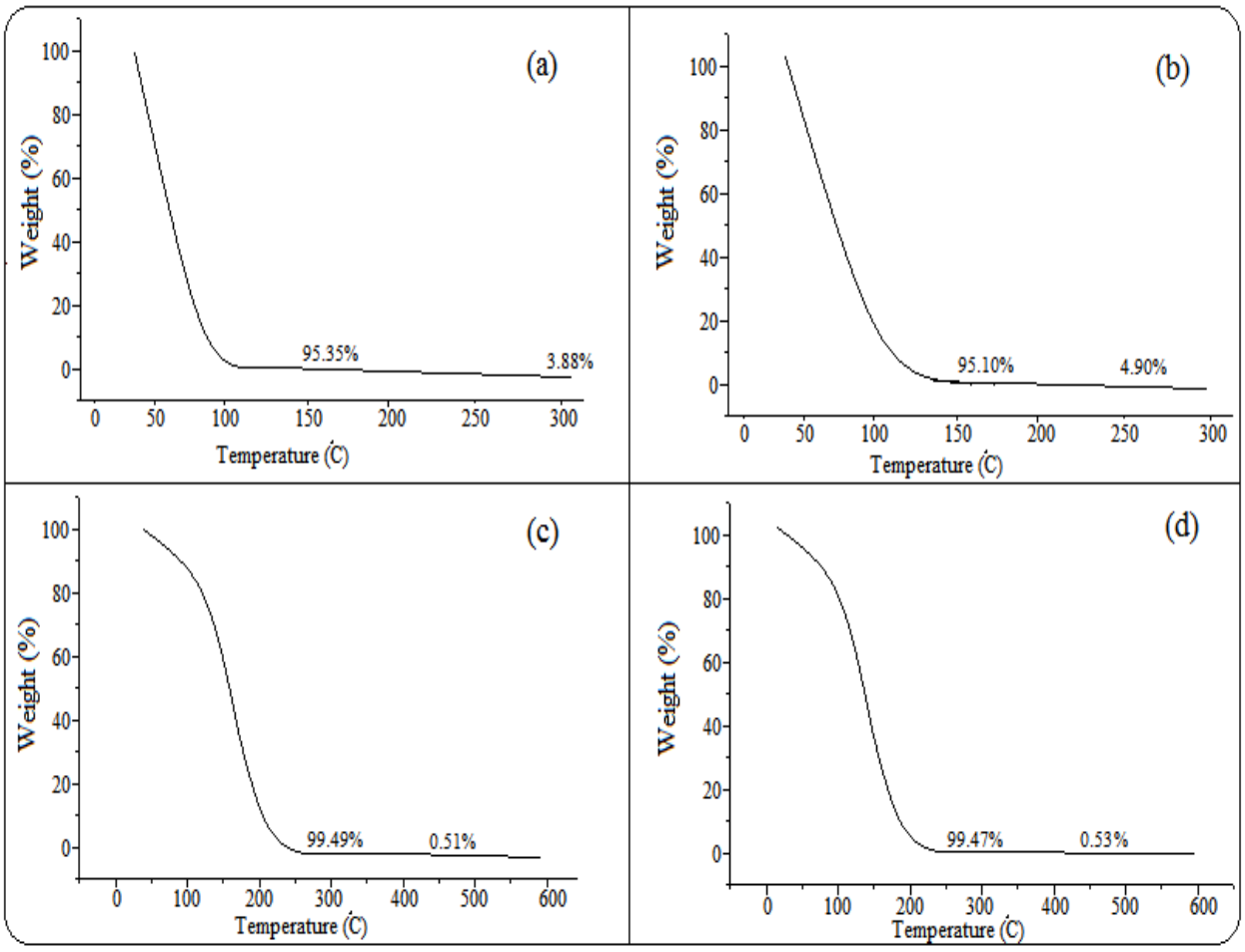

Figure 9. TGA thermograms of (a) HFP, (b) LFP, (c) HFH and (d) LFH

4.5. THE CALORIFIC VALUE OR ENTHALPY OF COMBUSTION AF, DF, LFH AND HFH

The calorific value (enthalpy of combustion or energy value or heating value) of a substance, usually a fuel or food, is the amount of heat released during the complete combustion of a specified amount of it. The calorific value is a characteristic for each substance. It is measured in units of energy per unit of the substance, usually mass, such as: kJ g^{-1}, MJ kg^{-1} kJ mol^{-1}, kcal kg^{-1}. Calorific value is commonly determined by use of a bomb calorimeter.

The calorific values of LFP, HFP, LFH, HFH, DF and AF were checked with help of bomb calorimeter (uncertainty $\pm$ 0.1% according to manufacturer of the equipment) in laboratory and compared with to standard ASTM values of DF and AF. The calorific values of the LFP and HFP were 36.50 MJ kg^{-1} and 37.10 MJ kg^{-1} respectively. After hydrogenation the calorific values of LFH and HFH increased to 44.22 MJ kg^{-1} and 44.20 MJ kg^{-1} respectively, which make a 17.07% increase in the calorific value of LFH and 16.06% increase in the calorific value of HFH. The calorific values of LFH and HFH were approximately the same as that of diesel fuels and aviation fuels. The LFH has a calorific value 44.22 MJ kg^{-1} and diesel fuel has a calorific value 44.31 MJ kg^{-1} while the HFH has a calorific value 44.20 MJ kg^{-1} and aviation fuels has a calorific value 43.35 MJ kg^{-1}. While according to ASTM the calorific value of AF and DF are 43.28 MJ kg^{-1} and 44.80 respectively.

4.6. FREEZING POINT OF LFH, HFH AND AF, DF

Table II represents the freezing point values for the base fuels (AF and DF) and the fractions (HFH and LFH). The freezing point should be low enough to prevent problems of fuel flow through lines, filters and valves in the fuel system of both turbines and diesel engines. However, this parameter should be stiffer for aviation fuel since the aircraft during flight reaches high altitudes and low temperatures. It is observed that the fractions present a freezing point within the parameters of quality demanded by the National Petroleum Agency, which establishes the value of -40 ºC for the AF and -10 ºC for the DF.

According to ASTM D 7153 the freezing point of aviation fuel is -47 and the freezing point of diesel fuels is varying from -8 to -18 ºC. According to our laboratory tests the freezing point of aviation fuel was -48 ºC and the freezing point of diesel fuels was -10 ºC. There was a

little (2.04%) difference in both freezing point tests of aviation fuels and this difference was probably due the difference between the equipments. The freezing points of LFH and HFH were -40 ºC and -30 ºC respectively.

Table II. Freezing point, flash point, density, viscosity and calorific value of all fractions

Fractions	**LFP**	**LFH**	**DF**	**HFP**	**HFH**	**AF**
Freezing point (ºC)	-30	-30	-10	-40	-40	-48
Flash point (ºC)	75	67	63	77	69	50
Calorific Value (MJ kg^{-1})	36.50	44.22	44.80	37.10	44.20	43.35
Density (g mL^{-1}) at 25 ºC	0.8522	0.8329	0.8203	0.8878	0.8525	0.8354
Viscosity (mm^2 s^{-1}) at 25 ºC	1.5422	0.8312	0.8410	2.5243	1.8274	1.8484

4.7. DENSITY AND VISCOSITY OF LFP, HFP, LFH, HFH, AF AND DF

Calorific power and density guarantee that the fuel used produces the necessary energy for certain autonomy. Density is an important feature because it is directly linked to the total energy content contained in a given mass of fuel. It is particularly useful for empirically determining the calorific value when used with other parameters such as the distillation curves and the aniline point for calculating the energy content of the fuel. Limiting a fuel density range is important for both the design and the proper functioning of the engine. Viscosity is limited to a maximum value in order to obtain a minimum loss of pressure in the low temperature flow as well as to allow adequate spraying of the fuel in the injector nozzles, enabling better combustion conditions. Viscosity can significantly affect the lubricity property of the fuel, and consequently

the fuel pump life. **Figure 10** shows the experimental curves whose extrapolation allows the calculation of the values of the densities, while **Figure 11** shows the experimental curves whose extrapolation allows the calculation of the viscosity values at -10 ºC, like aviation fuels (a), diesel fuels (b) , HFH (c) and the LFH (d). The values of the density and viscosity for AF, DF, LFH, HFH and their formulations at room temperature are shown in **Table II** and the values of the density and viscosity for AF, DF, LFH, HFH and their formulations at various temperatures (-10 to 50 ºC) are shown in **ANNEXES 4-10**.

At room temperature (25 ºC) the density (uncertainty $\pm$ 1.20%, according triplicate analysis) of LFH decreased from 0.8522 to 0.8329, which makes a 3.10% difference between the densities of LFP and LFH, while the density of HFH decreased from 0.8878 to 0.8525, which makes a 4% difference between the densities of HFP and HFH. Another hand, the densities of LFH and DF are 0.8329 and 8203 respectively, which makes 1.10% of the total difference while the densities of HFH and AF are 0.8525 and 0.8354, it makes only 1.19% of the total difference between the densities of HFH and AF.

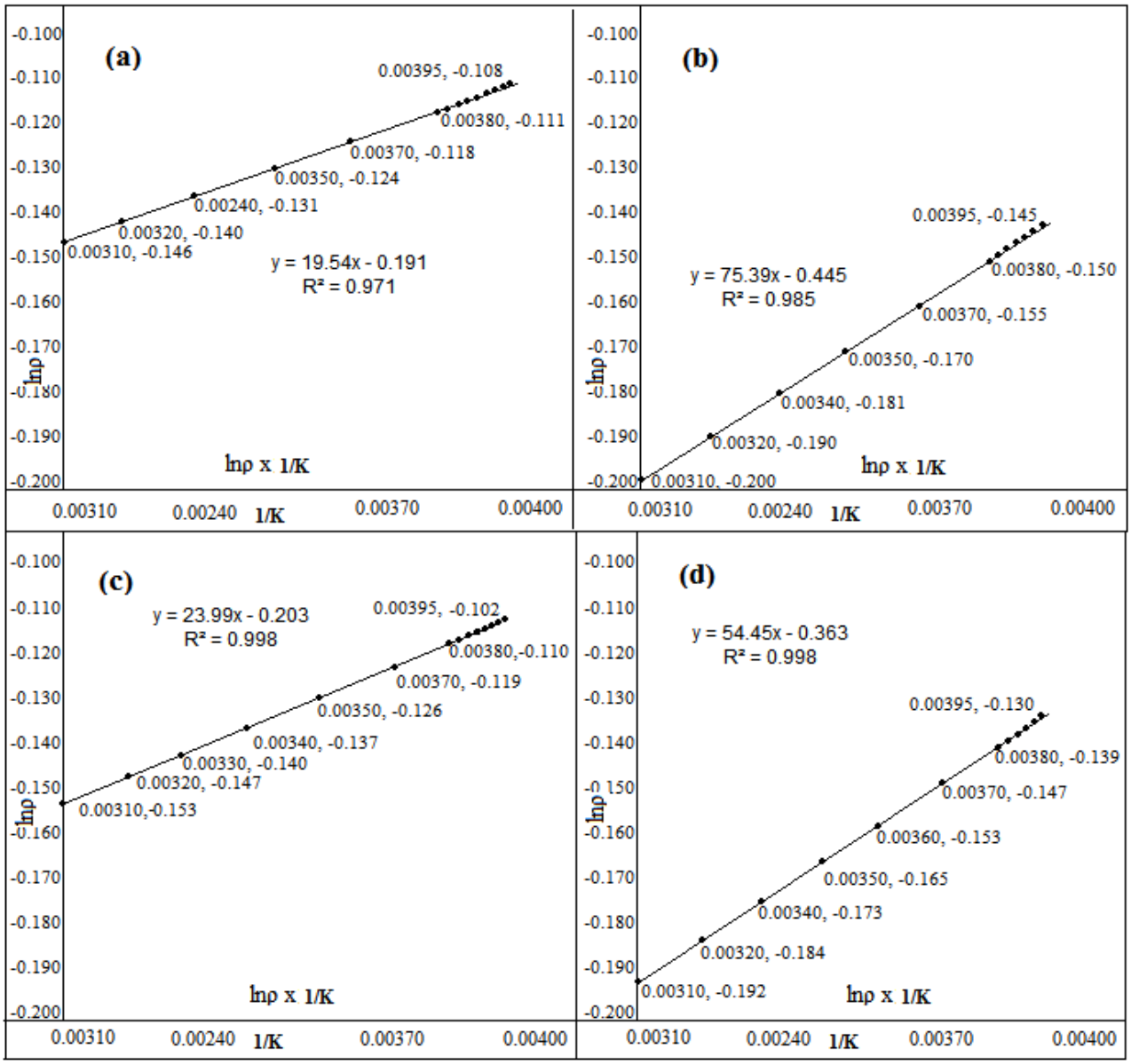

Figure 10. Density change of pure (a) AF, (b) DF, (c) HFH and (d) LFH at different temperatures

Table II shows the density and viscosity of all fractions like aviation fuels, diesel fuels, the LFH and HFH at room temperature. In Table II, we can see that the density and viscosity of LFH and HFH are a little lower than aviation fuels and diesel fuels. There are many parameters that influence the combustion properties. Density and viscosity are important parameters in combustion because these parameters mostly determine the droplet diameter distribution issuing

from the injector nozzle, and therefore impact the vaporization, ignition and combustion of the droplets. The droplet size from the spray increases the viscosity and density of the liquid. The viscosity and density of bio-oil are higher than those of petroleum fuels but by applying certain methods like hydrogenation, we can reduce the viscosity and density of bio-oil. That's why we can see in the graphs that viscosity the LFH is a little bit lower than diesel fuels and viscosity HFH is also a little bit lower than aviation fuels after hydrogenation. The Tables of density and viscosity of all pure samples are given in **ANNEXES 4-6**.

At room temperature (25 ^{o}C) the viscosity (uncertainty $\pm$ 1.27%, according triplicate analysis) of LFH decreased from 1.5422 to 0.8312, which makes 46.15% difference between the viscosities of LFP and LFH, while the viscosity of HFH decreased from 2.5243 to 1.8274, which makes 37.55% difference between the viscosities of HFP and HFH. Another hand, the viscosities of LFH and DF are 0.8312 and 0.8410 respectively, which makes 1.16% of the total difference and the viscosities of HFH and AF are 1.8274 and 1.8484, it makes only 1.13% of the total difference between the viscosities of HFH and AF.

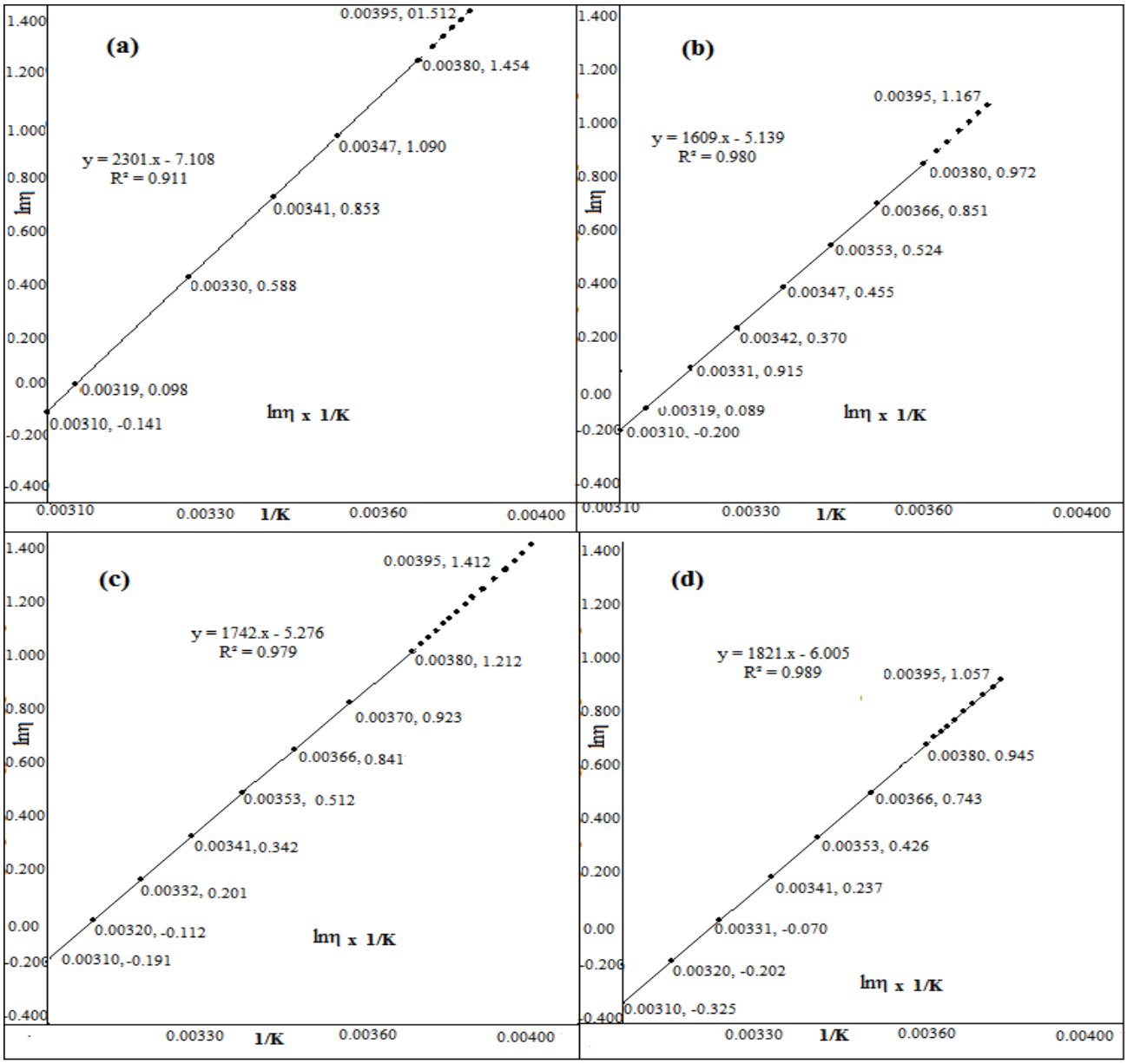

Figure 11. Viscosity change of pure (a) AF, (b) DF, (c) LFH and (d) HFH at different temperatures

4.8. VOLATIZATION

The volatility of a fuel is its ability to vaporize at different temperatures and can be expressed through distillation and flash point curves, among others.

4.8.1 DISTILLATION CURVES OF AF, DF, LFH AND HFH

The distillation curve is expressed by means of the temperature as a function of the fraction of the distillate volume providing important information regarding the composition of the fuel connected to its volatility and the operation of the engine. A distillation curve provides:

IB: The initial boiling point.

T10: Temperature at which 10% of the sample was distilled. This is linked to the slight fractions of the fuel, important for starting the engine.

T50: Temperature at which 50% of the sample was distilled. This is linked to the average fuel fractions, related to the heating and optimal engine operating range.

FB: Final boiling point.

T90: temperature at which 90% of the sample was distilled. This is linked to heavier fuel fractions, related to engine economy and performance.

Figure 12 shows the distillation curves of (a) HFH and (b) AF. It is observed that the profile of the distillation curve for the AF and the HFH fraction are similar, but the HFH fraction presents a lower PI (160 ºC), meaning the presence of compounds with lower volatility than the AF (165 ºC). The HFH fraction has heavier compounds.

.

4.8.1.1. Distillation curves of AF and HFH

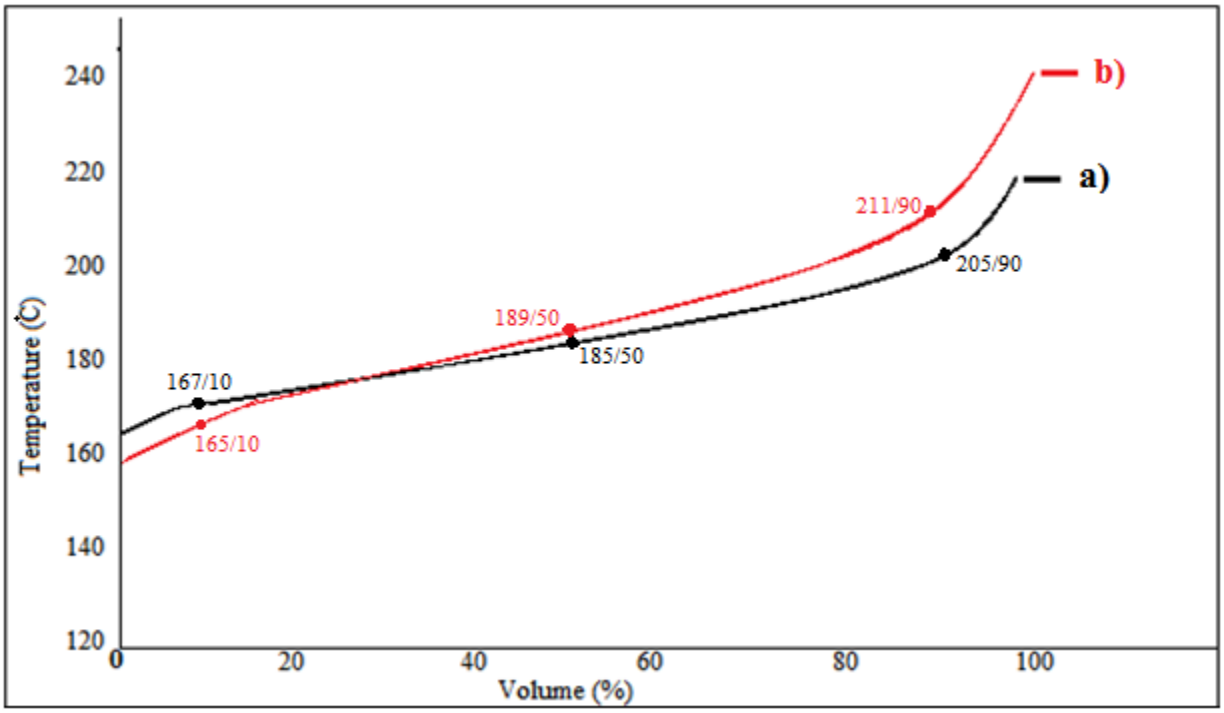

Figure 12. Distillation curve of (a) AF and (b) HFH

Figure 13 shows the distillation curves (a) DF and (b) LFH fraction. According to **Figure 13**, it is observed that the profiles of the distillation curves are similar however the LFH fraction presents in all its extension more volatile compounds than the DF.

4.8.1.2. Distillation curves of DF and LFH

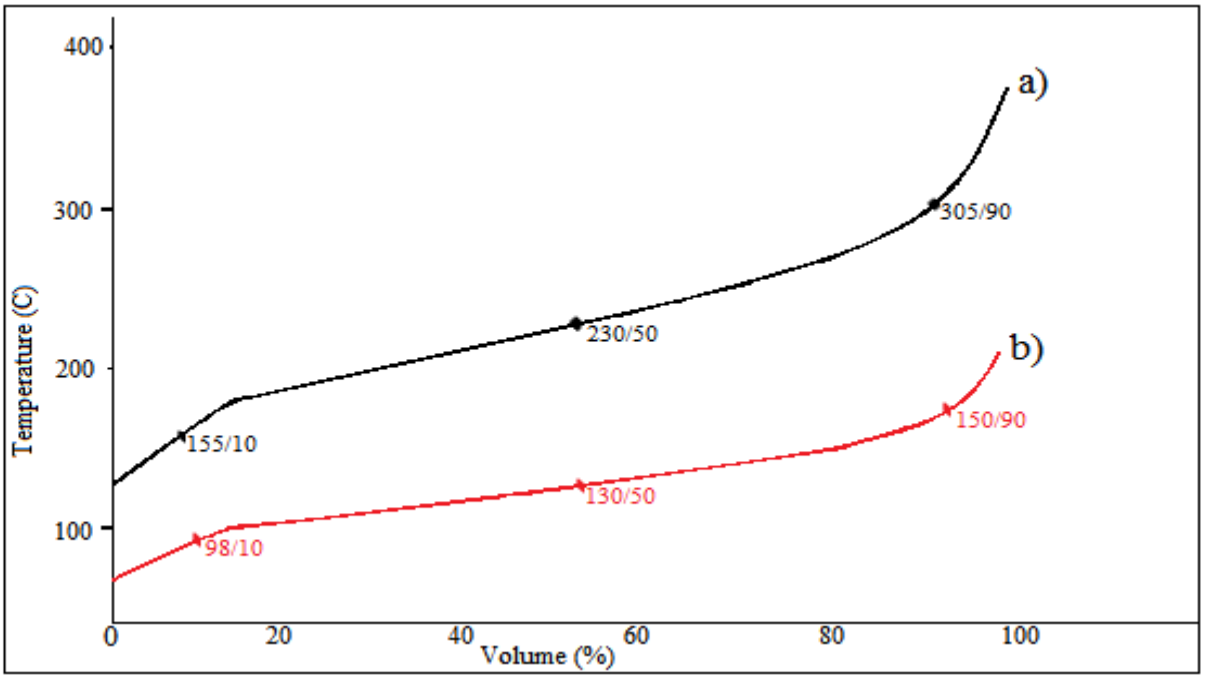

Figure 13. Distillation curve of (a) DF and (b) LFH

4.8.2. FLASH POINT OF LFH, HFH, DF AND AF

The flash point limitation is linked to the safety in the transport and handling of the product as well as the evaporative losses during storage. It also allows the detection of possible contaminations by lighter products. Bio-oil is mostly non-flammable and possesses only limited volatility, and ignite only at high temperatures. The flash point of bio-oil is varying from 50- 120 ^{o}C, depending on the chemical composition of bio-oil. Bio-oil contains some light compounds that evaporate at low temperatures and may cause a small short-duration flash in the presence of air and heat. These compounds include acetaldehyde, acetone and methanol. However, the flash is rapidly suppressed by a large amount of evaporated water. The flash points of AF, DF, LFH

and HFH are 50 ^{o}C, 63 ^{o}C, 67 ^{o}C and 69 ^{o}C respectively and the flash points of formulations are very close to pure fuels.

4.9. ENRICHMENT OF HYDROCARBONS IN BIO-OIL AFTER HYDROGENATION

Figure 14 shows the percentage area of chemical classes for bio-oil (a) before and (b) after hydrogenation.

Figure 14 (a) shows that there are many nitrogen and oxygen containing compounds in the bio-oil before hydrogenation. The main groups are ketones and alcohols. There was 30% nitrogen and 45% oxygen containing groups in LFP and HFP. Only a few hydrocarbons were detected in LFP and HFP. In HFP there were almost all high molecular weight compounds. Due to having these high molecular weight nitrogenated and oxygenated compounds, the bio-oil is unstable and difficult to use in engines because the presence of high amounts of nitrogen compounds in the composition of bio-oil may lead to the formation of oligomers and increase the emission of nitrogen oxide compounds (NOx) during the combustion process. However, the NOx emitted during combustion depends not only on the composition of the fuel but also on the mode of operation and the design of the burners and of the combustion chamber and on the fuel's other physicochemical characteristics (e.g., its cetane number (CN)). Eucalyptus biomass is composed of 38 − 45% cellulose, 16% hemicellulose, 25 − 37% lignin, and 9 − 15% of other organic and inorganic compounds. Cellulose is a natural high molecular weight polymer with the generic empirical formula of $H(C_6H_{10}O_5)n$ OH with up to 10,000 monomer units and a molecular weight of 1,600,000 a.m.u. Hemicelluloses are formed with copolymers of glucose and a variety of other monomers, mainly hydrates of carbon. They are amorphous and have a lower degree of polymerization than cellulose. During the process of pyrolysis, these compounds are cracked,

producing fractions of lower molecular weight while maintaining some of the characteristics of the original compounds.

After hydrogenation, we can see in **Figure 14 (b)** that more than 50% of nitrogenated species, 65% of oxygenated species and more than 40% of other groups are converted into hydrocarbons. More than 30 peaks of hydrocarbons were detected in the HFH. All these hydrocarbons have an area of 61% of the whole sample. The hydrocarbons detected in the HFH have high molecular weight as compared to hydrocarbons detected in the LFH. The compounds detected in both LFH and HFH can be classified into hydrocarbons, alcohols, phenol, ethers, aldehydes, ketones, carboxylic acids, and esters as shown in **ANNEX 11**. Hydrocarbons with C9–C17 are predominant in with a % area of 55% and 53% in both LFH and HFH respectively. In **Figure 14 (a)** we can see that there were only a few hydrocarbons in the bio-oil before hydrogenation which makes only 7% of the total HFP and 5% of the total LFP. These hydrocarbons are varying from C11–C15 and 93% of the HFP consists of nitrogenated, oxygenated and other reactive compounds before hydrogenation.

In **Figure 14 (b)** we can see that there were also many hydrocarbons in the bio-oil after hydrogenation which makes 61% of the total fraction and these hydrocarbons are very from C9 – C15 and only 39% of the total fraction of bio-oil consists of nitrogenated, oxygenated and other reactive compounds after hydrogenation. We noticed that there were aromatics, aliphatics as well as cyclic hydrocarbons in the bio-oil after hydrogenation. Residues and % area of hydrocarbons detected in LFP, HFP and LFH, HFH and % area of all groups detected in the LFH and HFH are shown in **ANNEX 11**.

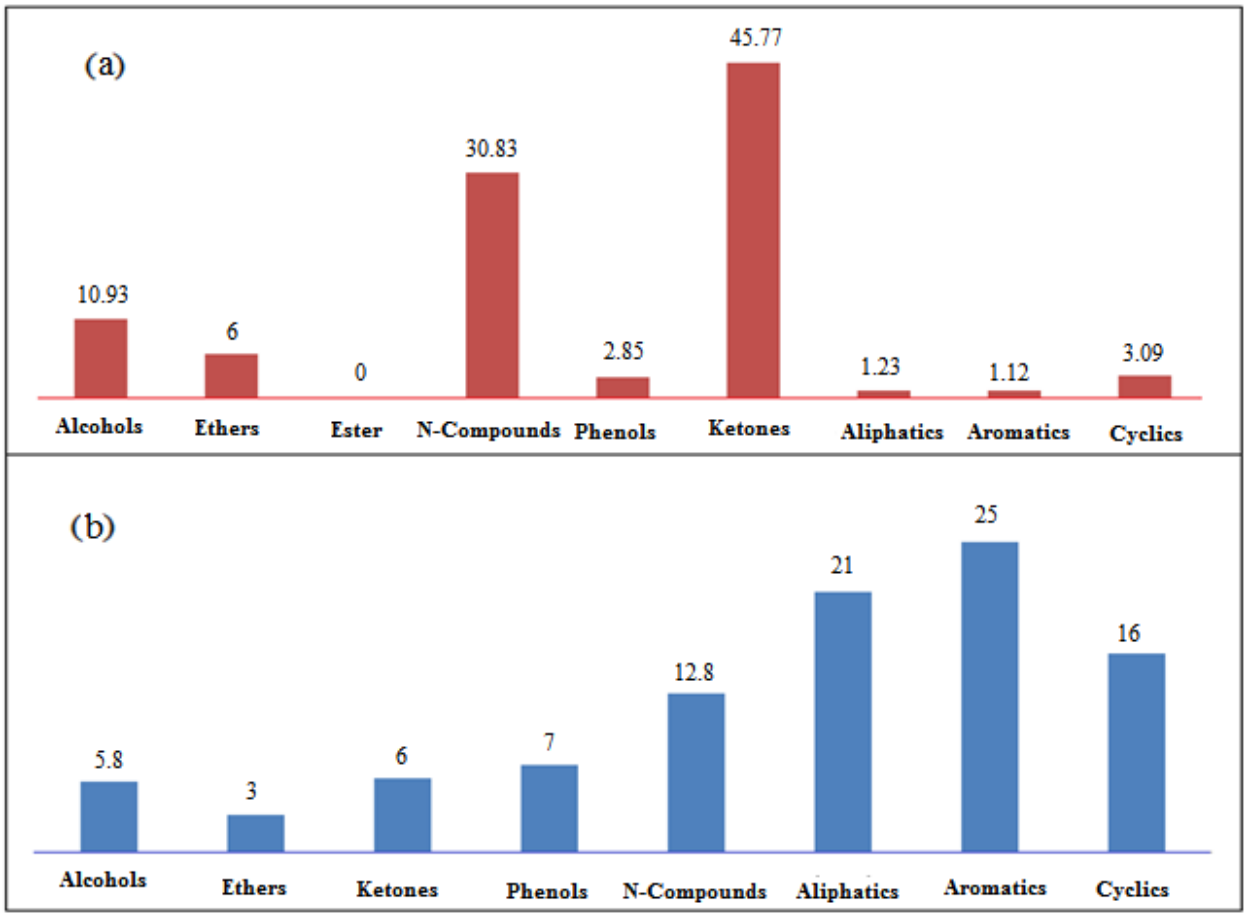

Figure 14. Percentage area of chemical classes of bio-oil (a) before and after (b) hydrogenation

4.10. NITROGEN AND OXYGEN CONTENTS OF BIO-OIL AFTER AND BEFORE HYDROGENATION

The nitrogen and oxygen contents of wood pyrolysis bio-oil are 45 – 65% and it is due to more than 300 oxygenated compounds that have been identified in the bio-oil. The distribution of these compounds depends on the type of biomass and the production process used. In the case of Eucalyptus, there was 30% nitrogen and 45% oxygen containing compounds in LFP and HFP. But these quantities decreased to 12% and 6% in LFH and HFH respectively. Due to high

nitrogen and oxygen contents, the bio-oil possesses different chemical and physical properties and behavior from other oils, this result in the difference in the combustion application of bio-oil. For example, the oxygen content of the bio-oil helps the combustion due to the lower need for combustion air and will also reduce the number of flue gasses generated.

5. ANALYSIS OF LFH AND HFH AFTER FORMULATIONS WITH DF AND AF

5.1. DENSITY ALL FRACTIONS AFTER FORMULATION

Figure 15 shows the densities of all four samples after formulations, like10% aviation fuels **(a)**, 20% aviation fuels **(b)**, 10% diesel fuels **(c)** and 20% diesel fuels **(d)**.

Figure 16 shows that the density of 10% and 20% formulation with aviation fuels are closed to the density of pure aviation fuels and the density of 10% and 20% formulations with diesel fuels are closed to the density of pure diesel fuels. It was observed that when HFH was added to aviation fuels, viscosity decreased and when LFH was added to diesel fuels its viscosity increased. The density of all formulated fractions was also checked at a temperature -10 to 50 ^{o}C and then it was extrapolated up to -20 ^{o}C. The temperature didn't show a great effect on density but when the temperature increased the density decreased.

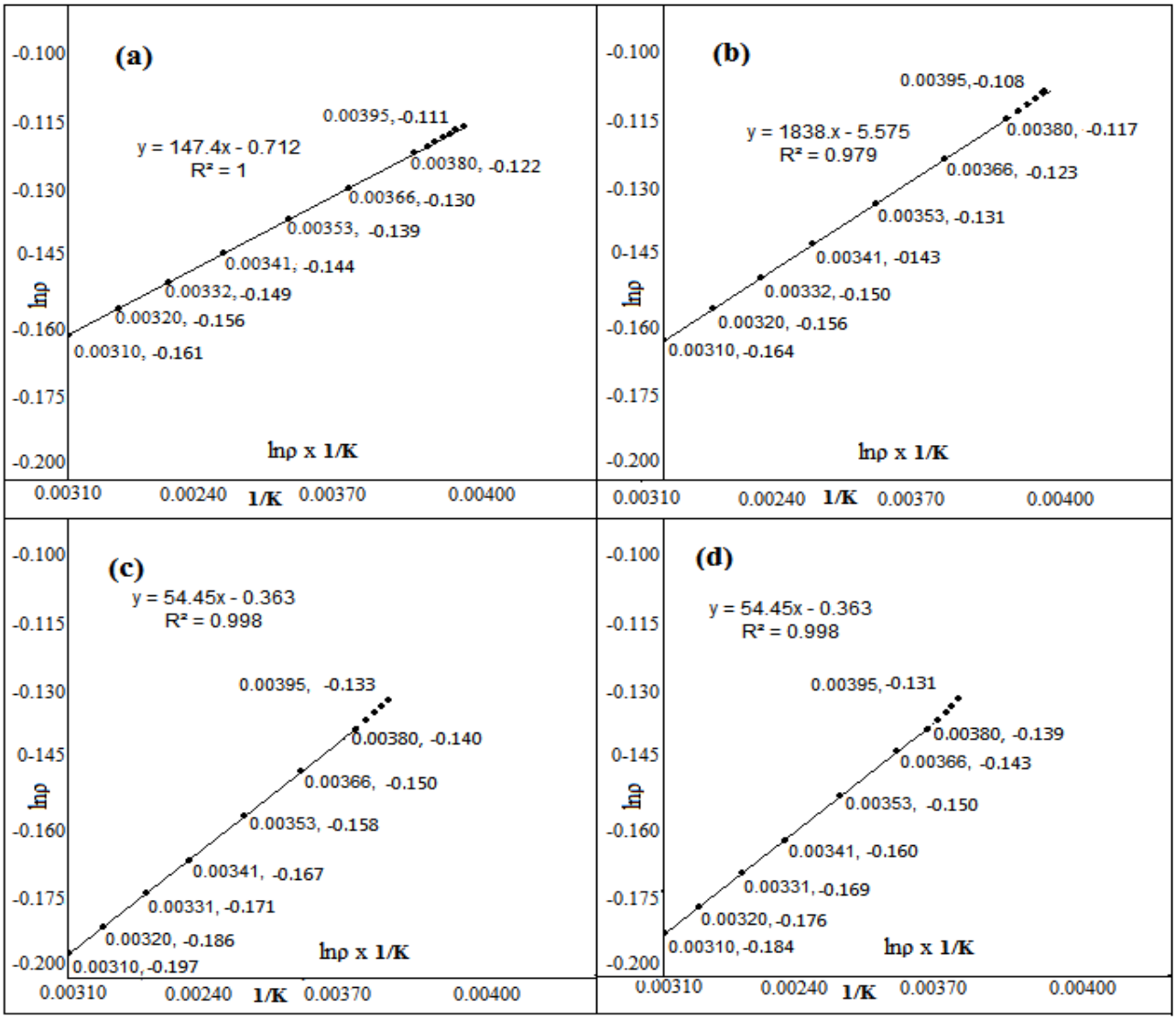

Figure 15. Density change of all formulations (a) 10% AF, (b) 20% AF, (c) 10% DF and (d) 20% DF at different temperature

5.2. VISCOSITY OF ALL FRACTIONS AFTER FORMULATIONS

Figure 16 shows the viscosities of all four formulated samples, like 10% aviation fuels (a), 20% aviation fuels (c), 10% diesel fuels (b) and 20% diesel fuels (d). Where we can see that the viscosity of 10% and 20% formulations with aviation are closed to the viscosity of pure aviation fuels and the viscosity of 10% and 20% formulations with diesel fuels are closed to the

viscosity of pure diesel fuels. There is a decrease in viscosity in all cases. As the temperature increases the viscosity decreases. With the addition of bio-oil, the viscosity increases because pure bio-oil has a higher viscosity than the aviation fuels, that's why formulated fractions have a little higher viscosity than pure aviation fuels. The tables of viscosity and density of all formulations are given in **ANNEXES 7-10**.

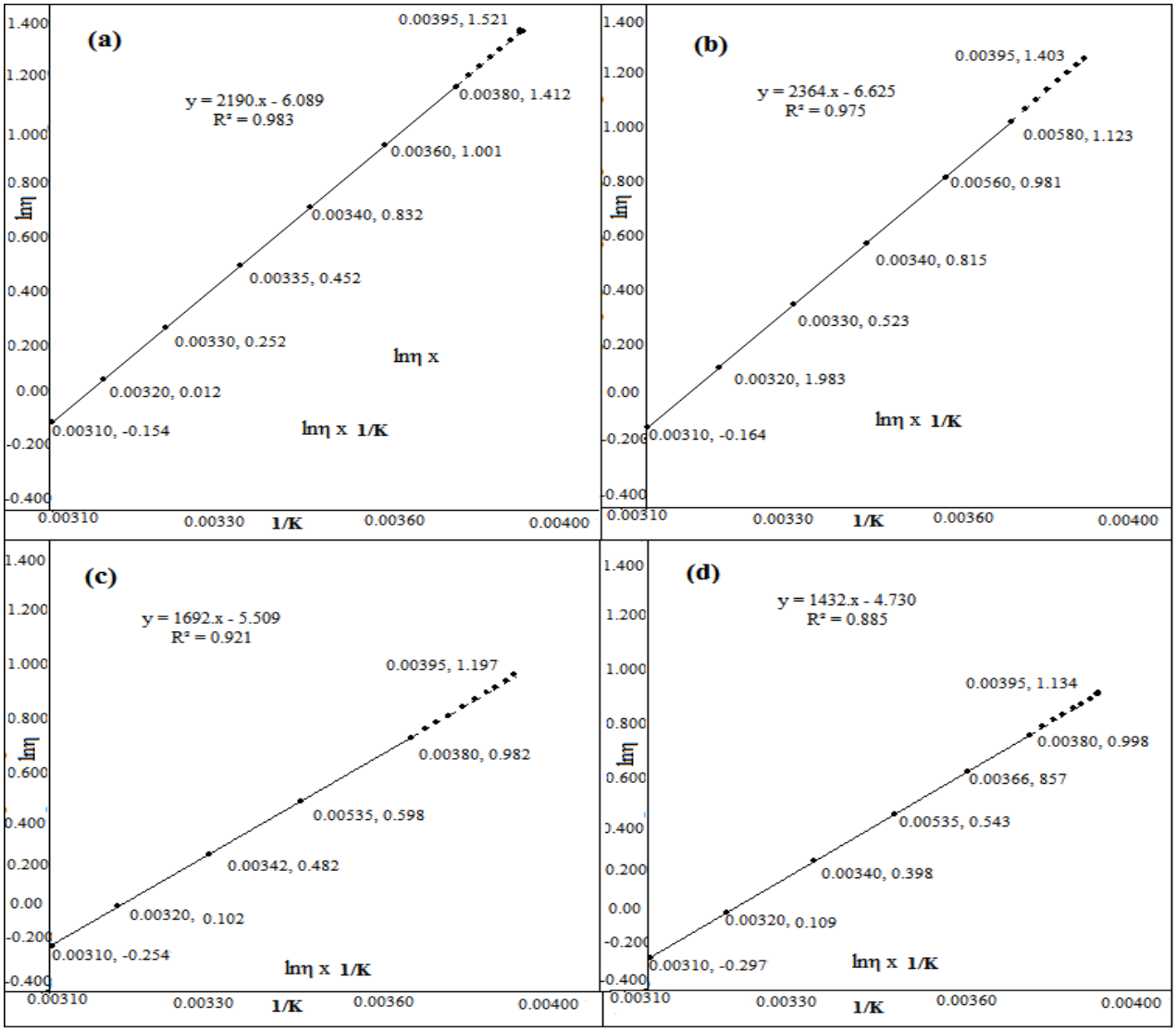

Figure 16. Viscosity change of all formulations (a) 10% AF, (b) 20% AF, (c) 10% DF and (d) 20% DF at different temperature

5.3. DISTILLATION CURVES OF FORMULATIONS AND PURE FRACTIONS

5.3.1. Distillation curves of pure AF, HFH, 10% HFH and 20% HFH

Figure 17 represents the distillation curves of pure HFH (a), pure AF (b), 10% HFH (c) and 20% HFH (d) distillation curves. The pure HFH curve is a little different from AF curve, anyhow, 10% and 20% HFH curves are a very close and similar to pure AF curve. This means that we can make formulations of HFH with AF to use it in an aviation turbine.

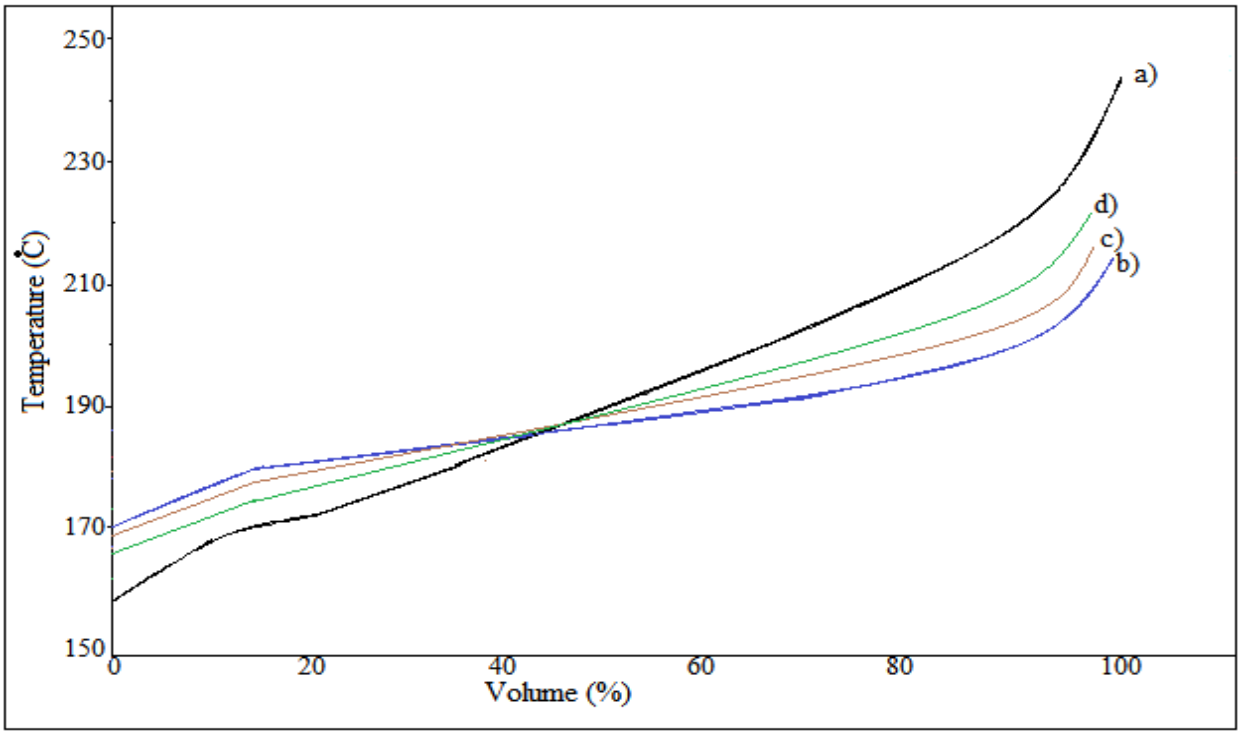

Figure 17. Distillation curves of (a) HFH, (b) AF, (c) 10% AF and (d) 20% AF

5.3.2. Distillation curves of pure DF, LFH, 10% LFH and 20% LFH

Figure 18 illustrates the distillation curves of pure DF (a), pure LFH (b), 10% LFH (c) and 20% LFH (d). The pure LFH distillation curve is clearly different from DF curve but 10% LFH and 20% LFH distillation curves are a somehow close to DF curve. This means that we can make formulations of LFH with DF to use it in a diesel engine.

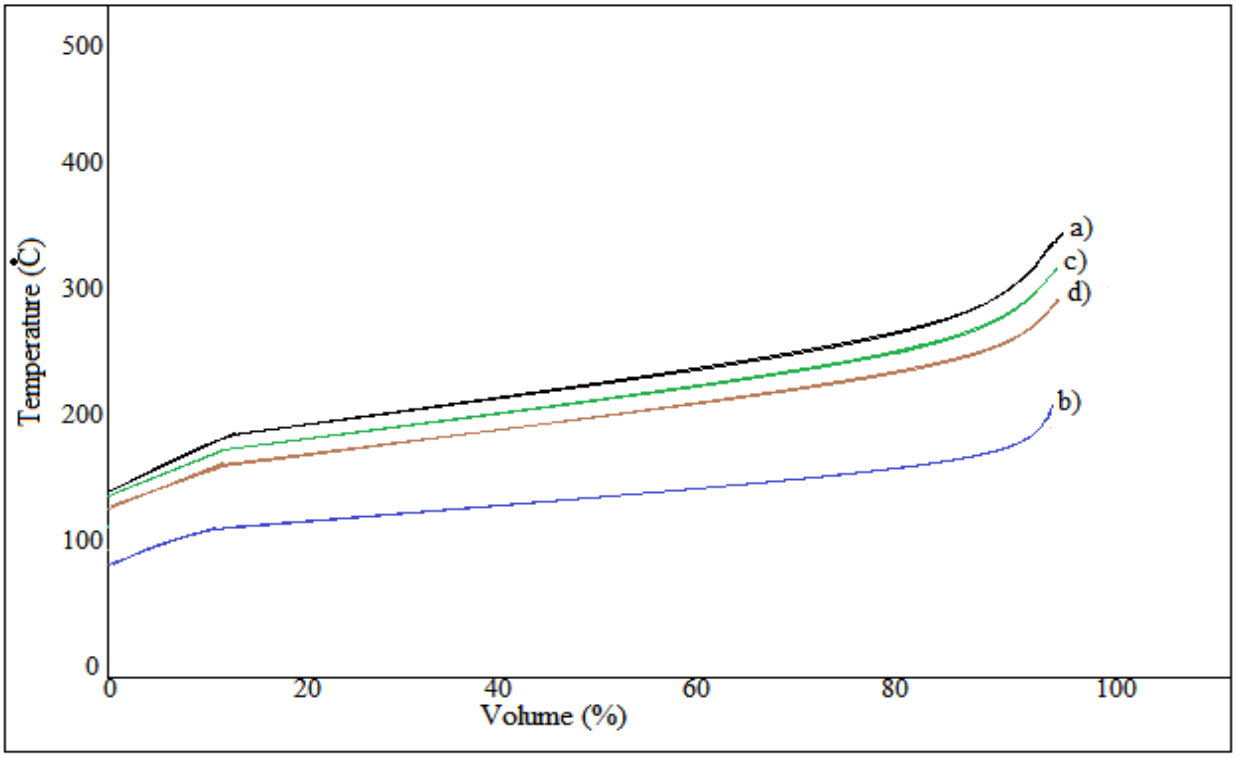

Figure 18. Distillation curves of (a) DF, (b) LFH, (c) 10% DF and (d) 20% DF

6. CONCLUSIONS

Bio-oil produced by the pyrolysis of agricultural wastes was a complex black sticky liquid containing many hundreds of compounds and various groups like alcohol, aldehydes, nitrogenated and oxygenated compounds as well as phenol ketones and some hydrocarbons. The hydrogenation of pyrolysis oil was performed in the presense of NiMo as a catalyst. Hydrogenation is a class of chemical reactions in which the net result is the addition of hydrogen to nitrogenated and oxygenated compounds present in bio-oil. NiMo (catalyst) was tested for its effect on the pyrolysis products of agricultural wastes (woody biomass). The influence of NiMo on improving the quality of bio-oil was investigated and found very promising in terms of reduction of lignin derived compounds, organic acids, heavy nitrogen and oxygen containing compounds, corrosiveness, and hydrocarbon production.

The aim of upgrading was to convert oxygen and nitrogen containing species as well as other reactive compounds in bio-oil to hydrocarbons through hydrogenation. Hydrogenation was found very useful to improve the quality and stability of bio-oil by decreasing the contents of organic acids, aldehydes, nitrogenated, oxygenated as well as other reactive compounds. The number of hydrocarbons is increased from 5% to 60% in the LFH and from 7% to 61% in the HFH.

Thus bio-oil can be used (as formulation) as transportation fuels because the important physico-chemical properties such as boiling point, freezing point, flash point, viscosity, density, the number of lower molecular weight hydrocarbons, distillation curve and enthalpy of combustion etc of bio-oil were found very close to petroleum fuels. It was observed that LFH can be used with diesel fuel because it has almost the same physico-chemical properties as diesel fuels and HFH showed almost the same physico-chemical properties as that of aviation fuels.

Important results from different analyses were as follow:

The GC-MS analysis of bio-oil after and before hydrogenation was completely different. The GC-MS results showed 5% hydrocarbons before hydrogenation while more than 60% hydrocarbons after hydrogenation. The GC-MS analysis also showed that there were a few phenolic compounds before hydrogenation while phenolics also increased (3−7%) after hydrogenation.

The TGA results were also very interesting after hydrogenation. The thermal stability of bio-oil was increased 100% after hydrogenation while the number of residues (after a complete burning of the sample) was decreased from 4% to 0.53%.

- **RESPONSE TO OBJECTİVES:**

1. It was found that pretreatment had a significant effect on thermal decomposition of wastes biomass. The product yield increases or decreases due to different pretreatments during pyrolysis.

2. NiMo catalyst had a significant effect on the hydrogenation of the higher molecular weight products of pyrolysis. Hydrogenated bio-oil without NiMo didn't show a big difference from pyrolysis oil while it was observed that more than 60% heavy compounds were converted in to hydrocarbons when NiMo was used as a catalyst during hydrogenation.

3. Both fractions of bio-oil (HFH and LFH) were characterized and compared with aviation and diesel fuels. The density, viscosity, freezing point, flash point, distillation curve and enthalpy of combustion of LFH and HFH were found much closer to diesel and aviation

fuels respectively.

4. The 10% and 20% formulation of bio-oil with aviation fuels and diesel fuels were also analyzed, studied and compared with pure avaition and diesel fuels. The 10% and 20% formulations of bio-oil showed almost the same physico-chemical properties and characteristics as pure aviation and diesel fuels.

5. The concept of upgrading and fuel quality was made easy and cleared to understand in this work. Pyrolysis oil before hydrogenation (upgrading) was found a black viscous and sticky liquid, which was impossible to use for any purpose. But after hydrogenation the same pyrolysis oil was found very clean and less viscous as compared to pyrolysis oil.

6. Many attempts were made to discover a proper pyrolysis temperature and a proper biomass and catalyst ratio, and finally, a proper pyrolysis temperature (850 ^{o}C) and a proper biomass and catalyst ratio (3:1) was discovered and it was observed that very low or very high temperature can create many problems during pyrolysis. For example, a temperature lower than 600 ^{o}C can cause blockage of the pyrolysis system and high amount of residues, and a temperature higher than 900 ^{o}C can cause blockage of the pyrolysis system and produce a high amount of uncondensible gases.

7. REFERENCES

1. S. Arbogast, D. Bellman, J. D. Paynter and J. Wykowski; *Fuel Processing Technology,* 106 (2013) 518-525.

2. A. A. Khan, W. Jong, P. J. Jansens and H. Spliethoff; *Fuel Processing Technology*, 90 (2009) 21-50.

3. R. Cataluña, P. M. Kuamoto, C. L. Petzhold, E. B. Caramão, M .E. Machado and R. Silva; *Energy and Fuels,* 27 (2013) 6831−6838

4. N. Laksmono, M. Paraschiv, K. Loubar and M. Tazerout*; Fuel Processing Technology*,106 (2013) 776-783.

5. P.M. Mortensen, J.D. Grunwaldt, P.A. Jensen, K.G. Knudsen, A.D. Jensen; *Applied Catalysis A.* 407 (2011) 1–19.

6. A.V. Bridgwater; *Biomass Bioenergy* 38 (2012) 68–94.

7. K.C. Kwon, H. Mayfield, T. Marolla, B. Nichols, M. Mashburn; *Renewable Energy* 36 (2011) 907–915.

8. T.V.Choudhary, C.B. Phillips; *Applied Catalysis A,* 397 (2011) 1–12.

9. S. Wang, Q. Cai, X. Wang, Z. Guo, Z. Luo; *Fuel Processing Technology,* 111 (2013) 86–93.

10. S. Wang, Q. Cai, Z. Guo, Y. Wang, X. Wang; *BioResources,* 7 (2012) 5019–5031.

11. R. Trane, S. Dahl, M.S. Skjøth-Rasmussen, A.D. Jensen; *International Jouranl of Hydrogen Energy,* 37 (2012) 6447–6472.

12. G. Hu, J. Li, G. Zeng; *J. Hazard. Mater.* 261 (2013) 470–490.

13. L. Ma, T. Wang, Q. Liu, X. Zhang, W. Ma, Q. Zhang*; Biotechnol. Adv.* 30 (2014) 859–873.

14. M.R. Rover, R.C. Brown, *J. Anal. Appl. Pyrolysis;* 104 (2013) 366–371.

15. H. Ben, A.J. Ragauskas; *Energy and Fuel*, 25(2011) 2322-32.

16. H. Ben, A.J. Ragauskas; *Bioresour Technol,* 147(2009) 577-584.

17. M.S.Mettler, D.G. Vlachos, P.J. Dauenhauer; *Energy Environ Sci.* 5 (2012) 797-809.

18. K. Papadikis, S. Gu, A.V. Bridgwater, H. Gerhauser; *Fuel ProcessTechnol,* 90 (2009) 504-512.

19. F. Motasemi, M.T. Afzal; *Renew Sust Energ Rev*. 28 (2013) 317-330.

20. J. Akhtar, N.S. Amin; *Renew SustEnerg Rev*. 16 (2012) 5101-5109.

21. A. Abbaszaadeh, B. Ghobadian, M.R. Omidkhah, G. Najafi; *Energy Convers Manage*, 63, (2012) 138–48

22. M.M. Wright, D.E. Daugaard, R.C. Brown; *Fuel*, 89 (2010) 2-10.

23. G.W. Huber, S. Iborra, A. Corma; Chemistry*, catalysts, and engineering, Chem. Rev*.106 (2006) 4044–409.

24. A.V. Bridgwater; *Biomass Bioenergy,* 38 (2012) 68–94.

25. D. Mohan, C.U. Pittman, P.H. Steele; *Energy Fuels.* 20 (2006) 848–889.

26. C. Amen-Chen, H. Pakdel, C. Roy; *Biomass Bioenergy.* 13 (1997) 25–37.

27. C.B. Xu, T. Etcheverry; Fuel, 87 (2011) 335–345.

28. A.S. Pollard, M.R. Rover, R.C. Brown; *J. Anal. Appl. Pyrolysis* 93 (2012) 129–138.

29. A.V. Bridgwater, D. Meier, D. Radlein; *Org. Geochem.* 30 (1999) 1479–1493.

30. Z.G. Guo, S.R. Wang, Y.L. Gu, G.H. Xu, X. Li, Z.Y. Luo; *Sep. Purif. Technol.* 76 (2010) 52–57.

31. L.F. Zilnik, A. Jazbinsek; *Sep. Purif. Technol.* 86 (2012) 157–170.

32. Y. Wei, H.W. Lei, L. Wang, L. Zhu, X.S. Zhang, Y.P. Liu; Energy Fuels. 28 (2104) 1207- 1212.

33.A. V. Bridgwater; *Thermal science,* 8 (2004) 21-49.

34. A. V. Bridgwater; *In: TUSTIN, J. IEA Bioenergy Annual Report* 2006,

35. D. Mohan, C. U. Pittman and P. H. Steele; *Energy Fuel,* 20 (2006) 848-889.

36. S. Li, S. Xu, S. Liu, C. Yang and Q. Lu; *Fuel Processing Technology*,85 (2004) 1201– 1211.

37. N. Özbay, B. B. Uzun, E. A. Varol and A. E. Pütün; *Fuel Processing Technology*, 87 (2006) 1013– 1019.

38. P. M. Mortensen, J. D. Grunwaldt, P. A. Jensen, K. G. Knudsen and A.D. Jensen; *Applied Catalysis A*. 407 (2011) 1–19.

39. X. F. Zhu, J. L. Zheng, Q. X. Guo and Q. S. Zhu; *Engineering Science*,7 (2005) 83–88.

40. Q. Zhang, Q. J. Chang, T. J. Wang and Y. Xu; *Petrochemical Technology*, 35 (2006) 493–498.

41. G.W. Huber, A. Corma; *Angew Chem Int Ed Engl.* 46 (2007) 7184-201.

42. Q. Zhang, J. Chang, T.J Wang, Y. Xu; *Energy Conversion and Management* 48 (2014) 87- 92.

43. V.A. Bridgwater, D. Meier, D. Radlein; *Org Geochem* 30 (2005) 1479-1493.

44. W. Liu, X. Wang, C. Hu, D. Tong, L. Zhu; *International Journal of Hydrogen Energy* 39 (2014) 6371-6383.

45. R.J. Nevagi, S.N. Dighe; *Eur J.Med Chem.* 97 (2015) 561-581.

46. M.V. Migliorini, M.E. Machado, E.B. Caramão; *Scientia Chromatographica* 54 (2013) 7-65.

47. L.R. Almeida, A.A. Hidalgo, M.L. Veja; *Estudos Tecnológicos* 7 (2011) 163- 176.

48. J. Kim, J.Y. Jaung; *Dyes and Pigments* 77 (2008) 474-477.

49. J.A. Pereira, A.M. Pessoa, M.N. Cordeiro, R. Fernandes, C. Prudêncio; *Eur J Med Chem.* 97 (2006) 664-672.

50. World Energy Outlook 2004; International Energy Agency (IEA); *Brussels.* 2004.

51. D.M. Alonso, J.Q. Bond, J.A. Dumesic; *Green Chem.* 12 (2010) 1493−1513.

52. A. Demirbas; *Appl. Energy* 88 (2011) 17–28.

53. D. Shen, R. Xiao, S. Gub, K. Luo; *RSC Adv.* 1 (2011) 1641−1660.

54. C. Perego, M. Ricci; *Catal. Sci. Technol.* 2 (2012) 1776−1786.

55. P. Girard, Z. Fallot; *Energy Sustainable Dev.* 2 (2006) 92−108.

56. J.C. Serrano, J.A. Dumesic; *Energy Environ. Sci.* 4 (2011) 83−99.

57. Y. Sano, K. Choi, Y. Korai, I. Mochida; *Energy Fuels* 18 (2004) 644–651.

58. J. Goldemberg; *Quim. Nova*, 32 (2009) 582− 587.

59. F. Galembeck, C.A..S Barbosa, R.A. Souza; *Quim. Nova.* 3 (2009) 571−581.

60. W. Cui, J. Cheng; *Plant Biology* 17 (2015) 16–23

61. W. Catallo, T. Shup, T. Eberhardt; *Biomass Bioenergy* 32 (2008) 140–145.

62. T. Viet, J. Lee, F. Ma, G. Kim, I. Ahn, C. Lee; *Fuel* 103 (2013) 553–561.

63. C. Xu, S. Hamilton, M. Ghosh; *Fuel* 88 (2009) 2097–2105.

64. W.S. Cardoso; *Quim. Nova.* 36 (2013) 623−627.

65. P. Duan, Y. Xu, X. Bai; *Energy Fuels.* 27 (2013) 4729–4738.

66. S. M. Stanciulescu and E.D. Hogan; *Biomass and bioenergy*, 24 (2003) 221-232.

67. A. Alahmer, J. Yamin, A. Sakhrieh, M.A. Hamdan; GCREEDER 2009, Amman-Jordan, March 31st – April 2nd 2009.

68. Q. Zhang, J. Chang, T. Wang, Y. Xu; *Energy Conversion and Management* 48 (2007) 87-92.

69. D. Chiramonti, M.Yaseen; *Biomass and bioenergy*, 25 (2003) 85-99.

70. A. Centeno, E. Laurent, B. Delmon; *J. Catal.* 154 (1995) 288–298

7. P. Degobert, "Automobiles and Pollution" *Society of Automotiv Engineers* ISBN 2- 7108-0676-2, 24.

72. D. Ayhan; *Energy Conversion Management.* 49 (2008) 2106–2116.

73. A. Cho, H. Kim, A. Iino, A. Takagaki, S.T. Oyama; *J. Catal.* 318 (2014) 151–161.

74. V.M.L. Whiffen, K.J. Smith, *Top. Catal*. 55 (2012) 981–990.

75. V.M.L. Whiffen, K.J. Smith, S.K. Straus; *Appl. Catal. A. Gen.* 419 (2012) 111–125.

76. O.D. Mante, F.A. Agblevor, S.T. Oyama; *Fuel* 117 (2014) 649–659.

77. S.T. Oyama, T. Gott, H. Zhao, Y.-K. Lee; *Catal. Today* 143 (2009) 94–107.

78. R. Prins, M.E. Bussell; *Catal. Lett.* 142 (2012) 1413–1436.

79. H.Y. Zhao, D. Li, P. Bui, S.T. Oyama; *Appl. Catal. A: Gen.* 391 (2011) 305–310.

80. D.C. Elliott; *Energy Fuels* 21 (2007) 1792–1815.

81. S. De, B. Saha, R. Luque; *Bioresour. Technol.* 178 (2015) 108–118.

82. H.M. Wang, J. Male, Y. Wang; *ACS Catal*. 3 (2013) 1047–1070.

83. T. Dickerson, J. Soria; *Energies* 6 (2013) 514–538.

84. D.A. Bulushev, J.R.H. Ross; *Catal. Today* 171 (2011) 1–13.

85. M. Guisnet, P. Magnoux, *Catal. Today* 36 (1997) 477–483.

86. S. Vitolo, B. Bresci, M. Seggiani, M.G. Gallo; *Fuel* 80 (2001) 17–26.

87. F. Li, Y. Yuan, Z. Huang, B. Chen, F. Wang; *Appl. Catal. B* 165 (2015) 547–554.

88. C. Zhou, X. Xia, C. Lin, D. Tonga, J. Beltramin; *Chem. Soc. Rev.* 40 (2011) 5588−5607.

89. S. Xiu, A. Shahbazi; *Renew. Sustain. Energy Rev.* 16 (2012) 4406–4414.

90. F. Bilgili; *Renew. Sustain. Energy Rev.* 16 (2012) 5349–5354.

91. J. Carlos Serrano-Ruiz, J.A. Dumesic; *Energy Environ. Sci.* 4 (2011) 83–99.

92. R. Gentilli, L. Tognotti, G. Benelli, "Feasibility of Using Wood Flash-Pyrolysis Oil in Diesel Engines", SAE 982529.

93. G.W. Huber, S. Iborra, A. Corma; *Chem. Rev.* 106 (2006) 4044–4098.

94. A.V. Bridgwater; *Biomass Bioenergy* 38 (2012) 68–94.

95. G.D. Roy, "Non-Renewable energy sources; *Hanna Publications.*

96. A.V. Bridgwater, D. Meier, D. Radlein; *Org. Geochem.* 30 (1999) 1479–1493.

97. C. Bertoli, J.D. Alessio, N. Giacomo, M. Lazzaro; *SAE.* 2975. 2000-01.

98. J.A. Pereira, A.M. Pessoa, M.N. Cordeiro, R. Fernandes, C. Prudêncio; *Eur J Med Chem* 97 (2006) 664-672.

99. S. Czernik, K. D. Johnson and B. Stewart; *Biomass and Bioenergy*, 7 (1994) 187-192.

100. D. Chiaramonti, A. Oasmaa, Y. Solantausta; *Renewable and Sustainable Energy.* 11(2011) 1056-1086.

101. N, Özbay, B.B. Uzun, E.A. Varol; *Fuel Processing Technology* 87 (2011) 1013-1019.

102. C.E. Goering, A.W. Schwab, M.J. Daugherty, A.J. Heakin; *Trans ASAE* 25 (2007)1472-1477.

103. R.W. Pryor, M.A. Hanna, J.L. Schinstock, L.L.Bashford; *Trans ASAE* 26 (1993) 0333-0337.

104. P.N. Giannelos, F. Zannikos, S. Stournas, E. Lois, G. Anastopoulos *Ind Crop Prod* (2002) 16: 1-9

105. M. Guisnet, P. Magnoux; *Catal. Today* 36 (1997) 477–483

106. S. Vitolo, B. Bresci, M. Seggiani, M.G. Gallo; *Fuel* 80 (2001) 17–26

107. W.B. Widayatno, G. Guan, J. Rizkiana, X. Hao, Z. Wang, C. Samart, A. Abudula; *Fuel* 132 (2014) 204–210

108. S.E. Wanke, P.C. Flynn; *Catal. Rev. Sci. Eng.* 12 (1975) 93–135.

109. P.T. Williams, P.A. Horne; *J. Anal. Appl. Pyrol.* 31 (1995) 39–61.

110. R.C. Veses, P.M. Kuamoto, C.L. Petzhold, E.B. Caramão, R.D Silva; *Energy Fuels* 27 (2013) 6831−6838

ANNEX 1

Main compounds identified in both fractions of bio-oil before hydrogenation

Compounds identified in the HFP

COMPOUNDS NAMES	FORMULAS	COMPOUNDS NAMES	FORMULAS
H-Pyrrole, 4-ethyl-2,3-dimethyl	$C_6H_{13}N$	1-Propyne, 2-bromo-	C_3H_3Br
5,6,7,8-Tetrahydroindolizine	$C_8H_{11}N$	Ethanol, 2,4-diethoxy-	$C_6H_{14}O_3$
Amino-4-methylpyrrole-3 carbonitrile	$C_6H_7N_3$)	1H-Indole, 2,5-dimethyl-	$C_{10}H_{11}N$
Methyl 4-O-methyl-d-arabinoside	$C_6H_{10}OS_2$	3-O-Methyl-d-glucose	$C_7H_{14}O_6$
Diallylmethylsilane	$C_7H_{14}Si$	Ethanol, 2,2-diethoxy-	$C_6H_{14}O_3$
Oxotetrahydrofuran-2-carboxylic acid	$C_5H_6O_4$	1H-Indole, 2,6-dimethyl-	$C_{10}H_{11}N$
1-Phospha-1-butyne, 3,3-dimethyl	C_5H_9P	Ethanol, 2,2-diethoxy-	$C_6H_{14}O_3$
5,6,7,8-Tetrahydroindolizine	$C_6H_{11}N$	Furfural	$C_5H_4O_2$
1H-Indole, 2,3-dihydro-	C_8H_9N	1,3,5-Trisilacyclohexane	$C_3H_{12}Si_3$
4-Methylimidazole-5-	$C_6H_{16}N_{20}$	Histidine, 1-methyl-	$C_7H_{11}N_3O_2$
4-Acetonylcycloheptanone	$C_{10}H_{16}0_2$	4-(Trimethylsilyl) morpholine	$C_7H_{17}NOSi$
Phenol, 4-(2-aminoethyl)-	$C_8H_{11}NO$	Diethyl-phenylsilane	$C_{10}H_{16}Si$
1-Propyne, 3-bromo-	C_3H_3Br	Tetrahydro-1,3-thiazine-2-thione	$C_4H_7NS_2$
4-Acetonylcycloheptanone	$C_{10}H_{16}O_2$	Ethanol, 2,2-diethoxy-	$C_6H_{14}O_3$
1,2-Bis (dimethylphosphino) ethane	$C_6H_{16}P_2$	4-(Trimethylsilyl) morpholine	$C_7H_{17}NOSi$
Quinoline, 5,6,7,8-tetrahydro-	$C_9H_{11}N$	9H-Fluorene, 9-bromo-	$C_{13}H_9Br$
Methyl 4-O-methyl-d-arabinoside	$C_6H_{14}O_5$	2,3-Anhydro-d-galactosan	$C_6H_8O_4$
3-Ethoxypropionic acid	$C_6H_{10}O_3$	Ethanol, 2,2-diethoxy-	$C_6H_{14}O_3$
Ethanol, 2,2-diethoxy	$C_6H_{14}O_3$	Pregna-3,5-dien-9-ol-20-one	$C_{21}H_{30}O_2$
Naphthalene, 1,2,-tetrahydro-1-nonyl-	$C_{19}H_{30}$	Ethanol, 2,2-diethoxy-	$C_6H_{14}O_3$
1,4-Dithiane-1-oxide	$C_4H_8OS_2$	Ethanol, 2,2-diethoxy-	$C_6H_{14}O_3$
3-Oxo-.alpha.-ionol	$C_{13}H_{20}O_2$	Glycero-galacto-heptose	$C_7H_{14}O_7$
2,3-Anhydro-d-galactosan	$C_6H_8O_4$	Glycerol-galacto-heptose	$C_7H_{14}O_7$
Pregna-3,5-dien-9-ol-20-one	$C_{21}H_{30}O_2$	Ethanol, 2,2-diethoxy-	$C_6H_{14}O_3$

Quinoline, 5,6,7,8-tetrahydro-	$C_9H_{11}N$	Methyl 4-methyl-arabinoside	$C_7H_{14}O_5$
Cyclohexylamine	$C_6H_{13}N$	Indene,3-dihydro-4-methyl	$C_{10}H_{12}$
phenol	C_6H_6O	2,5-Diaminotoluene	$C_7H_{10}N_2$
pentanone	$C_5H_{10}O$	Cyclohexanone	$C_6H_{10}O$
Cyclohexenyl-ethanone	$C_8H_{12}O$	2,5-Diaminotoluene	$C_7H_{10}N_2$

Compounds identified in LFP

COMPOUNDS NAMES	**FORMULAS**	**COMPOUNDS NAMES**	**FORMULAS**
Pentanol	$C_5H_{12}O$	Cyclohexanone	C_6H_8O
cyclopentane, methyl ethylidene	C_8H_{14}	phenol	C_6H_6O
1-Methyl-2-n-hexylbenzene	$C_{13}H_{20}$	4-methylphenol	C_7H_8O
pentanone	$C_5H_{10}O$	Pyrrole	C_4H_5N
Hexanone	$C_6H_{12}O$	3-methylbut-3-enenitrile	C_5H_7N
1H-Indene, 1-ethylidene-	$C_{11}H_{10}$	Cyclohexylamine	$C_6H_{13}N$
Toluene	C_6H_7	Cyclohexylamine	$C_6H_{13}N$
Benzene, 1-ethyl-3-methyl-	C_9H_{12}	2,6-Dimethylpiperidine	$C_7H_{15}N$
octanone	$C_8H_{16}O$	4-Methylpyridine	C_6H_7N
Heptanone	$C_7H_{14}O$	Phenethylamine	$C_8H_{11}N$
Hexenol	$C_6H_{12}O$	1,5-Diazabicyclonon-5-ene	$C_7H_{12}N_2$
cyclopentanone	C_5H_8O	Phenylenediamine	$C_6H_8N_2$
Cyclohexanone	$C_6H_{10}O$	2,5-Diaminotoluene	$C_7H_{10}N_2$
endo-Norborneol	$C_7H_{12}O$	Tetramethylsuccinonitrile	$C_8H_{12}N_2$
2-cycloheptenone	$C_7H_{10}O$	Diallylaminopropionitrile	$C_9H_{14}N_2$
Heptanone	$C_7H_{14}O$	Benzene, (1-methylpentyl)-	$C_{12}H_{18}$
Acetylcyclohexene	$C_8H_{12}O$	1-Aza-bicycloheptan-3-ol	$C_6H_{11}NO$
acetophenone	C_8H_8O	Triacetone amine	$C_9H_{17}NO$
cyclohexenyl, ethanone	$C_8H_{12}O$	1-Amino-1-cyclopentanemethan	$C_6H_{13}NO$
3,5-Trimethyl-2-cyclohexene-1-one	$C_9H_{14}O$	Amino-1-dimethylamin	$C_{10}H_{16}N_2$
cyclohexanone, ethylidene	$C_8H_{12}O$	Isonipecotonitrile	$C_6H_{10}N_2$

cyclopentenone, methylene	$C_9H_{12}O$	4-Cyanopiperidine	$C_6H_{10}N_2$
indenone, hexahydro	$C_9H_{12}O$	4-Methyl-2-propyl-H-imidazole	$C_7H_{12}N_2$
ethane, diethoxy	$C_6H_{14}O_2$	4-methyl-2-propyl-1H-imidazole	$C_7H_{12}N_2$
furan methanol	$C_5H_6O_2$	pyridine, propenyl	$C_{10}H_{13}N$

ANNEX 2

Main compounds identified in both fractions of bio-oil after hydrogenation

Compounds detected in the HFH

COMPOUNDS NAMES	FORMULAS	COMPOUNDS NAMES	FORMULAS
Benzene, 1-ethyl-3-methyl-	C_9H_{12}	Benzene, (1-methylbutyl)-	$C_{11}H_{16}$
Benzene, 1,2,3-trimethyl-	C_9H_{12}	Azulene	$C_{10}H_8$
1,3-dithio-, S-ethyl ester	$C_6H_{10}OS_2$	Indane	C_9H_{10}
1H-Pyrrole, 4-ethyl-2,3-dimethyl-	$C_8H_{13}N$	Dodecane	$C_{12}H_{26}$
5,6,7,8-Tetrahydroindolizine	$C_8H_{11}N$	6-Dodecene	$C_{12}H_{24}$
3-Decene	$C_{10}H_{20}$	3-Dodecene	$C_{12}H_{24}$
Benzene, 1,2,3-trimethyl-	C_9H_{12}	Benzene, hexyl-	$C_{12}H_{18}$
Benzene, 2-propenyl-	C_9H_{10}	Benzene, (1-methylpentyl)-	$C_{12}H_{18}$
Indane	C_9H_{10}	1,3-Propanedithiol	$C_3H_8S_2$
11-Dodecen-2-one, 7,7-dimethyl-	$C_{14}H_{26}O$	Naphthalene, 1-methyl-	$C_{11}H_{10}$
Diallylmethylsilane	$C_7H_{14}Si$	Tridecane	$C_{13}H_{28}$
5,6,7,8-Tetrahydroindolizine	$C_8H_{11}N$	3-Tridecene	$C_{13}H_{26}$
1H-Indole, 2,3-dihydro-	C_8H_9N	Benzene, 2-propenyl-	C_9H_{10}
12-Methyl-E,E-2,13-octadecadien-1-ol	$C_{19}H_{36}O$	1H-Indene, 1-ethylidene-	$C_{11}H_{10}$
1,3-Propanedithiol	$C_3H_8S_2$	Naphthalene, 2-methyl-	$C_{11}H_{10}$
Undecane	$C_{11}H_{24}$	1-Isopropenylnaphthalene	$C_{13}H_{12}$
3-Undecene	$C_{11}H_{22}$	Naphthalene, 1-methyl-	$C_{11}H_{10}$
3-Undecene	$C_{11}H_{22}$	Tetradecane	$C_{14}H_{30}$
Benzene, 4-ethenyl-1,2-dimethyl-	$C_{10}H_{12}$	3-Tetradecene	$C_{14}H_{28}$
1,7-Heptane	C_7H_{10}	Pentadecane	$C_{15}H_{32}$
3-Ethoxypropionic acid	$C_5H_{10}O_3$	Undecenol, 2,10-dimethyl-	$C_{13}H_{26}O$
Ethanol, 2,2-diethoxy-	$C_6H_{14}O_3$	camphor	$C_{10}H_{16}O$
Methyl isopropylidene-	$C_9H_{16}O_5$	3-Ethoxypropionic acid	$C_5H_{10}O_3$
Benzene, pentyl-	$C_{11}H_{16}$	Benzene, (1-methylpentyl)-	$C_{12}H_{18}$

Compounds identified in the LFH

COMPOUNDS NAMES	FORMULAS	COMPOUNDS NAMES	FORMULAS
2,4-Dimethylstyrene	$C_{10}H_{12}$	Naphthalene, 1,2,3,4-tetrahydro-	$C_{10}H_{12}$
Undecane	$C_{11}H_{24}$	Benzene, (1-methylbutyl)-	$C_{11}H_{16}$
3-Undecene	$C_{11}H_{22}$	furan methanol	$C_5H_6O_2$
3-Undecene	$C_{11}H_{22}$	Cyclohexanone	C_6H_8O
cyclopentane, methyl ethylidene	C_8H_{14}	phenol	C_6H_6O
1-Methyl-2-n-hexylbenzene	$C_{13}H_{20}$	Benzene, 2-propenyl-	C_9H_{10}
pentanone	$C_5H_{10}O$	Indane	C_9H_{10}
Hexanone	$C_6H_{12}O$	Indene	C_9H_8
1H-Indene, 1-ethylidene-	$C_{11}H_{10}$	Benzene, butyl-	$C_{10}H_{14}$
Toluene	C_6H_7	Cyclohexylamine	$C_6H_{13}N$
Benzene, 1-ethyl-3-methyl-	C_9H_{12}	Naphthalene, 1-methyl-	$C_{11}H_{10}$
octanone	$C_8H_{16}O$	Tridecane	$C_{13}H_{28}$
Benzene, hexyl-	$C_{12}H_{18}$	Benzene, (1-methylpentyl)-	$C_{12}H_{18}$
Benzene, (1-methylpentyl)-	$C_{12}H_{18}$	Naphthalene, 1-methyl-	$C_{11}H_{10}$
Naphthalene, 1-methyl-	$C_{11}H_{10}$	3-Tridecene	$C_{13}H_{26}$
Cyclohexanone	$C_6H_{10}O$	2,5-Diaminotoluene	$C_7H_{10}N_2$
endo-Norborneol	$C_7H_{12}O$	Tetramethylsuccinonitrile	$C_8H_{12}N_2$
Azulene	$C_{10}H_8$	Diallylaminopropionitrile	$C_9H_{14}N_2$
Dodecane	$C_{12}H_{26}$	octanone	$C_8H_{16}O$
6-Dodecene	$C_{12}H_{24}$	1-Aza-bicycloheptan-3-ol	$C_6H_{11}NO$
3-Dodecene	$C_{12}H_{24}$	Triacetone amine	$C_9H_{17}NO$
cyclohexenyl, ethanone	$C_8H_{12}O$	1-Amino-1-cyclopentanemethan	$C_6H_{13}NO$
3,5-Trimethyl-2-cyclohexene-1-one	$C_9H_{14}O$	2-Amino-1-dimethylamine	$C_{10}H_{16}N_2$
1H-Indene,2,3-dihydro-4-methyl-	$C_{10}H_{12}$	Isonipecotonitrile	$C_6H_{10}N_2$
Benzene, pentyl-	$C_{11}H_{16}$	4-Cyanopiperidine	$C_6H_{10}N_2$

ANNEX 3

Hydrocarbons identified in both fractions of bio-oil after and before hydrogenation

Main hydrocarbons detected in LFP

NO	COMPOUNDS NAMES	FORMULAS
1	3-Dodecene	$C_{12}H_{24}$
2	3-Dodecene	$C_{12}H_{24}$
3	2-Tridecene	$C_{13}H_{26}$
3	Tridecane	$C_{13}H_{28}$
4	3-Tridecene	$C_{13}H_{26}$
5	3-Tetradecene	$C_{14}H_{28}$

Main hydrocarbons identified in HFP

NO	HYDROCARBONS NAMES	FORMULAS
1	1H-Indene, 1-ethylidene-	$C_{11}H_{10}$
2	1-Isopropenylnaphthalene	$C_{13}H_{12}$
3	Tetradecane	$C_{14}H_{30}$
4	3-Tetradecene	$C_{14}H_{28}$
5	Pentadecane	$C_{15}H_{32}$

Main hydrocarbons detected LFH

COMPOUNDS NAMES	FORMULAS	COMPOUNDS NAMES	FORMULAS
3-Decene	$C_{10}H_{20}$	Benzene, hexyl-	$C_{12}H_{18}$
Benzene, 1,2,3-trimethyl-	$C9H_{12}$	Benzene, (1-methylpentyl)-	$C_{12}H_{18}$
Benzene, 2-propenyl-	C_9H_{10}	Naphthalene, 1-methyl-	$C_{11}H_{10}$
Indane	C_9H_{10}	Tridecane	$C_{13}H_{28}$
Undecane	$C_{11}H_{24}$	Benzene, (1-methylpentyl)-	$C_{12}H_{18}$

3-Undecene	$C_{11}H_{22}$	Naphthalene, 1-methyl-	$C_{11}H_{10}$
3-Undecene	$C_{11}H_{22}$	3-Tridecene	$C_{13}H_{26}$
Benzene,4-ethenyl-1,dimethyl-	$C_{10}H_{12}$	1H-Indene, 1-ethylidene-	$C_{11}H_{10}$
Naphthalene,1,2,3,4-tetrahydro-	$C_{10}H_{12}$	Naphthalene, 2-methyl-	$C_{11}H_{10}$
Benzene, (1-methylbutyl)-	$C_{11}H_{16}$	1-Isopropenylnaphthalene	$C_{13}H_{12}$
Azulene	$C_{10}H_{8}$	Tetradecane	$C_{14}H_{30}$
Dodecane	$C_{12}H_{26}$	3-Tetradecene	$C_{14}H_{28}$
6-Dodecene	$C_{12}H_{24}$	Pentadecane	$C_{15}H_{32}$

Main hydrocarbons identified in HFH

HYDROCARBONS NAMES	**FORMULAS**	**HYDROCARBONS**	**FORMULAS**
2,4-Dimethylstyrene	$C_{10}H_{12}$	3-Dodecene	$C_{12}H_{24}$
Undecane	$C_{11}H_{24}$	Benzene, hexyl-	$C_{12}H_{18}$
3-Undecene	$C_{11}H_{22}$	Benzene, (1-methylpentyl)-	$C_{12}H_{18}$
3-Undecene	$C_{11}H_{22}$	Naphthalene, 1-methyl-	$C_{11}H_{10}$
Benzene, 4-ethenyl-1,2-dimethyl	$C_{10}H_{12}$	Benzene, 2-propenyl-	$C_{9}H_{10}$
1H-Indene, 2,3-dihydro-4-methyl-	$C_{10}H_{12}$	Indane	$C_{9}H_{10}$
Benzene, pentyl-	$C_{11}H_{16}$	Indene	$C_{9}H_{8}$
Naphthalene, 1,2,3,4-tetrahydro-	$C_{10}H_{12}$	Benzene, butyl-	$C_{10}H_{14}$
Benzene, (1-methylbutyl)-	$C_{11}H_{16}$	Naphthalene, 1-methyl-	$C_{11}H_{10}$
Azulene	$C_{10}H_{8}$	Tridecane	$C_{13}H_{28}$
Dodecane	$C_{12}H_{26}$	Benzene, (1-methylpentyl)-	$C_{12}H_{18}$
6-Dodecene	$C_{12}H_{24}$	Naphthalene, 1-methyl-	$C_{11}H_{10}$

ANNEX 4

Change in density of LFH and HFH at different temperatures

Change in density of LFH at different temperatures

T(ºC)	volume (mL)	mass (g)	ρ (g mL^{-1})	T (K)	1/K	ln ρ
-10	11.721	10	0.8531	263	0.003802	-0.156719
0	11.811	10	0.8466	273	0.003663	-0.164128
10	11.884	10	0.8414	283	0.003534	-0.17067
20	11.916	10	0.8392	293	0.003413	-0.17877
30	11.949	10	0.8368	303	0.003311	-0.18428
40	11.984	10	0.8344	313	0.003195	-0.18983
50	12.094	10	0.8271	323	0.003096	-0.19468

Change in density of HFH at different temperatures

T (°C)	volume (mL)	mass (g)	ρ (g mL^{-1})	T (K)	1/K	ln ρ
-10	11.290	10	0.8857	263	0.003802	-0.11241
0	11.362	10	0.8801	273	0.003663	-0.11565
10	11.410	10	0.8764	283	0.003534	-0.11866
20	11.452	10	0.8656	293	0.003413	-0.12155
30	11.792	10	0.8480	303	0.003323	-0.12451
40	11.885	10	0.8413	313	0.003195	-0.12729
50	11.910	10	0.8396	323	0.003096	-0.12896

ANNEX 5

Change in viscosity of LFH and HFH at different temperatures

Change in viscosity of LFH at different temperatures

T(ºC)	Time (s)	T (K)	1/K	η (mm^2/s)	ln η
-10	270	263	0.003802	2.6722	1.057790294
0	239	273	0.003663	2.1032	0.741937345
10	219	283	0.003534	1.6531	0.500775288
20	183	293	0.003413	0.9673	-0.03303985
30	175	303	0.003311	0.8523	-0.18464425
40	161	313	0.003195	0.8273	-0.18982967
50	156	323	0.003096	0.7223	-0.19479908

Change in viscosity of HFH at different temperatures

T (°C)	Time (s)	η (mm^2/s)	T (K)	1/K	ln η
-10	370	4.4228	263	0.003802	1.48678327
0	330	3.3433	273	0.003663	1.20697436
10	286	2.5681	283	0.003534	0.94780622
20	243	2.0375	293	0.003413	0.711723572
30	205	1.7557	303	0.003321	0.50512943
40	171	0.8634	313	0.003195	0.21026093
50	149	0.8001	323	0.003096	0.09540108

ANNEX 6

Change in viscosity of pure DF and AF at different temperatures

Change in viscosity of DF at different temperatures

T (ºC)	Time (s)	T (K)	η (mm^2/s)	1/K	ln n
-10	245	263	2.5724	0.003802	0.944839
0	215	273	1.9736	0.003663	0.679859
10	191	283	1.5533	0.003534	0.440382
20	173	293	0.9578	0.003413	-0.04312
30	162	303	0.8427	0.003301	-0.17114
40	141	313	0.8179	0.003195	-0.20102
50	131	323	0.7128	0.003096	-0.33855

Change in viscosity of AF at different temperatures

T(ºC)	1/K	T(K)	Time (s)	η (mm^2/s)	ln (visc)
-10	0.003802	263	179	4.618	1.529962
0	0.003663	273	135	3.9771	1.380553
10	0.003534	283	119	3.2171	1.16848
20	0.003425	293	102	2.4484	0.895435
30	0.003321	303	86	1.8484	0.61432
40	0.003195	313	77	1.0934	0.089292
50	0.003096	323	70	0.8678	-0.14179

ANNEX 7

Change in viscosity of AF with 10% and 20% HFH (mixture) at different temperatures

Change in viscosity of AF with 10% HFH (mixture) at different temperatures

T(ºC)	Time (s)	1/K	T(K)	η (mm^2/s)	Lnη
-10	309	0.003802	263	4.521	1.508733
0	259	0.003759	273	3.8743	1.354365
10	236	0.003731	283	3.1976	1.162401
20	208	0.003704	293	2.4789	0.907815
30	188	0.003663	303	1.7487	0.558873
40	175	0.003597	313	1.0838	0.080473
50	152	0.003534	323	0.8575	-0.15373

Change in viscosity of AF with 20% HFH (mixture) at different temperatures

T(ºC)	Time (s)	1/K	T(K)	η (mm^2/s)	Lnη
-10	299	0.003802	263	4.5113	1.506585
0	250	0.003759	273	3.8549	1.349345
10	226	0.003731	283	3.1771	1.155969
20	199	0.003704	293	2.4581	0.899389
30	185	0.003663	303	1.7389	0.553253
40	171	0.003597	313	1.0737	0.071111
50	150	0.003534	323	0.8478	-0.16511

ANNEX 8

Change in density of AF with 10% and 20% HFH at different temperatures

Change in density of AF with 10% HFH at different temperatures

T (°C)	volume (mL)	mass(g)	ρ (g mL^{-1})	T (K)	1/K	ln p
-10	11.655	10	0.8580	263	0.0038023	-0.15154
0	11.774	10	0.8493	273	0.003663	-0.17207
10	11.980	10	0.8347	283	0.003534	-0.19109
20	12.143	10	0.8235	293	0.003413	-0.20892
30	12.481	10	0.8011	303	0.003311	-0.22558
40	12.771	10	0.7830	313	0.003195	-0.24106
50	12.965	10	0.7713	323	0.003096	-0.25565

Change in density of AF with 20% HFH at different temperatures

T (°C)	volume (mL)	mass (g)	ρ (gmL^{-1})	T (K)	1/K	ln ρ
-10	11.330	10	0.8844	263	0.003802	-0.12277
0	11.572	10	0.8641	273	0.003663	-0.14303
10	11.965	10	0.8357	283	0.003534	-0.19237
20	12.277	10	0.8145	293	0.003413	-0.21035
30	12.632	10	0.7981	303	0.003321	-0.22552
40	12.823	10	0.7861	313	0.003195	-0.24067
50	12.956	10	0.7718	323	0.003096	-0.25373

ANNEX 9

Change in viscosity of DF with 10% and 20% LFH at different temperatures

Change in viscosity of DF with 10% LFH at different temperatures

T(°C)	Time (s)	η (mm^2/s)	T (K)	1/K	ln η
-10	270	2.5929	263	0.003802	0.952777
0	240	1.9938	273	0.003601	0.690042
10	206	1.5637	283	0.003532	0.447055
20	183	0.9598	293	0.003411	-0.04103
30	165	0.8469	303	0.003313	-0.16617
40	151	0.8199	313	0.003221	-0.19857
50	134	0.7168	323	0.003121	-0.33296

Change in viscosity of DF and 20% LFH at different temperatures

T (°C)	Time (s)	η (mm^2/s)	T (K)	1/K	ln η
-10	279	2.6121	263	0.003802	0.960154
0	251	1.9999	273	0.003663	0.693097
10	211	1.5777	283	0.003534	0.455968
20	187	0.9599	293	0.003413	-0.04093
30	169	0.8481	303	0.003321	-0.16476
40	155	0.8214	313	0.003195	-0.19675
50	141	0.7193	323	0.003096	-0.32948

ANNEX 10

Change in density of DF with 10% and 20% LFH at different temperatures

Change in density of DF with 10% LFH at different temperatures

T (°C)	volume (mL)	mass (g)	ρ (g mL^{-1})	T (K)	1/K	ln P
-10	11.852	10	0.8437	263	0.003802	-0.157544
0	11.941	10	0.8374	273	0.003534	-0.178743
10	12.021	10	0.8318	282	0.003413	-0.188542
20	12.132	10	0.8242	293	0.003300	-0.198329
30	12.212	10	0.8188	303	0.003195	-0.204813
40	12.293	10	0.8134	313	0.003096	-0.213193
50	12.346	10	0.8099	323	0.003003	-0.223019

Change in density of DF with 20% LFH at different temperatures

T (°C)	volume (mL)	mass (g)	ρ (g mL^{-1})	T (K)	1/K	Ln P
-10	11.780	10	0.8486	263	0.003802	-0.145882
0	11.953	10	0.8366	273	0.003534	-0.175545
10	12.011	10	0.8325	282	0.003413	-0.186209
20	12.135	10	0.8240	293	0.003312	-0.192372
30	12.221	10	0.8182	303	0.003195	-0.201382
40	12.411	10	0.8057	313	0.003096	-0.219152
50	12.585	10	0.7945	323	0.003003	-0.227277

ANNEX 11

Percent area of all groups present in bio-oil before and after hydrogenation

Groups	% Area before hydrogenation	% Area after hydrogenation
Alcohols	10.93	5.89
Aldehydes	0	0.45
Ketones	45	12
Ethers	6.26	3
Esters	0	0
Phenols	2.85	7.80
Nitrogenous	30	6
Aromatics hydrocarbons	0.24	25.24
Cyclic hydrocarbons	3.09	16.42
Aliphatic hydrocarbons	0	21.84

Percent area of hydrocarbons and residues identified after and before hydrogenation

Fractions	Hydrocarbons detected before hydrogenation (%)	Hydrocarbons detected after hydrogenation (%)	% Residues after hydrogenation
Light (80-160 ºC)	7	60	16
Heavy (160-240 ºC)	5	61	15